NRL Report 4354

ANALYSIS OF SYSTEMS FOR THE RECORDING OF EXPONENTIAL SIGNALS

R. V. Talbot, J. R. Shipman, F. E. Huggin,
and C. B. Dobbie

April 1954

Reprinted June 1960

APPROVED FOR PUBLIC
RELEASE - DISTRIBUTION
UNLIMITED

NAVAL RESEARCH LABORATORY
Washington, D.C.

NRL Report 4354

ANALYSIS OF SYSTEMS FOR THE RECORDING OF EXPONENTIAL SIGNALS

R. V. Talbot, J. R. Shipman, F. E. Huggin,
and C. B. Dobbie

April 1954

Reprinted June 1960

NAVAL RESEARCH LABORATORY
Washington, D.C.

CONTENTS

List of Illustrations v

Acknowledgments vii

Abstract viii

Problem Status viii

Authorization viii

Section 1 - INTRODUCTION 1

1.1 Purpose 1
1.2 Background 1
1.3 The Exponential Signal 2

Section 2 - DETECTORS 3

2.1 Introduction 3
2.2 Delta Function 3
2.3 Detector Response - Case 1 6
2.4 Detector Response - Case 2 7
2.5 Detector Response - Case 3 8
2.6 Summary 9

Section 3 - TRANSMISSION LINES 10

3.1 Introduction 10
3.2 General Response Characteristics 10
3.3 Delta Function Response 13
3.4 Exponential Function Response 15
3.5 Step Function Response 16
3.6 Response to Other Driving Functions 18
3.7 Solid Dielectric Lines 19
3.8 Limitations due to Higher Modes 21

Section 4 - AMPLIFIERS 22

4.1 Introduction 22
4.2 Network Analysis 22
4.3 Comparison of Amplifier Performance on Exponential, Sinusoidal and Step Function Signals 25
4.4 The Frequency-Amplitude Spectrum of an Exponential 26
4.5 Response of Simple Shunt Fed Amplifier to Exponential Signals 27
4.6 Amplifier Linearity Considerations 29
4.7 Circuit Measurements 31
4.8 Conclusions 32

Section 5 - DISPLAY SYSTEMS AND CATHODE-RAY TUBES 34

5.1 Introduction 34
5.2 Display Systems 34
5.3 Characteristics of the Rossi Display 36
5.4 Cathode-Ray Tube Characteristics 36

CONTENTS(Cont'd)

5.5 Transit Time Distortion 38
5.6 Recording Small Amplitude Signals 39
5.7 Recording Large Amplitude Signals 40
5.8 Selection of the Cathode-Ray Tube for a Recording System 40
5.9 Summary 42
5.10 List of Symbols 42

Section 6 - CONCLUSIONS AND RECOMMENDATIONS 44

APPENDIX A - DETECTOR CALCULATIONS 45

A.1 Detector Response - Case 1 45
A.2 Detector Response - Case 2 53
A.3 Detector Response - Case 3 55

APPENDIX B - TRANSMISSION LINE RESPONSE CONSIDERATIONS 59

APPENDIX C - RESPONSE OF ELECTRICAL NETWORKS TO EXPONENTIAL DRIVING FUNCTIONS 60

APPENDIX D - COMPARISON OF AMPLIFIER RESPONSE TO SINUSOIDAL, STEP FUNCTION AND EXPONENTIAL SIGNALS 62

D.1 Introduction 62
D.2 Circuit Analysis 62
D.3 Response of Cascaded Vacuum-Tube Stages to a Sinusoidal Function 63
D.4 Response of Cascaded Vacuum Tube Stages to a Step Function 63
D.5 Response of Cascaded Vacuum Tube Stages to an Exponential Function 65
D.6 Comparison of Sinusoidal, Step Function and Exponential Response 65

APPENDIX E - SPECTRUM ANALYSIS OF EXPONENTIAL SIGNALS 68

E.1 General 68
E.2 Frequency - Amplitude Analysis 68

APPENDIX F - RESPONSE OF SIMPLE SHUNT FED AMPLIFIER TO EXPONENTIAL SIGNALS 72

APPENDIX G - AMPLIFIER LINEARITY CONSIDERATIONS 74

APPENDIX H - PARAMETERS OF THE ROSSI DISPLAY 77

H.1 General 77
H.2 Unresolved Displacement at Start of the Survey 77
H.3 Writing Speed Requirements 78
H.4 Number of Generations that can be Recorded 79
H.5 Determining Alpha from the Rossi Display 80
H.6 Error in Measuring Alpha by a Rossi Display 81

APPENDIX I - TRANSIT TIME EFFECTS OF DEFLECTION PLATES 83

FIGURES

Fig. No.	Title	Page
1	Basic Recording System Block Diagram	87
2	Sensitivity Reduction Factors for the Coaxial Photocell	88
3	Response of Transmission Line to Delta Function Input	89
4	Transmission Line Time Constant	90
5	Response of Transmission Line to Step Function Input	91
6	Optimum GRF vs. ω_H/ω_L	92
7	Universal GRF Curves for n=1 to n=5	93
8	Magnitude and phase angle of the Sinusoidal Components of an Exponential Signal vs. ω/α	94
9	Ivy Amplifier Circuit Diagram	95
10	Ivy Amplifier Frequency Response	96
11	Ivy Amplifier Exponential Response ($\alpha=0.925\times10^8$)	97
12	418-A Distributed Amplifier Exponential Response ($\alpha=0.925\times10^8$)	98
13	Single 418-A Amplifier Exponential Response ($\alpha=0.925\times10^8$)	99
14	100 Mc and 200 Mc Filters – Exponential Response ($\alpha=0.925\times10^8$)	100
15	Ivy Amplifier Exponential Response ($\alpha=2.38\times10^8$)	101
16	418-A Distributed Amplifier Exponential Response ($\alpha=2.38\times10^8$)	102
17	Single 418-A Amplifier Exponential Response ($\alpha=2.38\times10^8$)	103
18	100 Mc and 200 Mc Filters – Exponential Response ($\alpha=2.38\times10^8$)	104
19	Ivy Amplifier Exponential Response ($\alpha=4.7\times10^8$)	105
20	418-A Distributed Amplifier Exponential Response ($\alpha=4.7\times10^8$)	106
21	Single 418-A Amplifier Exponential Response ($\alpha=4.7\times10^8$)	107
22	100 Mc and 200 Mc Filters – Exponential Response ($\alpha=4.7\times10^8$)	108
23	418-A Distributed Amplifier Frequency Response (V.G. at O DB = 77)	109
24	Single 418-A Amplifier Frequency Response (V.G. at O DB = 37.5)	110
25	100 Mc and 200 Mc Filters – Frequency Response	111

Fig. No.	Title	Page
26	Measured and Calculated Gain vs. Alpha	112
27	418-A Distributed Amplifier Circuit Diagram	113
28	Single 418-A Amplifier Circuit Diagram	114
29	Variation of X-Y Angle vs. Alpha	115
30	D.C. Calibration Raster	116
31	Block Diagram of System for Measuring Writing Speed	117
32	Writing Speed Comparison	118
33	Sensitivity Reduction Factor for Deflection Plates with Sinusoidal Input	119
34	Sensitivity Reduction Factor for Deflection Plates with Exponential Input	120
35	Response of Terminated Detector to Delta Function Input	121
36	Response of Open-Circuited Detector to Delta Function Input	122
37	Response of Transmission Line to Ramp Function Input	123
38	Response of Transmission Line to Cosine Squared Input	124
39	Response of Transmission Line to Triangular Input	125
40	Rise Time and GRF vs. f_A	126
41	Gain of Single 418-A Amplifier vs. Alpha	127
42	Amplitude and Alpha Nonlinearity (Ivy Amplifier)	128
43	The Exponential Signal and the Rossi Display	129
44	Writing Speed vs. Alpha for Rossi Display	130
45	Nomograph Relating Field, Resolution and $\ln A/G$	131
46	$\ln (e^{1/m} - 1)$ vs. m	132
47	Rossi Display (f = 400 mc)	133
48	Rossi Display (f = 800 mc)	134
49	Rossi Display (f = 1000 mc)	135
50	Rossi Display (f = 3000 mc)	136
51	Exponential Signal Displayed on Linear Time Base ($\alpha = 3.75 \times 10^8$) ($f = 1000$ mc)	137
52	Probable Error in Measurement of Alpha vs. m	138

ACKNOWLEDGMENTS

The authors express particular appreciation to Dr. E. H. Krause, under whose leadership this work was conducted and without whose encouragement it would not have been possible. A large amount of the analysis of detectors and transmission lines was done by E. G. Harris. Additional work on the transmission line section was done by L. R. White.

ABSTRACT

This report is an analysis of the requirements of a recording system to be used in recording single nonrecurrent signals of the form $Ke^{\alpha t}$ with the range of α (alpha) being from approximately 1×10^8 to 20×10^8 sec^{-1}. The recording of such signals is particularly important in nuclear measurements on atomic weapons.

Particular attention is given to the response of the more important system components such as detectors, transmission lines, signal amplifiers and cathode-ray tubes. The capabilities and limitations of each are discussed. It is found that for a linear system the primary effect of each component is to cause a reduction in the relative amplitude of the signal, resulting in a reduction in the dynamic range of the system.

Some attention is also given to the response of certain system elements to other type signals including impulse functions, step functions, ramp functions and sinusoids. The effects of nonlinear elements are considered rather briefly.

From this analysis conclusions are drawn and recommendations made concerning the selection of the most suitable system elements and the arrangement of these elements. Where possible, suggestions have been given as to possible future developments.

PROBLEM STATUS

Certain phases of the system analysis are concluded with this report; other work on the problem continues.

AUTHORIZATION

NRL Problem H05-01

Manuscript submitted March 15, 1954

ANALYSIS OF SYSTEMS FOR THE RECORDING OF EXPONENTIAL SIGNALS

SECTION 1 - INTRODUCTION

1.1 Purpose

In the testing of atomic weapons one of the most direct criteria of weapon performance is the neutron multiplication rate, commonly referred to as alpha. Measurements of this parameter have been made for nearly every weapon tested and it is expected that such measurements will continue to be made in the future. A considerable effort has been made in the development of the recording systems used in determining alpha. It is the purpose of this report to analyze such recording systems with particular attention being given to the more important components.

A number of different methods for determining alpha have been considered. Because of the time and amplitude resolution required only a very few methods are practical. It is expected that as new techniques are developed simpler and more accurate methods may become possible. However, this report will be confined to an analysis of present systems with consideration given to capabilities and limitations.

1.2 Background

The measurement of alpha has been made in all weapons evaluation tests. The primary method of measurement has remained the same although many improvements in the system have been made. Figure 1 shows the basic recording system used in the alpha measurement. The system consists primarily of a detector which receives radiation from the weapon and generates an electrical signal which is a function of the radiation received. The signal is transmitted to a cathode-ray tube display through a transmission line. The beam of the cathode-ray tube is unblanked by a circuit which is triggered by the signal, the signal then being delayed sufficiently to permit the unblanking to occur before the signal arrives. The signal is then applied to one deflection axis of the tube while a sinusoidal timing wave is applied to the other deflection axis. The resulting trace is recorded on film, using a large aperture camera.

Continued research has led to the development of improved detectors. Photodiodes have been developed for delivering high level signals. Photomultipliers have been used to obtain increased sensitivity where desired. Transmission line development has led to the use of high quality coaxial lines which produce less signal distortion and attenuation and yet provide simpler and more reliable installations.[1] Cathode-ray tube development has resulted in tubes having improved deflection sensitivity, smaller trace widths, larger fields and higher writing speeds permitting more accurate measurement of alpha over a greater range of time. Further increase in signal coverage has been obtained by the development of signal amplifiers capable of amplifying low level exponential signals to a level where they can be recorded on the cathode-ray tubes. Other development has included signal inverters, improved timing oscillators and cathode-ray tube circuitry, and better photographic techniques.

---

[1] "Styroflex Coaxial Cable," NRL Report 4160

1.3 The Exponential Signal

It is assumed that the gamma rate, the neutron rate, and the fission rate are all proportional over much of a normal bomb reaction. Thus a measurement of gamma multiplication rate from the radiation at the detector should provide a measurement of the neutron multiplication rate, α, in the weapon. If a rate-type detector, such as a photodiode scintillation detector, is used the output will be proportional to the gamma rate.

For an interval of time $0 < t \leq t_{max}$ the fission rate $n_F(t)$ and the gamma rate $n_\gamma(t)$ increase exponentially in time. During this time α may be defined by the relation

$$\frac{dn_\gamma(t)}{dt} = \alpha\, n_\gamma(t)$$

The detector output voltage V(t) is then given by

$$V(t) = V(t_o)\, e^{\alpha(t-t_o)} = V_o e^{\alpha t}$$

where $V(t_o)$ is the threshold output voltage reached at time t_o, corresponding in practice to several generations of the reaction. After the time $t = t_{max}$ the fission rate no longer follows an exponential law with constant α. In order to discuss the problem for $t > t_{max}$ it is possible to define a variable $\alpha(t)$ as follows

$$\frac{dV(t)}{dt} = \alpha(t)\, V(t)$$

or

$$V(t) = V(t_o)\, e^{\int_{t_o}^{t} \alpha(t')dt'}$$

where $\alpha(t')$ is constant for $t_o \leq t \leq t_{max}$ and variable for $t > t_{max}$.

During the time when alpha is constant, this exponential signal has a number of significant characteristics, many of which will be discussed in later sections of this report. These include the following: the value of α cannot be affected by a linear system; while α is constant a change in signal level cannot be distinguished from a time delay; circuit elements which are reactive for sinusoidal driving functions are purely resistive for the exponential driving function.

1.4 Recording System Considerations

The basic system for the measurement of alpha was described in Sec 1.2. Following sections present analyses of the major components of the system including photodiode detectors, transmission lines, signal amplifiers and cathode-ray tubes. In order to obtain the maximum amount of information the system may utilize various arrangements of components. These may include: the use of detectors of different sensitivities, each detector signal being displayed on an indicator; the use of cathode-ray tubes of different sensitivities to display various levels of a given signal; and the use of amplifiers to provide even more coverage of low level signals.

As mentioned in Section 1.3, a linear system cannot change the value of α. The effects produced are primarily those of an effective attenuation of the exponential signal. This effect will be evaluated for each of the components discussed. Since detectors and amplifiers have a limited linear range they may introduce nonlinearity which can affect the apparent value of α.

SECTION 2 - DETECTORS

2.1 Introduction

In order to convert the weapon radiation into an electrical signal a detector is required. The three main types that have been used are the ionization chamber, and the photodiode and photomultiplier with scintillator.

Large coaxial ionization chambers, which have been used in the past, are basically integrating detectors and are not generally as suitable as the rate detectors developed later.

The second type of detector used consisted of a large coaxial photodiode surrounded by a cylinder of liquid scintillator composed of 0.5% terphenol in toluene. Two coaxial photodiodes have been used, the C7154 tube manufactured by R.C.A. and the CPT tube manufactured by the Capehart-Farnsworth Company. These tubes are essentially the same electrically except that the CPT tube has external connections to the plate and cathode at both ends of the tube whereas the C7154 has the connections at one end only. A detailed theoretical analysis follows which will determine the "sensitivity reduction factor" as a function of α for a simplified detector which is an approximation to both photodiode detectors which have been used. It is a more accurate approximation to the detector using the CPT tube.

The third type of detector used consisted of the same type of liquid scintillator illuminating an RCA 5819 photomultiplier. The response of this detector has not been evaluated. It is possible to estimate its response from the transit time spread in pulses generated by single particles such as cosmic rays. Experimental checks indicate this spread to be less than 5×10^{-9} seconds.

2.2 Delta Function Response

The purpose of this section of the report is to determine the "sensitivity reduction factor" for the large coaxial photodiode detector when it is used to detect radiation fields varying as $Ce^{\alpha t}$ for various values of α.

The factor may be obtained by first calculating the weighting function (sometimes called the memory function) of the detector and, from this, calculating the response of the detector to a γ-ray intensity of the form $Ce^{\alpha t}$. This approach is frequently used in the analysis of linear systems. A rudimentary account of the method is given here.[2]

Let the response of the detector (current output at the terminal) be $1 \cdot f_{\Delta t}(t)\,\Delta t$ when a very narrow γ-ray pulse of unit density and duration Δt falls on the front face of the scintillator at time $t = 0$ as shown in the sketch below.

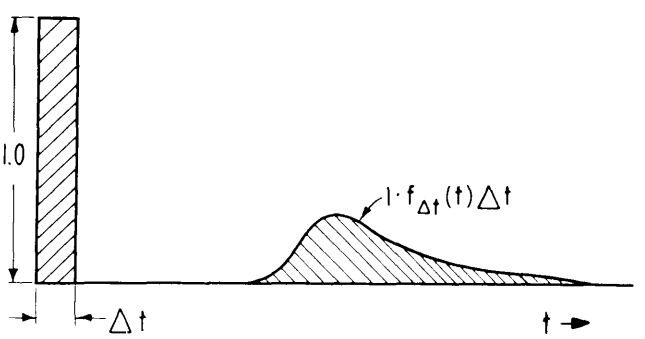

[2] James, Nichols and Philips, "Theory of Servomechanisms," Chapt. 2, Vol. 24 Rad. Lab. Series, McGraw-Hill

The factor $1 \cdot \Delta t$ is included since, when the response of any system is many times wider in time than the input, the amplitude of response is proportional to the area of the input. The subscript Δt is to indicate that the shape of the response is dependent upon the width of the γ-ray pulse. Then $C' f_{\Delta t}(t)\Delta t$ is the response to a γ-ray pulse of intensity C' and width Δt and $1/(\Delta t) \cdot f_{\Delta t}(t)\Delta t = f_{\Delta t}(t)$ is the response to a pulse of intensity $1/(\Delta t)$ and width Δt. Such a pulse would contain unit energy if the intensity is measured in units of energy per unit time. Let $f(t) = \lim_{\Delta t \to o} f_{\Delta t}(t)$

If a pulse of intensity C' and width Δt occurs at the time $t = \lambda$ instead of $t = 0$, the response will be $Cf_{\Delta t}(t - \lambda)\Delta t$. Now the response to any function $F(t)$ can be determined by approximating $F(t)$ by a series of narrow pulses of width Δt or $\Delta\lambda$ in the following way.

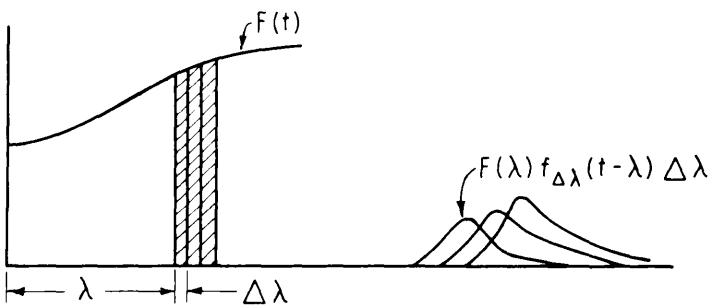

The pulse that occurs at $t = \lambda$ has the intensity $F(\lambda)$. The response to it is $F(\lambda) f_{\Delta\lambda}(t - \lambda)\Delta\lambda$.

The response to $F(t)$ can be found by summing the response to the narrow pulses making up $F(t)$. This response is approximately

$$\sum_{n=-\infty}^{n=t/\Delta\lambda} F(n\Delta\lambda)\, f_{\Delta\lambda}(t-n\Delta\lambda)\, \Delta\lambda . \tag{2.1}$$

The approximation is improved by taking $\Delta\lambda$ smaller and finally in the limit as $\Delta\lambda$ 0 the response to $F(t)$ is

$$I_{o_{F(t)}} = \int_{-\infty}^{t} F(\lambda)\, f(t-\lambda)\, d\lambda \tag{2.2}$$

which by a change of variable may be put in the form

$$I_{o_{F(t)}} = \int_{o}^{\infty} F(t-\lambda)\, f(\lambda)\, d\lambda . \tag{2.3}$$

Thus the problem of finding the response to any function F(t) has been reduced to the problem of finding the weighting function f(t), which is the response to a pulse of intensity $1/(\Delta t)$ and width Δt in the limit as $\Delta t \rightarrow 0$. Such a pulse is the Dirac Delta function $\delta(t)$ with the properties

$$\delta(t) = 0 \text{ for } t \neq o$$

$$\int_{-\eta}^{+\eta} g(t)\ \delta(t)\ dt = g(o) \tag{2.4}$$

Where g(t) is an arbitrary function and η is any finite value of time.

If there were no distortion in the system f(t) would be equal to k $\delta(t)$, and the response of the system to F(t) would be (using the second property stated above)

$$\int_{o}^{\infty} F(t-\lambda)k\delta(\lambda)d\lambda = k\ F\ (t) \tag{2.5}$$

a trivial result.

The distortion which occurs in the detector is due to two causes. (1) The scintillator decays according to the law $e^{-t/\tau}$. That is, after a γ-ray is absorbed in an element of volume of the scintillator, low energy photons are emitted at a rate proportional to $\epsilon^{-t/\tau}$. (2) There is distortion due to variable lengths of paths taken by γ-rays, low energy photons and electrical waves in the detector.

These two kinds of distortion can be considered separately and then combined in the following manner. Suppose the scintillator is assumed to decay instantaneously ($\tau = 0$) and the response to $\delta(t)$ is calculated and found to be $f_1(t)$. This result could then be used to find the response to $\delta(t)$ for <u>finite</u> τ in the following way.

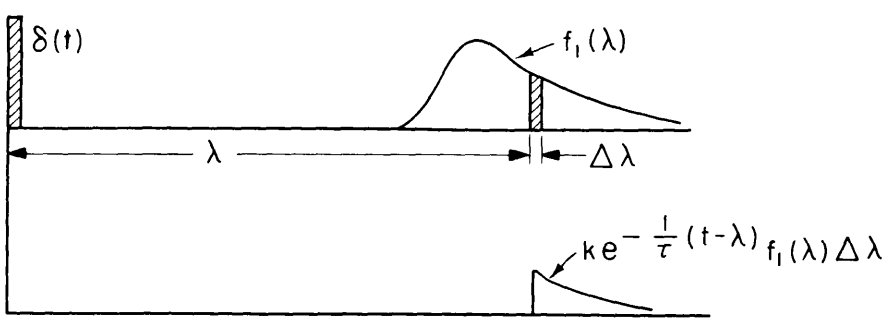

The small shaded area in the above figure contains the energy $f_1(\lambda)d\lambda$. Due to the finite decay time of the scintillator it is "smeared out" in the time as $ke^{-1/\tau(t-\lambda)}$. At time t the contributions from all previous times must be added up. So the total response is

$$f(t) = k\int_{o}^{t} e^{-\frac{1}{\tau}(t-\lambda)}\ f_1\ (\lambda)\ d\lambda$$

$$= k\ e^{-\frac{1}{\tau}} \int_{o}^{t} e^{-\frac{1}{\tau}}\ f_1\ (\lambda)\ d\lambda \tag{2.6}$$

The procedure for calculating the response of the detector to an arbitrary signal (γ-ray intensity) is then seen to be the following. (1) The finite decay time of the scintillator is neglected and $f_1(t)$, the response of the detector to a δ - function is calculated. (2) Equation 2.6 is used to calculate $f(t)$, the response of the detector to a δ-function when the finite decay time of the scintillator is taken into account. (3) $f(t)$ is then used in equation 2.2 or equation 2.3 to calculate the response to the arbitrary function $F(t)$.

The function $f_1(t)$, discussed in Appendix A, depends on the geometry of the detector, the termination of the detector and the orientation of the detector with respect to the source of radiation. In the following sections the results of Appendix A will be used to calculate the response of the detector to a signal of the form $Ce^{\alpha t}$ by the procedure outlined above.

2.3 Detector Response - Case 1, Detector Terminated in its Characteristic Impedance with the Axis of the Detector Pointing at the Source of Radiation

It is shown in Appendix A that when the axis of the detector is pointing towards the source of radiation and the detector is terminated in its characteristic impedance so that no reflection occurs from the end nearest the source, $f_1(t)$ may be approximated by the function

$$f_1(t) = \begin{cases} 0 & t < a \\ A\left[e^{-\frac{1}{\tau_1}(t-a)} - e^{-\frac{1}{\tau_2}(t-a)}\right] & t > a. \end{cases} \tag{2.7}$$

Where $\tau_1 = 0.137 \times 10^{-9}$ sec

$\tau_2 = 0.130 \times 10^{-9}$ sec.

This function is plotted in Fig. 35. Constants A and a do not occur in the final result so their values are of no importance. Using equation 2.6

$$f(t) = \begin{cases} 0 & t < a \\ A\,k\left\{\frac{\tau\tau_1}{\tau_1-\tau}\left[e^{-\frac{1}{\tau_1}(t-a)} - e^{-\frac{1}{\tau}(t-a)}\right]\right. \\ \left. - \frac{\tau\tau_2}{\tau_2-\tau}\left[e^{-\frac{1}{\tau_2}(t-a)} - e^{-\frac{1}{\tau}(t-a)}\right]\right. & t > a \end{cases} \tag{2.8}$$

This can now be used to calculate the response of the detector to a γ-ray intensity of the form $Ce^{\alpha t}$. By equation 2.3 it is

$$I_{o_{Ce^{\alpha t}}} = \int_0^\infty Ce^{\alpha(t-\lambda)} f(\lambda)\, d\lambda$$

$$= Ak\, Ce^{\alpha\tau} \frac{\tau(\tau_1-\tau_2)}{(1+\alpha\tau_1)(1+\alpha\tau_2)(1+\alpha\tau)} e^{-\alpha a}. \tag{2.9}$$

The response to a constant unit γ-ray intensity, obtained by setting $C = 1$, $\alpha = 0$ is

$$I_o(\text{unit}) = kA\tau\ (\tau_1 - \tau_2)$$

Since the quantity I_0(unit) is susceptable to experimental measurement, it is convenient to express the detector response in terms of it. Then

$$I_{o_{(Ce^{\alpha t})}} = Ce^{\alpha(t-a)} \quad \frac{1}{(1+\alpha\tau_1)(1+\alpha\tau_2)(1+\alpha\tau)} I_o(\text{unit}). \tag{2.10}$$

It is seen that the response has the same exponential form as the signal but is delayed by the time a and reduced in amplitude by the factor

$$\frac{1}{(1+\alpha\tau_1)(1+\alpha\tau_2)(1+\alpha\tau)}$$

called the sensitivity reduction factor for the detector. Figure 2 shows a plot of this function. Its value is given in the table below for several values of α using $\tau = 2 \times 10^{-9}$ sec for the decay time of the terphenyl-toluene scintillator.[3]

α (sec^{-1})	$\frac{1}{(1+\alpha\tau_1)\ (1+\alpha\tau_2)\ (1+\alpha\tau)}$
0	1
2×10^8	0.679
5×10^8	0.440
10×10^8	0.260
15×10^8	0.174
20×10^8	0.125
25×10^8	0.0935
30×10^8	0.0729

2.4 Detector Response - Case 2, Open Circuited Detector with the Axis of the Detector Pointing at the Source of Radiation

In Section A.2 of Appendix A, $f_1(t)$ is calculated for the case in which the end of the detector nearest the source of radiation is open circuited so that complete reflection occurs. It is found that

$$f_1(t) = R_1(t) + R_2(t) \tag{2.11}$$

where

$$R_1(t) = \begin{cases} o & \text{for} \quad t < 0 \\ A\left[e^{-\frac{1}{\tau_1}(t-a)} - e^{-\frac{1}{\tau_2}(t-a)}\right] & , \ t > \alpha \end{cases}$$

$$R_2(t) = \begin{cases} 0, & t < a \\ Ke^{-\frac{\beta c}{2}(t-a)}, & a < t < b \\ 0, & t < b \end{cases}$$

[3] S. H. Liebson, "Temperature Effects in Organic Fluors," Nucleonics, Vol. 10, No. 7, July 1952

and

$$A = \frac{1}{2(\tau_1 - \tau_2)}$$

$$K = \frac{\beta c}{4\left[1 - e^{-(\beta c/2)(b-a)}\right]}$$

$$\tau_1 = 0.1357 \times 10^{-9} \text{ sec.}$$

$$\tau_2 = 0.130 \times 10^{-9} \text{ sec.}$$

$$a = 1.1 \times 10^{-9} \text{ sec.}$$

$$b = 2.3 \times 10^{-9} \text{ sec.}$$

$$\beta = 0.042 \text{ cm}^{-1}$$

$$c = 3 \times 10^{10} \text{ cm/sec.}$$

The procedure used in the preceding section may be used to calculate the sensitivity reduction factor below.

$$\frac{1}{(1+\alpha\tau)}\left[\frac{1}{2(1+\alpha\tau_1)(1+\alpha\tau_2)} + \frac{\beta c}{4(\alpha+\frac{\beta c}{2})}\;\frac{\left[1-e^{-(\alpha+\frac{\beta c}{2})(b-a)}\right]}{\left[1-e^{-\frac{\beta c}{2}(b-a)}\right]}\right] \tag{2.12}$$

The value of this factor is given for several values of α in the following table and Fig. 2 shows a plot of the function.

α (sec^{-1})	Sensitivity Reduction Factor
0	1.0
2×10^8	0.664
5×10^8	.405
10×10^8	.235
15×10^8	.153
20×10^8	.106
25×10^8	.0785
30×10^8	.0602

2.5 Detector Response - Case 3, Open Circuited Detector with the Radiation Entering from the Side.

In Section A.3 of Appendix A, $f_1(t)$ is calculated for the case in which the radiation enters an open circuited detector from the side. This function is plotted in Figure 36. It is seen that $f_1(t)$ may be approximated by the function

$$f(t) = \begin{cases} 0 & t < 0 \\ \dfrac{t}{a} & 0 < t < a \\ 1 & a < t < b \\ \dfrac{c-t}{c-b} & b < t < c \\ 0 & t > c \end{cases} \tag{2.13}$$

Where $a = 0.53 \times 10^{-9}$ sec.

$b = 1.2 \times 10^{-9}$ sec.

$c = 1.73 \times 10^{-9}$ sec.

Using this function the sensitivity reduction factor is found to be

$$\frac{(1-e^{-\alpha a})}{ab\alpha^2} \frac{(1-e^{-\alpha b})}{(1+\alpha\tau)} \tag{2.14}$$

The value of this factor is given for several values of α in the table below. Figure 2 shows a plot of the function.

α (sec^{-1})	Sensitivity Reduction Factor
0	1.0
2×10^8	0.604
5×10^8	.336
10×10^8	.151
15×10^8	.0804
20×10^8	.0468
25×10^8	.0292
30×10^8	.0194

2.6 Summary

This section has evaluated the sensitivity reduction factor, for various orientations of the detector during the time that alpha is constant. From Figure 2 it is seen that the detector should be irradiated from the end in order to obtain maximum output, especially for high values of alpha. Some improvement in relative response is obtained by terminating the detector at the end opposite the transmission line. However this gain is offset by the fact that the steady state response of the open circuited detector is twice that of the terminated detector.

SECTION 3 - TRANSMISSION LINES

3.1 Introduction

It is necessary to employ transmission lines in the recording system to carry the signals from the detectors to the indicators. Since these signals are usually contained in a wide frequency spectrum it is necessary to use a high quality transmission line. Coaxial lines are most suitable for such an application because they have good frequency response characteristics, are well shielded electrically, and have good mechanical properties. These lines are intended to produce a minimum effect upon the signal, but to properly design a recording system it is necessary to know what effects they do produce. In general, it also is necessary to know what these effects are in order to determine the actual input signal from a recorded output signal.

One effect which may be present is ionization in the cable produced by gamma radiation. This can be eliminated by properly shielding the lines from the radiation. Line losses produce other effects. If these losses were independent of frequency the only result would be signal attenuation. However, since they include frequency dependent effects the result is, in general, a distortion of the signal.

Other effects may be produced by discontinuities in the transmission line due to supporting insulators or to variations in cable impedance.[4] These can be minimized by proper cable design and installation.

The cable loss effects are due mainly to the fact that the electromagnetic waves do not penetrate the conductors completely but are confined to a "skin" whose effective depth varies with frequency according to the relation

$$d = \frac{1}{\sqrt{\pi f \mu \sigma}} \quad \text{meters} \tag{3.1}$$

where f = frequency

μ = conductor permeability

σ = conductor conductivity

This results in a variation in both resistance and inductance of the cable with frequency. These are the effects to be evaluated in determining the response characteristics of the lines.

3.2 General Response Characteristics

The current I, on a transmission line must obey the so-called "telegraphers equation"

$$\frac{\partial^2 I}{\partial z^2} - LC \frac{\partial^2 I}{\partial t^2} - (LG + RC) \frac{\partial I}{\partial t} - RG\, I = 0 \tag{3.2}$$

where

L = inductance per unit length,

C = capacitance per unit length,

[4] "Greenhouse Final Report," NRL Report 3978, Vol V

R = resistance per unit length,

G = shunt conductance per unit length.

There is a similar equation for the voltage.

An approximate solution of this equation will be obtained for a sinusoidal current of frequency ω; then by using a Fourier integral (i.e., by superimposing currents of different frequencies) the current at any point of the line when the input current is a δ-function will be calculated. This result can then be used to calculate the response to an arbitrary input current.

If the current depends on the time only, through the factor $e^{i\omega t}$, the above equation may be written

$$\frac{\partial^2 I}{\partial z^2} = (R + i\,\omega L)(G + i\,\omega C)\, I. \tag{3.3}$$

This has the solution

$$I(z,t) = I_o e^{\,i(\omega t - kz)} \tag{3.4}$$

where

$$k = \sqrt{(R + i\,\omega L)\,(G + i\,\omega C)}. \tag{3.5}$$

For an air dielectric coaxial transmission line G is usually negligibly small. This assumption cannot be made with solid dielectric lines.

As stated above both the resistance and the inductance are functions of frequency. The analysis of this effect is quite complicated, involving the solution of Maxwell's equations inside the cable. This problem has been solved approximately by Stratton.[5] For a good conductor he finds that

$$R = \frac{1}{\sqrt{4\pi}}\,\frac{f\mu_1}{\sigma_1}\left(\frac{1}{a_1} + \frac{1}{a_2}\right) \quad \text{ohms/meter} \tag{3.6}$$

$$L = \frac{\mu_2}{2\pi}\left[\ln\frac{a_2}{a_1} + \frac{1}{\sqrt{4\pi}}\,\frac{1}{\mu_2}\sqrt{\frac{\mu_1}{f\sigma_1}}\left(\frac{1}{a_1} + \frac{1}{a_2}\right)\right] \quad \frac{\text{Henrys}}{\text{Meter}} \tag{3.7}$$

and

$$C = \frac{2\pi\epsilon_2}{\ln\left(\frac{a_2}{a_1}\right)} \quad \text{Farads/meter} \tag{3.8}$$

where a_1 = Radius of inner conductor

a_2 = Radius of outer conductor

f = frequency

[5] J. A. Stratton, Electromagnetic Theory, Page 545

σ_1 = conductivity of conductors

μ_1 = Permeability of conductors

μ_2 = Permeability of dielectric

ϵ_2 = Permittivity of dielectric.

It is seen that L may be separated into two parts, L_1 and L_2 where L_1 is independent of frequency and L_2 is a function of frequency. Equation (3.5) may then be written as

$$k = \sqrt{-\omega^2 L_1 C - \omega^2 L_2 C + i\,\omega\, R\, C}$$

$$= i\omega\sqrt{L_1 C}\left[1 + \frac{\omega^2 L_2 C - i\,\omega\, R\, C}{\omega^2 L_1 C}\right]^{1/2}. \tag{3.9}$$

Because the second term inside the bracket is much less than unity the expression may be expanded and only the first two terms of the expansion retained.

Then

$$k \cong i\,\omega\sqrt{L_1 C} + \frac{1}{2}\sqrt{\frac{C}{L_1}}(R + i\,\omega\, L_2) \tag{3.10}$$

Using the values of R, L, and C found by Stratton this becomes

$$k \cong i\,\frac{\omega}{v} + K\sqrt{i\,\omega} \tag{3.11}$$

where

$$v = \frac{1}{\sqrt{L_1 C}} = \frac{1}{\sqrt{\mu_2 e_2}}$$

and

$$K = \frac{1}{2}\sqrt{\frac{\epsilon_2 \mu_1}{\sigma_1 \mu_2}}\left(\frac{1}{a_1} + \frac{1}{a_2}\right)\frac{1}{\ln\frac{a_2}{a_1}}$$

$$(a_2/a_1 = 2.36 \text{ for } Z_o = 51.5 \text{ ohms})$$

For air dielectric (dielectric constant of unity) and copper conductors

$$\mu_1 = \mu_2$$

$$\epsilon_2 = \epsilon_o = 8.854\times10^{-12} \text{ Farads/meter}$$

and

$$\sigma_1 = 5.8\times10^{7} \text{ Mho/meter}$$

from which $K = (0.765 \times 10^{-9})/a_2$, where a_2 is the radius of the outer conductor. Then from equation (3.4) the current is

$$I(z,t) = I_o e^{i\omega(t-\frac{z}{v})} e^{-Kz\sqrt{i\omega}} \tag{3.12}$$

By the Fourier integral theorem the current due to an arbitrary input may be written as

$$I(z,t) = \frac{1}{\sqrt{2\pi}} \int_{-\infty}^{+\infty} \bar{I}(\omega) e^{i\omega(t-\frac{z}{v})} \epsilon^{-Kz\sqrt{i\omega}} d\omega \tag{3.13}$$

3.3 Delta Function Response

The response of the transmission line to a delta or impulse function will first be determined. This will form the basis for the analysis of the response to any other driving function. For the δ-function input, equation 3.13 becomes

$$\delta(t) = \frac{1}{\sqrt{2\pi}} \int_{-\infty}^{+\infty} \bar{I}(\omega) e^{i\omega t} d\omega \tag{3.14}$$

where $I(o,t) = \delta(t)$

The inverse transform is

$$\bar{I}(\omega) = \frac{1}{\sqrt{2\pi}} \int_{-\infty}^{+\infty} \delta(t) e^{-i\omega t} dt \tag{3.15}$$

$$= \frac{1}{\sqrt{2\pi}}$$

which combined with equation (3.13) gives

$$I(z,t) = \frac{1}{2\pi} \int_{-\infty}^{+\infty} e^{i\omega(t-\frac{z}{v})} e^{-Kz\sqrt{i\omega}} d\omega \tag{3.16}$$

Making the substitution

$$t' = t - \frac{z}{v}$$

$$p = i\omega$$

in equation 3.16

$$I(z,t') = \frac{1}{2\pi i}\int_{-i\infty}^{+i\infty} e^{pt'}\, e^{-Kz\sqrt{p}}\, dp \tag{3.17}$$

$I(z,t')$ is just the inverse Laplace transform of $\epsilon^{-kz\sqrt{p}}$. This is given below:

$$I(z,t) = \begin{cases} 0 & \text{for } t < \frac{z}{v} \\ \dfrac{Kz}{2\sqrt{\pi}(t-\frac{z}{v})^{3/2}}\, e^{-\frac{K^2z^2}{4\left(t-\frac{z}{v}\right)}} & \text{for } t > \frac{z}{v}. \end{cases} \tag{3.18}$$

Then, the response to the impulse function, R_I (t), is

$$R_I(t') = \sqrt{\frac{\tau}{\pi}}\left(\frac{1}{t'}\right)^{3/2} e^{-\tau/t'} \text{ where } \tau = \frac{K^2z^2}{4} \text{ and } t' = t-\frac{z}{v}. \tag{3.19}$$

This is the current in the cable due to a δ-function input current and may be used to calculate the response to any input current S(t) from

$$R(t) = \int_{-\infty}^{t} S(\lambda)R_I(t-\lambda)d\lambda$$

or (3.20)

$$R(t) = \int_{o}^{\infty} S(t-\lambda)R_I(\lambda)d\lambda.$$

In the expression for the current response to the δ-function it will be noted that time t′ is as measured at the output end of the cable. The quantity τ has the dimensions of time and corresponds to a "time constant" for the cable. In order to obtain a plot of the function it is desirable to be able to express time in terms of this time constant. Therefore the expression

$$R_I^*(t') = \frac{1}{\sqrt{\pi}}\left(\frac{\tau}{t}\right)^{3/2} e^{-\frac{\tau}{t}} \tag{3.21}$$

is plotted in Fig. 3. For any particular cable length, or "time constant,"

$$R_I(t') = \frac{R^*(t')}{\tau}. \tag{3.22}$$

The factor τ is of considerable interest since it determines the response characteristics of the line. In Figure 4, τ/z^2 is plotted against the radius a_2, with points shown for commonly used transmission lines. Thus for a line having a nominal 7/8 inch diameter and 1000 ft. long, τ is seen to be $130 \times (1000)^2 \times 10^{-18} = 1.3 \times 10^{-10}$ sec.

3.4 Exponential Function Response

Of particular interest in weapons testing applications is the response to a signal whose amplitude increases exponentially with time. For times of interest the signal current can be expressed as

$$I = I_o e^{\alpha t}. \tag{3.23}$$

Thus, if the input current $S(t) = e^{\alpha t}$, from Equation 3.20

$$R(t) = \int_0^\infty e^{\alpha(t-\lambda)} \frac{Kz}{2\pi(\lambda-\frac{z}{v})^{3/2}} e^{-\frac{Kz^2}{4(\lambda-\frac{z}{v})}} d\lambda. \tag{3.24}$$

The result of integrating this expression is

$$R(t) = e^{\alpha(t-z/v)} - Kz\sqrt{\alpha} \tag{3.25}$$

or

$$R(t) = e^{\alpha t'} - Kz\sqrt{\alpha} \quad \text{where } t' = t-z/v.$$

The details of the integration are omitted since this result can be simply obtained by replacing $i\omega$ by α in equation (3.12).

The factor

$$e^{-Kz\sqrt{\alpha}} = e^{-2\sqrt{\alpha\tau}} \tag{3.26}$$

is the attenuation factor for exponential inputs. Since

$$e^{-Kz\sqrt{i\omega}} = e^{-Kz\sqrt{\omega}\left(\frac{1+i}{\sqrt{2}}\right)} \tag{3.27}$$

the attenuation factor for sinusoidal inputs is

$$e^{-Kz\sqrt{\frac{\omega}{2}}}. \tag{3.28}$$

The attenuation of an increasing exponential function is seen to be equal to the attenuation of a sine wave of equivalent frequency

$$\omega = 2\alpha \qquad \text{(radians/sec)} \tag{3.29}$$

or

$$F_{eq.} = \frac{2\alpha}{2\pi} = \frac{\alpha}{\pi} \qquad \text{(cycles/sec)} \tag{3.30}$$

The factor $e^{-\alpha z/v}$ is the time delay factor which is a function of the cable length z. It is obvious that the effect of the cable has been to delay the exponential and reduce its amplitude, but that it has not affected the parameter "alpha" itself. Thus, if the input signal were

to continue increasing indefinitely with a constant value of alpha the output signal would reach any desired amplitude. However, because the input signal rises exponentially over only a limited range and because it is generally desired to make measurements at the lowest reaction level possible, transmission line losses are undesirable. It should be noted here that any change in alpha, or departure from the exponential form, requires a further analysis of the response.

3.5 Step Function Response

If the input current, S(t), is a step function

$$S(t) = \begin{cases} o & t < o \\ 1 & t > o \end{cases} . \tag{3.31}$$

The response to S(t) is

$$\begin{aligned} R(t) &= \int_{-\infty}^{t} S(\lambda) R_I(t-\lambda) d\lambda \\ &= \int_{o}^{\infty} S(t-\lambda) R_I(\lambda) d\lambda \\ &= \int_{o}^{t} R_I(\lambda) d\lambda . \end{aligned} \tag{3.32}$$

Since $S(t - \lambda) = 1$ For $t > \lambda > 0$
and $S(t - \lambda) = 0$ For $\lambda > t$.

Hence the response to the step function is found by integrating the response to the impulse function in Equation (3.18). Since

$$R_I(t) = \begin{cases} 0 \quad \text{for } t < \frac{z}{v} \\ \frac{Kz}{2\sqrt{\pi}\,(t-\frac{z}{v})^{3/2}} \; e^{-\frac{Kz^2}{4(t-z/v)}} \quad \text{for } t > \frac{z}{v} \end{cases} \tag{3.33}$$

$$R(t) = \frac{Kz}{2\sqrt{\pi}} \int_{\frac{z}{v}}^{t} \frac{e^{-\frac{K^2 z^2}{4(\lambda-\frac{z}{v})}}}{(\lambda-\frac{z}{v})^{3/2}} d\lambda \quad \text{for } t > \frac{z}{v} . \tag{3.34}$$

By letting

$$y = \frac{Kz}{2(\lambda - \frac{z}{v})^{1/2}}$$

the limits of the integration are

$$y = \frac{Kz}{2(t - \frac{z}{v})^{1/2}}$$

$$y = \infty$$

which gives

$$R(t) = \frac{2}{\sqrt{\pi}} \int_{\frac{Kz}{2\sqrt{t-\frac{z}{v}}}}^{\infty} e^{-y^2} dy \tag{3.35}$$

$$= \frac{2}{\sqrt{\pi}} \int_{o}^{\infty} e^{-y^2} dy - \frac{2}{\sqrt{\pi}} \int_{o}^{\frac{Kz}{2\sqrt{t-\frac{z}{v}}}} e^{-y^2} dy$$

$$= 1 - \operatorname{erf} \frac{Kz}{2\sqrt{t-\frac{z}{v}}} \tag{3.36}$$

$$= \operatorname{erfc} \frac{Kz}{2\sqrt{t-\frac{z}{v}}} = \operatorname{erfc} \sqrt{\frac{\tau}{t'}}$$

where

$$\tau = \frac{K^2 z^2}{4}.$$

$$t' = t - \frac{z}{v}.$$

The response of a transmission line to a step function is shown in Figure 5. Amplitude is plotted as a function of time, in terms of the time constant of the line. The characteristic long tail of the complementary error function as the argument approaches zero, or as t'/τ approaches infinity, results in an output current which requires many time constants to approach unity. Consider the previous case of a 7/8 inch transmission line, 1000 feet long, with a step function input. The time required for the output to reach 95% of the input is found, from Figure 5 to be $t/\tau = 500$. From Figure 4, $\tau = 1.1 \times 10^{-10}$ and $t = 500 \times 1.3 \times 10^{-10} = 65 \times 10^{-9}$ or 65 ns. If 3 1/8 inch line had been used: $\tau = 9.1 \times 10^{-12}$ and $t = 4.5 \times 10^{-9}$ or 4.5 ns.

It is of interest to note that the response at 10 time constants ($t' = 10\,\tau$) is approximately 65%. The response of a simple RC circuit is 65% at one time constant.

3.6 Response to Other Driving Functions

The response to the sinusoidal function, the impulse function, the exponential and the step function have been obtained by direct integration. In general, the response to other driving functions must be obtained indirectly by a graphical evaluation of the superposition integral. Appendix B shows response curves for various other functions and explains their use.

Of particular interest is the response to the ramp function. In the experimental determination of the response characteristics of a transmission system it is frequently most convenient to send a fast rising pulse through the system and record the shape of the pulse at the input and output of the system. Ideally this would be done with a step function. However, any generated function has a finite rise time. Thus, the simplest approximation to the input pulse may be the ramp function. Appendix B gives the response to the ramp function for a rather limited range in rise time and line lengths. However in many cases the response to the ramp function can be determined from the theoretical step function and impulse function response curves. By using this approximation, whenever valid, the analysis is made much simpler.

The difference between the unit step function and the ramp function (of unit height) is a triangular function of unit value at zero time and of zero values at time T, the ramp function rise time. Since the system is linear, the response to the unit step exceeds the response to the ramp by the response to the triangular function just described. It is clear then that for large values of time the ramp function response is approximately equal to the unit step response since the response to the triangular function approaches zero with increasing time.

For any time t' which is less than $2/3\,\tau$ or greater than $T + 2/3\,\tau$ the response to the triangular function will lie between the response to a Dirac impulse function acting at time $t' = 0$ and a Dirac impulse function acting at time $t' = T$, with the additional stipulation that these impulses are taken to have area $1/2\ T$, the area of this triangular function, instead of the usual area 1.0. The response to this impulse acting at time zero is, from Equation 3.21,

$$R = \frac{1}{2}\frac{T}{\tau}\frac{1}{\sqrt{\pi}}\left(\frac{\tau}{t'}\right)^{3/2} e^{-\tau/t'} \tag{3.37}$$

and the response to the impulse acting at time T is given by

$$R = \frac{1}{2}\frac{T}{\tau}\frac{1}{\sqrt{\pi}}\ (\tau/t'-T)^{3/2}\ e^{-\tau/t'-T}. \tag{3.38}$$

Figure 3 is a plot of this function, except for the factor $1/2\ T/\tau$. For times between $2/3\,\tau$ and $T + 2/3\,\tau$ the response is fairly well approximated by the difference in the response to the step function and the Dirac function acting at $t = 0$.

Comparison of the response to the step function and the ramp function for large times, t', shows that the difference between the responses is represented more nearly by the response to an impulse function occurring at time zero than to an impulse function occurring at time T, as would be expected. Therefore a very good approximation for large time is

$$\text{Ramp Response} = \text{Step response} - (\text{Impulse response}^* \times T/(2\tau))$$

It is obvious that if the cable time constant, τ, is much larger than the rise time T, the ramp response becomes approximately the same as the step response. It is also obvious that the ramp response is approximately the same as the step response for large values of time since the impulse response becomes smaller with increasing time. The step response may be used for the ramp response when $t'/\tau > 10$ and $t'/T > 10$, or when $t'/\tau > 1$ and $t'/T > 100$. The impulse correction should be used for shorter times.

3.7 Solid-Dielectric Lines

The preceding analysis has assumed a transmission line with a lossless dielectric between the inner and outer conductors. In the case of a line with solid dielectric, such as the polyethylene dielectric flexible cables, this assumption is not valid and the results are not directly applicable. Unfortunately it is impossible to obtain similar solutions for this case because the dielectric has a loss factor which varies with frequency. Since the resulting equations cannot be solved directly, graphical solutions are required.

An approximate response characteristic can be obtained from the measured attenuation of a solid dielectric line. From Equation 3.12 the real part of the attenuation factor is

$$e^{-Kz\sqrt{\omega/2}}$$

and the attenuation per unit length is

$$K\sqrt{\omega/2} \text{ nepers/meters.}$$

For air dielectric lines the measured attenuation is found to correspond to this calculated value. For solid dielectric lines the calculated value is not correct since it does not take the dielectric loss into account. It is found from measurements that the attenuation can be expressed approximately as

$$K_1(f)^n$$

where f is the frequency and where n in general is not 1/2, and K_1 is not equal to K. However, if the previously derived response functions are to be used n must be taken as 1/2. Then, over a limited frequency the measured attenuation can be approximated by

$$K_2\sqrt{f}.$$

Thus a value for K_2 can be determined from the measured attenuation characteristics, which can be substituted for K in the various response functions to determine the response of the solid dielectric line over a limited frequency range. In order to determine K_2 it is necessary to determine the frequency spectrum of the driving function. In general for most functions there is an upper frequency below which most of the energy is being contained. If the attenuation can be approximated by $K\sqrt{f}$ in this range an approximate value of τ can be determined, from which the response can then be calculated.

For an exponential driving function an analysis of the frequency spectrum indicates that it is reasonable to match the attenuation at $f = \alpha/\pi$. Consider the response of 1000 ft. of solid dielectric RG-17/U cable to an exponential with $\alpha = 2 \times 10^8$. The measured attenuation at the equivalent frequency of 63.5 mc is approximately 0.7 db/100 ft. From Equation 3.28, the attenuation factor is

*From Figure 3

$$e^{-K_2 \sqrt{\alpha/2}}.$$

Then the attenuation is $K\sqrt{\pi f}$ nepers/meter

or $$4.7\times10^2 \; K\sqrt{f} \quad \text{db/100 ft.}$$

and $$K = \frac{0.7}{4.7\times10^2 \sqrt{63.5\times10^6}} = 1.87\times10^{-7}$$

From the expression for τ, equation 2.33 and for z = 1000 ft (305 meters)

$$\tau = \frac{K^2 z^2}{4} = \frac{(1.87\times10^{-7}\times305)^2}{4} = 8.1\times10^{-10} \text{ sec.}$$

From equation 3.26 the relative response is

$$e^{-2\sqrt{2\times10^8\times8.1\times10^{-10}}} = e^{-0.804} = 0.45$$

which corresponds to the measured attenuation of 0.7 db per 100 ft. Thus in 1000 ft. of RG-17/U the exponential signal is reduced to 45% of its original amplitude.

It is of interest to consider this same transmission line with a ramp function input having a rise time, T, of 1 x 10^{-9} seconds. From a Fourier analysis of the ramp function it can be shown that the major components of the signal are frequencies below the reciprocal of the rise time. Thus in this example $f_{max} = 1/10^{-9} = 1000$ mc/s. An examination of the attenuation characteristics of RG-17/U shows that the attenuation can be approximated by $K_2\sqrt{f}$ where K_2 is chosen to match the measured attenuation at 400 mc/s. The resulting calculated attenuation will be higher than the measured for frequencies below 400 mc and somewhat lower in the 400 to 1000 mc range. The measured attenuation at 400 mc is about 2.4 db/100 ft.

Then $$K = \frac{2.4}{4.7\times10^2 \sqrt{4\times10^8}} = 2.55\times10^{-7}$$

and $$\tau = \frac{(2.55\times10^{-7} \times 305)^2}{4} = 1.5\times10^{-9} \text{ sec.}$$

Then $\tau/T = 1.5$, which corresponds to $\sqrt{1.5 \times 400} = 24.5$ unit lengths.

The ramp function response is discussed in Appendix B. The largest value plotted in Figure 37 is 10 unit lengths. However, from Section 3.6 it is seen that the response corresponds approximately to the step function response for $t'/T > 10$ or $t' > 15 \times 10^{-9}$ sec. At times less than this the response is approximated by the difference between the response to a step function and a modified impulse function.

For a line length of 400 ft. $\tau = 0.24 \times 10^{-9}$ and $\tau/T = 0.24$. The response would then correspond to curve 10 of Figure 37.

The response of solid dielectric lines is complicated by a tendency to periodic variations in impedance along their length as a result of manufacturing processes. This results in a signal loss due to reflection as well as the attenuation loss. Also there is a rapid increase in attenuation above about 3000 megacycles because the braided outer conductor no longer acts as a continuous surface.

3.8 Limitations due to Higher Modes

In the analysis presented it has been assumed that the coaxial lines were excited only in the T E M mode. It is possible to excite other modes at higher frequencies which can absorb the energy at these frequencies. The principal interfering higher order mode is the T $E_{1,1}$ mode which is excited only by frequencies above $f_c = (3 \times 10^{10}) / [(r_1 + r_2)]$ where r_1 and r_2 are the radii of the inner and outer conductors. The largest line considered here is the 3 1/8 inch line. For this line

$$f_c = \frac{3 \times 10^{10}}{\pi\,(0.65 + 1.51)(2.54)} = 1.74 \times 10^9.$$

Thus the higher order modes will not be excited below about 1740 mc in the 3 1/8 inch line.

Since it appears that most of the energy in the exponential signal is contained in frequencies below $f = \alpha/\pi$ it seems reasonable to assume that absorption of energy by higher order modes will not be significant for values of alpha below about 50×10^8 and hence should present no problem. Again, for a ramp function rising in 1×10^{-9} seconds most of the energy is contained in frequencies below $f = 1/T = 10^9$, or 1000 mc. Hence it would appear that there should be no problem for pulses with this rise time.

SECTION 4 - AMPLIFIERS

4.1 Introduction

In atomic weapons measurements it is desirable to cover an extremely wide range of signal levels in order to obtain the maximum amount of information. Because of the accuracy requirements of the over-all system and voltage overload problems with various components, there is a limit to the dynamic range which can be recorded by each complete system unit. However, wide range coverage can be obtained by means of a number of detectors placed at different distances from the weapon (or a number of detectors of different sensitivities placed at the same location) each connected through a transmission line to a recording system. Efficiency and economy is obtained by using as wide a range of coverage as possible from each detector-transmission line combination.

For a given cathode-ray tube in the recording system a certain range of signal levels is recorded when displayed directly on the tube. Some variation in this range can be obtained by using different types of cathode-ray tubes. Signals of higher level than that required to provide maximum trace deflection can be recorded by attenuating the signals while signal levels below that required for maximum deflection require the use of signal amplifiers. One function of amplifiers is to raise the voltage level of exponential signals so that lower reaction levels can be investigated. Because this should be accomplished with minimum distortion of the signal there must be minimum amplitude distortion over the field of the cathode-ray tube and minimum frequency distortion at the frequencies required to pass that particular exponential. Thus, amplifier design must consider the cathode-ray tube which will be used (which determines the amount of linear output voltage needed), the magnitude of the available input voltage (which together with the output voltage requirement determines the gain required), and the alpha of the exponential (which determines the frequency range which should be passed by the amplifier).

The design of these amplifiers is based on a knowledge of the response of basic amplifier circuits and other electrical networks to exponential signals. Because there is rather limited information available in the literature on this subject[6,7,8] a fairly complete analysis of these problems is included in this report. In addition, consideration is given to the practical limitations of vacuum tube circuits, the equivalent amplitude-frequency spectrum of an exponential signal, and the effect of amplitude nonlinearity in amplifiers for exponential signals. Certain conclusions regarding the bandwidth necessary to pass an exponential and recommendations for minimizing nonlinearity are given.

The theoretical investigations are supported by actual tests of several amplifiers with three different exponential signals having nominal alphas of 1×10^8, 2.5×10^8, and 5×10^8 per second. Amplifier circuit recommendations are made.

4.2 Network Analysis -

It is shown in Appendix C, "Response of Electrical Networks to Exponential Driving Functions" that a series RLC circuit responds to an exponential driving voltage of the form $Ee^{\alpha t}$ as though the capacitor was an impedance equal to $1/\alpha C$ ohms, the inductance an impedance equal to αL ohms and the resistor a pure resistance equal to R ohms. In other

[6] "Response of Electrical Circuits to Exponential Driving Forces" by Walter H. Weber, LA-1323 Los Alamos Scientific Laboratory, October 1951.

[7] "Greenhouse Final Report" NRL 3974-3978.

[8] "Amplification and Transmission of Exponentially Increasing Signals" by E. Suydam, Los Alamos Scientific Laboratory, LA-670, March 1949.

words, $j\omega$ of the sinusoidal impedance is replaced by α for the exponential impedance. This is a general rule which may be used to determine the performance of a network on exponential signals on the basis of its sinusoidal performance. Therefore, the exponential impedance (Z_e) of a series RLC circuit to an exponential voltage is:

$$Z_e = R + \alpha L + \frac{1}{\alpha C}. \tag{4.1}$$

It will be noted that there are no imaginary terms in this expression and that all terms are positive. Consequently there can be no resonance effects in these circuits and as a result the usual frequency compensating networks are ineffective. The relationships for R, L, and C from Equation 4.1 will be used throughout this report and are the basis for the circuit analysis which follows.

Consider the equivalent circuit of a typical pentode RC coupled vacuum tube stage:

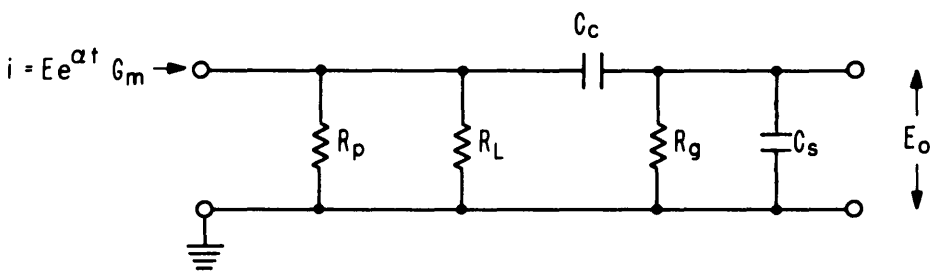

where C_s = The total shunt capacity to ground in this circuit including the output capacity of this stage, stray circuit capacity, and the input capacity of next stage,

C_c = Coupling capacity,

G_m = Mutual conductance of this stage,

R_g = Grid resistor of next stage,

R_p = Dynamic plate resistance of this stage, and

R_L = Plate load resistor.

If

$$R_1 = \frac{R_p R_L}{R_p + R_L}.$$

Then

$$E_o = E\, e^{\alpha t}\, G_m \left[\frac{R_1}{1 + \frac{R_1}{R_g} + \frac{C_s}{C_c} + \alpha R_1 C_s + \frac{1}{\alpha R_g C_c}} \right]. \tag{4.2}$$

Writing

$$\omega_H = \frac{1}{R_1 C_s}.$$

Where ω_H corresponds to the angular frequency at which the high frequency response is down by 3 db from the mid-frequency response and

$$\omega_L = \frac{1}{R_g C_c}.$$

where ω_L corresponds to the angular frequency at which the low frequency response is down by 3 db from the mid-frequency response.

Equation 4.2 reduces to

$$E_o = E\, e^{\alpha t}\left[\frac{G_m R_1}{1 + \frac{R_1}{R_g} + \frac{C_s}{C_c} + \frac{\alpha}{\omega_H} + \frac{\omega_L}{\alpha}}\right]. \tag{4.3}$$

For n such stages in cascade

$$E_o = E\, e^{\alpha t}\left[\frac{G_m R_1}{1 + \frac{R_1}{R_g} + \frac{C_s}{C_c} + \frac{\alpha}{\omega_H} + \frac{\omega_L}{\alpha}}\right]^n. \tag{4.4}$$

It is of interest to note that if the amplifier is of the low pass type ($\omega_L \rightarrow 0$) Equation 4.4 reduces to

$$E_o = Ee^{\alpha t}\left[\frac{G_m R_1}{1 + \frac{\alpha}{\omega_H}}\right]^n \tag{4.5}$$

and if the amplifier is the high pass type ($\omega_H \rightarrow \infty$) Equation 4.4 reduces to

$$E_o = Ee^{\alpha t}\left[\frac{G_m R_1}{1 + \frac{\omega_L}{\alpha}}\right]^n. \tag{4.6}$$

Equation 4.4 is of interest because it indicates that bandwidth is necessary in amplifying an exponential. Limiting either low frequency or high frequency response results in an effective gain reduction which is a function of alpha. It also indicates that the gain of a stage on an exponential signal approaches the familiar $G_m R_1$ as the upper limit. Furthermore, this expression shows that for fixed $G_m R_1$ the gain for a given alpha can be increased by increasing R_g and C_c, and by decreasing C_s since the low frequency cutoff (ω_L), the high frequency cutoff (ω_H), and the C_s/C_c and the R_1/R_g ratios are improved by these changes.

The quantity n (the number of such RC-coupled stages in cascade) appears as the exponent of the gain determining portion of the equation (i.e., the portion of the equation in parenthesis). This portion may be broken down into two basic parts. These are: $G_m R_1$ which is the basic mid-frequency gain of the amplifier, and

$$\left[\frac{1}{1 + \frac{R_1}{R_g} + \frac{C_s}{C_c} + \frac{\alpha}{\omega_H} + \frac{\omega_L}{\alpha}}\right]$$

which is the circuit parameter and alpha sensitive portion, to be called the gain reduction factor (GRF). The value of the GRF never exceeds unity.

Equation 4.4 also shows that for any given ω_H and ω_L there is an optimum alpha (α_M) for which that particular amplifier will give maximum output (i.e., optimum GRF). This optimum alpha is:

$$\alpha_m = \sqrt{\omega_H\, \omega_L}\,. \tag{4.7}$$

However, one should not be misled into thinking that, because there is an optimum alpha for any given ω_H, ω_L condition, that bandwidth can be restricted to obtain maximum output for a given alpha. This is not the case because the output at any alpha is always increased by

extending the passband. A plot of Equation 3, showing the optimum GRF available versus the ratio of high frequency to low frequency cutoff (ω_H/ω_L), is shown in Figure 6.

4.3 Comparison of Amplifier Performance on Exponential, Sinusoidal, and Step Function Signals

Reference to the GRF portion of Equation 4.5 $\left[1/(1+\alpha/\omega_H)\right]^n$ shows that as n increases this factor decreases rapidly in value since the GRF never exceeds unity. This result is not unexpected since the effective 3db cutoff frequency of the amplifier (f_A) on sinusoidal voltages is also decreasing. What is unusual is that if the cutoff frequency is adjusted in each case so that the 3 db point of the over-all amplifier remains constant as n increases there is a continuing reduction in the exponential gain. A plot of the GRF versus ω_H/α for values of n from one to five are shown on Figure 7.

Table 4.1 shows the manner in which the GRF and the stage cutoff frequency ($f_H = (\omega_H/2\pi)$) varies with n for an alpha of 2.5×10^8 and a constant 3 db cutoff frequency (f_A) of 100 mc.

TABLE 4.1

n	f_A	f_H	GRF
1	100 mc	100 mc	.716
2	100	157	.636
3	100	197	.574
4	100	224	.517
5	100	260	.49
6	100	286	.456
7	100	309	.432
8	100	333	.405
9	100	353	.38
10	100	373	.36

It will be noted that the GRF varies by two to one over the range of n from one to ten for an amplifier with the same over-all 3 db cutoff frequency (f_A) of 100 mc. This clearly shows that the GRF on an exponential is a function of the slope of the rolloff curve and that in order to predict the performance of an amplifier on an exponential that both the ω_H and n of the amplifier must be known. The slope of the sinusoidal rolloff curve in db per octave is equal to 6n.

It is also of interest to note at this point (from Appendix D) that the rise time (from 10 to 90%) of an amplifier on a step function is given by the expression:

$$t_{10-90} = \frac{0.35}{f_A} \tag{4.8}$$

where f_A is the over-all amplifier 3 db upper cutoff frequency. It should be noted that n does not appear in this expression. The conclusion to be drawn is that the slope of the sinusoidal rolloff curve is of no significance in the step function rise time case (as defined herein), but that it is of great importance in the case of an exponential signal. Furthermore, it is not possible to predict the performance of an amplifier on an exponential signal solely on the basis of the amplifier rise time. This same argument pertaining to exponential gain as a function of the slope of the rolloff curve holds for the high pass amplifier (Equation 4.6) and the bandpass amplifier (Equation 4.4). Appendix D, "Comparison of Amplifier Performance on Exponential, Sinusoidal, and Step Function Signals" provides a more complete analysis of this problem.

4.4 The Frequency-Amplitude Spectrum of an Exponential

Appendix E describes a method of determining the approximate bandpass requirements of a device intended to pass an exponential signal. This can be accomplished by converting the exponential into an amplitude-frequency spectrum by Fourier analysis. The resultant relative amplitude-frequency spectrum is of the form

$$f(\omega) \sim \frac{1}{\alpha - j\omega} . \tag{4.9}$$

The amplitude of this spectrum increases at the same rate as the original exponential, but the relative amplitude-frequency relationships within the spectrum remain constant with time. A plot of this amplitude-frequency spectrum is shown on Figure 8. The normalized amplitude of the spectrum is shown as Curve A and the phase angle is shown as Curve B, plotted against ω/α.

This amplitude-frequency spectrum makes it appear that the contribution from the components in the range from $\omega = 0$ to $\omega = \alpha$ is more important than that from the components above $\omega = \alpha$. However this curve represents the amplitude of each frequency in the spectrum. In general, devices used to pass the exponential are such that the frequency interval they pass (the bandpass) is proportional to a midfrequency ω_o.

For steady-state sinusoids the resultant voltage from the components within a bandpass interval is the rms sum of these components. Although the components of the exponential are not in such a steady-state condition it is found that for practical cases such a concept is useful. The weighted spectrum showing the contribution from the components in the bandpass interval with midfrequency ω_o is

$$f(\omega_o) \sim \frac{\sqrt{\omega_o}}{\alpha - j\omega_o} \tag{4.10}$$

and the absolute value is

$$\left| f(\omega_o) \right| \sim \sqrt{\frac{\omega_o}{\alpha^2 + \omega_o^2}} . \tag{4.11}$$

This expression for the voltage of each interval versus the ω/α ratio is shown as Curve C on Figure 8. It should be noted that now the maximum amplitude occurs at an angular frequency equal to alpha and that the curve drops off symmetrically both sides of this point (on a frequency proportional or logarithmic plot). The result is that for an amplifier with a one decade passband which can be placed anywhere desired in the frequency spectrum the most efficient operation on an exponential would result when this decade is geometrically centered at an angular frequency equal to alpha. This agrees with the relationships previously developed for optimum alpha (α_M), i.e., $\alpha_M = \sqrt{\omega_H \omega_L}$. The significance here is that frequency proportional intervals spaced geometrically either side of alpha make equal contributions to the exponential. Furthermore, energy contributions beyond a certain number of decades either side of the angular frequency equal to alpha point are of no significance. For example, the relative magnitude of the voltage in the decade at one decade either side of the angular frequency equal to alpha is 0.445, at two decades it is 0.14, and three decades it is 0.0447.

On this basis maximum gain is obtained from an amplifier which is adjusted to give as much gain as possible over the angular frequency range centered on alpha. The uniformity of gain within this range is less important since the exponential gain appears to depend upon the integral of a curve which represents the product of the amplitude response of the amplifier and the amplitude of the weighted spectrum of the exponential. On the other hand the design of wide band pulse amplifiers is based on maintaining uniform gain and phase shift over as wide a range of frequencies as possible in order to pass fast rising flat topped pulses

with minimum distortion. Thus the usual methods of achieving improved performance in wide band pulse amplifiers are not only generally not best for amplifying exponentials but may result in performance that is inferior to that obtained without compensation.

It should be noted that the phase characteristics of the sinusoidal components of the exponential signal as expressed in Equation 4.9 have been lost in Equation 4.11. This method of analysis also neglects the phase characteristics of the networks involved and for that reason yields only an approximate solution to the problem.

4.5 Response of Simple Shunt Fed Amplifier to Exponential Signals

The above condition for maximum gain of an exponential is more nearly satisfied by a simple shunt-fed capacity coupled vacuum tube circuit than by any other circuit utilizing conventional tubes (See Appendix F, "Response of Simple Shunt-Fed Amplifier to Exponential Signals." It is desirable that the impedance of the shunt feed inductance, L, be as large as possible, consistent with minimizing the shunt capacity to ground; that the grid resistor R_g, and the G_m be large; and, of course, that the vacuum tube capacities be small. The equivalent circuit for such a shunt fed amplifier is shown below, together with limiting conditions on the components.

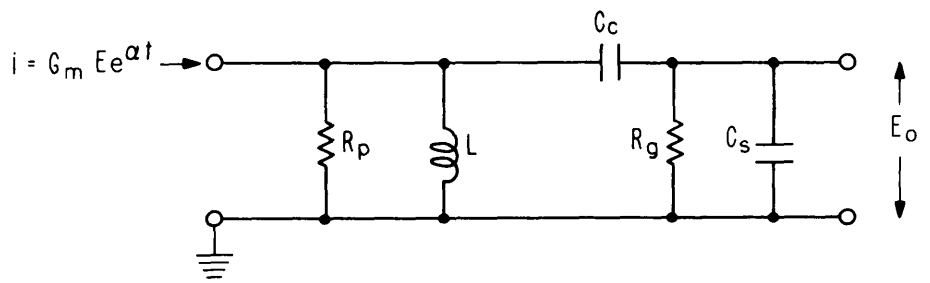

$$L \gg \left(\frac{R_p R_g}{R_p + R_g}\right)\frac{1}{\alpha}, \quad C_c \gg C_s, \quad R_g \gg \frac{1}{\alpha C_c}$$

It was noted previously that the exponential gain was a function of the slope of the sinusoidal rolloff curve and further that the steeper the rolloff the less the gain. This effect in itself prohibits the usual amplifier frequency compensating circuits for use in amplifying exponential signals, and in particular makes the use of distributed amplifiers for this purpose undesirable. If a number of tubes must be used in order to obtain sufficient current to achieve a desired output voltage, they should be placed in parallel with a minimum of isolation between them. Under these conditions the voltage gain from grid to plate will increase with the number of tubes in parallel if the external load resistance is small compared to $1/\alpha\, C_S$. (This is the case for an amplifier working into a traveling wave deflector type cathode-ray tube such as the TW-9.) However, it must also be remembered that the input now consists of several grids in parallel and the voltage on them will be reduced because of the added grid circuit capacitive loading, with a resultant reduction in the over-all gain. On the other hand, if the load impedance is large with respect to $1/\alpha\, C_S$ there is nothing to be gained by paralleling tubes. This is the case for an amplifier working into a conventional electrostatic deflection cathode-ray tube. The grid to plate gain will remain essentially constant, but the grid voltage will decrease (because of the added grid circuit capacitive loading) giving a net gain which is less than that for a single tube. To summarize then, the optimum gain using conventional vacuum tubes is obtained with cascaded shunt-fed capacitively-coupled stages which give as much gain over as wide a frequency range as possible.

If conditions in the above circuit are such that the impedance $1/\alpha C_S$ is the sole controlling factor (i.e., $R_p, \alpha L$, and $R_g >> 1/\alpha C_S$, and $C_c >> C_S$) the circuit reduces to

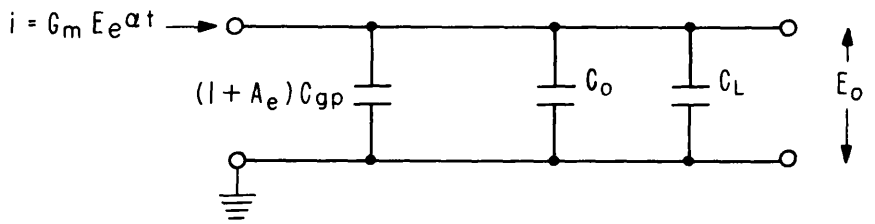

Where: C_L = Input capacity of next stage,

C_o = Plate to screen, cathode and heater capacity,

C_{gp} = Plate to grid capacity, and

A_e = Exponential gain = $G_m/\alpha C_S$

where $C_S = C_L + C_o + (1 + A_e) C_{gp}$.

The exponential gain, A_e, for this circuit is then given by the expression

$$A_e = \frac{-\left[\frac{C_o + C_L + C_{gp}}{C_{gp}}\right] \pm \sqrt{\left[\frac{C_o + C_L + C_{gp}}{C_{gp}}\right]^2 + \frac{4\,G_m}{\alpha\,C_{gp}}}}{2} \tag{4.12}$$

Table 4.2 lists the input, output, and grid-plate capacities, the G_m, and the alpha for which the gain is unity ($\alpha = G_m/C_S$) for several of the best currently available tubes.

TABLE 4.2

Tube Designation	Type	C_o* (mmf.)	C_I* (mmf.)	C_{gp}* (mmf.)	G_m (Micromhos)	α_1 for* unity gain $\alpha_1 = \frac{G_m}{C_o + C_I + G_{gp}}$ x10⁸	α_2 for* unity gain $\alpha_2 = \frac{G_m}{C_o + C_{gp}}$ x10⁸
407-A	(Double (Triode	1.0	2.2	1.3	5,500	12.2	23.9
418-A	Tetrode	2.7	16.0	.05	25,000	13.3	91.0
4X150-A	Tetrode	4.7	16.1	.02	12,000	5.77	24.5
6AH6	Pentode	2.0	10	.03	9,000	7.5	44.3
6AK5	Pentode	2.1	4	.03	5,000	8.1	23.5
6AN5	Pentode	4.8	9	.075	8,000	5.8	16.4
6BC5	Pentode	1.8	6.5	.03	6,000	7.2	32.8
6BK7	(Double (Triode	1.0	3.0	1.9	8,500	14.4	29.3
6CB6	Pentode	1.9	6.5	.02	6,200	7.5	32.3
6CL6	Pentode	5.5	11	.12	11,000	7.0	19.6
12AV7	(Double (Triode	.5	3.1	1.9	8,500	15.4	35.4
12AW6	Pentode	1.5	6.5	.025	5,000	6.2	32.8
12BY7	Pentode	3.0	11.1	.055	12,000	9.1	33.8

* C_o = Plate to cathode, heater, screen grid capacity.
C_I = Grid to cathode, heater, screen grid capacity.
C_{gp} = Grid to plate capacity.
α_1 = The alpha for which one stage will yield unity gain when working into the input capacity of a similar stage.
α_2 = The alpha for which one stage will yield unity gain when working into zero input capacity.

It should be noted that lead inductance and grid conductance have not been taken into consideration in constructing this chart and that both of these effects will result in an alpha lower than that shown for unity gain.

Reference to Table 4.2 shows that it is very difficult to realize any useful gains for an alpha greater than 10×10^8 with cascaded vacuum tube stages. Obviously some other means of amplification must be found for this region if any appreciable gains are to be realized. The traveling wave type amplifier shows some promise for this application. Development tubes have been reported which will work over a frequency range of 100-300 mc and yield a voltage gain of ten. From Equation 4.3 and for an alpha of 10.9×10^8 (α_M)

$$A_e = 10 \left[\frac{1}{1+1.153 + \frac{10.9\times10^8}{18.85\times10^8} + \frac{6.28\times10^8}{10.9\times10^8}} \right] = \frac{10}{3.3} = 3.3$$

where

$$\frac{R_1}{R_g} = \frac{C_c}{C_s}$$

and

$$\frac{R_1}{R_g} = \frac{\alpha}{\alpha_H} = \frac{\omega_L}{\alpha}$$

which corresponds to maximum exponential gain.

A voltage gain of this magnitude for an alpha of 10.9×10^8 is appreciable and if these tubes can be cascaded useful gains at these high alphas could be realized.

4.6 Amplifier Linearity Considerations

Amplifiers ordinarily have a definite range over which the output signal linearly follows the input signal. Above this linear range the output does not increase as rapidly as the input signal. This amplitude nonlinearity is exceedingly undesirable with exponential signals because of the difficulty of determining from the recorded trace whether there has actually been a change in alpha or whether amplifier nonlinearity is present. Thus, the data obtained from amplifiers is useful only up to the point at which the amplifier nonlinearity produces inaccuracies in alpha greater than can be allowed.

The Ivy amplifier is typical of those that have been used in the past for amplifying exponential signals. (See Figure 9 for schematic diagram of Ivy amplifier and Figure 10 for typical cw response curve.) It consists of two seven section 6AN5 distributed amplifier output stages operating push-pull to drive the vertical deflection plates of a 5XP-type cathode-ray tube. The grid line of each output stage is driven by a single 418-A video amplifier stage which in turn receive their signal from the two section 6AN5 distributed amplifier inverter stage. This amplifier has a nominal voltage gain of 105, a 250 cycle to 80 mc bandpass, and is capable of delivering 125 volts output with less than 2% nonlinearity. This output voltage will deflect the beam across about 70% of the useful field of the type 5XP cathode-ray tube with which it is used. Because all of the useful field of the cathode-ray tube is not used the dynamic range over which alpha can be measured with this tube is reduced when employing an amplifier and hence there is a resultant reduction in the accuracy with which alpha can be determined. (See Section 5.)

Linear amplifiers to drive low impedance devices such as coaxial cables and traveling wave cathode-ray tubes are particularly difficult to obtain. For example, if one desires an amplifier to deliver 100 volts into the 50 ohm deflection structure of the TW-9 traveling wave cathode-ray tube it is necessary for this amplifier to deliver up to 2 amperes of linear output. It is necessary to use relatively large high-frequency transmitting type tubes in order to obtain currents of this magnitude and high voltage power supplies capable of delivering these relatively large currents.

A further disadvantage in using amplifiers with the TW-9 cathode-ray tube is that it has an electrically unbalanced deflection system and must therefore be driven by a single-sided amplifier. The proposed TW-11 cathode-ray tube utilizing two opposed 125 ohm traveling wave deflection structures shows promise of relieving this condition. This tube would be easier to drive because of its higher impedance deflection structure and, in addition, would permit the use of push-pull amplifiers since the deflection structure is electrically balanced. The use of push-pull amplifiers would result in a considerable increase in linearity for a given number of tubes and output voltage.

The degree of nonlinearity of any particular amplifier on an exponential signal is a function of both the input level and alpha. For example, the percentage deviation from true alpha for an Ivy amplifier is approximately four times the percentage nonlinearity of the amplifier. Thus at the Ivy amplifier 2% amplitude nonlinearity point the apparent alpha value would be 8% below the true alpha. The only really satisfactory method of measuring exponential signal nonlinearity is by testing with a known exponential signal having the alpha and amplitude likely to be encountered in practice. However, if an exponential test signal is not available the usual pulse calibration linearity data may be utilized in analyzing the resultant exponential data for alphas which result in an amplifier gain reduction factor near unity. (See Appendix G, "Amplifier Linearity Considerations," for a development of this method.)

In order to obtain sufficient voltage with receiving type tubes to properly deflect the cathode-ray tube, with the uniform bandwidths required for pulse amplification, it is necessary to use distributed amplifier output stages. The impedance of the output line of an amplifier of this type (using a specific tube) is determined by the upper cutoff frequency when used with conventional electrostatic deflection cathode-ray tubes. For example, both output lines of the Ivy amplifier have a nominal upper cutoff frequency of 120 mc which in turn sets their impedance at 330 ohms with the tubes that were used. Assuming that each side of the amplifier delivers 62.5 volts in order to obtain the full 125 volts output, it is evident that each side must deliver 190 milliamperes signal current. If now an upper cutoff frequency of 240 mc is desired, the impedance of each output plate line would drop to 165 ohms, and each side would have to deliver 380 milliamperes to achieve the full 125 volt push-pull output. These two examples serve to indicate the manner in which the linearity problem depends upon the voltage output and bandwidth requirements.

One other phase of this problem is that in which the impedance of the amplifier output line instead of being determined by the upper cutoff frequency is determined primarily by the impedance of the device which the amplifier is driving. A good example of this is an amplifier which must drive a TW-9 and whose output impedance would then be set in the vicinity of 50 ohms. As pointed out previously it takes two amperes to get 100 volts from this device. In this case curtailing bandwidth (by adding shunt capacity across the output line) would result in no improvement in linear output range since linear output is essentially a function of the line impedance which has previously been set by the TW-9 deflection structure.

These examples show that every effort should be made to maintain as high an impedance as possible in the amplifier output line and points out the difficulties encountered in driving low impedance devices.

It has been shown previously that the simple shunt-fed amplifier gives optimum performance on an exponential signal. The linearity problems on an amplifier of this type are not as difficult as on the distributed amplifier because all the signal current is effectively utilized to charge the shunt output capacity of the amplifier tube and the capacity of the cathode-ray tube deflection plates. The technique here is to parallel tubes up to the point at which the output capacity of all the tubes in parallel is equal to or less than the capacity of the cathode-ray tube deflection plates. The problem then becomes one of obtaining the proper output current linearity versus input voltages under these minimum load conditions.

4.7 Circuit Measurements

In an effort to verify the theoretical calculations of circuit response to exponential signals, and to develop improved means of amplifying exponentials, actual circuits tests have been made on various components by means of an exponential pulse generator.[9] The output of the exponential pulser has been shaped such that the signal rises with an exponential of constant alpha and then is made to break as rapidly as possible to a constant voltage. The resultant "square topped" exponential lends itself readily to the analysis using Rossi displays because of the rapid break in alpha and because retrace is easily avoided. The point at which the signal breaks from the constant alpha is used as the reference point in comparing the exponential voltages. (In the figures discussed below, this point is marked by an arrow on each curve and, in addition, the curves are adjusted in time such that the alpha break points occurs at the same instant in each figure.) The gain of the device in each case is the ratio of the output difference voltage to the input difference voltage at (or before) the reference or alpha break point.

Curve A of Figures 11 through 14 shows a plot of the "square topped" input exponential ($\alpha = 0.925 \times 10^8$) while the additional curves in each case show the output voltage from various devices tested. (These are: Ivy Amplifier No. 6 in Fig. 11, 418-A Distributed Amplifier in Fig. 12, Single 418-A Amplifier in Fig. 13 and various filters. This information was obtained from 1000 mc Rossi displays and is shown as the voltage difference per cycle (1 millimicrosecond per cycle) on the logarithmic scale versus time on the linear scale. Figures 15 through 18 and Figures 19 through 22 show this same information for alphas of 2.38×10^8 and 4.7×10^8 respectively. The regular step pattern of the points on these curves at the lowest alpha (0.925×10^8) are actually a true representation of the output of the exponential pulser. At this low alpha the steps occur at 1.5 ns intervals and are quite easily resolved with the 1000 mc Rossi used in these tests. At the higher alpha the steps out of the pulser are not as pronounced because of rise time limitations within the pulser and are not so easily resolved because of the shorter period between steps (i.e., 0.6 ns for alpha = 2.38×10^8 and 0.3 ns for alpha = 4.7×10^8).

Table 4.3 tabulates the cw gain and response characteristics for each device tested and also the calculated and the measured exponential gain. The cw response curves for each of the devices is shown on Figures 10 and 23 through 25. The agreement between the calculated and the measured exponential gain indicates the validity of the theoretical analysis and of the measuring techniques employed.

TABLE 4.3

Device	SINUSOIDAL CHARACTERISTICS				EXPONENTIAL GAIN	
	f_H	n	Mid-frequency Gain	Alpha	A_e Calculated	A_e Measured
1. Ivy Amp. #6	70×10^6	2	105	$.925 \times 10^8$	71.7	82.3
				2.38×10^8	44.3	41.2
				4.7×10^8	24.5	See text.
2. 418-A Distributed Amplifier	100×10^6	2	77	$.925 \times 10^8$	58.6	54
				2.38×10^8	40.5	37.7
				4.7×10^8	25.2	See text.
3. Single 418-A Amplifier			$G_m = .0239$	$.925 \times 10^8$	27.4	29.2
			$C_o + C_L = 8.3$ mmf	2.38×10^8	11.3	10.4
			$C_{gp} = .05$ mmf	4.7×10^8	5.9	5.56
4. 100 Mc Filter	110×10^6	2	1	$.925 \times 10^8$	.778	.845
				2.38×10^8	.553	.548
				4.7×10^8	.354	.4
5. 200 Mc Filter	290×10^6	4	1	$.925 \times 10^8$	.797	.905
				2.38×10^8	.61	.71
				4.7×10^8	.4	.698
6. 100-200 Mc Filters in cascade	120×10^6	3	1	$.925 \times 10^8$	.705	.808
				2.38×10^8	.44	.436
				4.7×10^8	.234	.315

[9] "Pulse Synthesis by Networks" by D. Kirk, NRL Report 4342.

The exponential gain data presented in Table 4.3 is shown in graphical form in Figure 26 in which the measured and calculated gain in each case are plotted against alpha.

The exponential gain at $\alpha = 4.7 \times 10^8$ for both the Ivy Amplifier and the 418-A Distributed Amplifier are not shown in Table 4.3 because the output of both is so nonlinear at this high alpha that there is no straight line portion on the plot of sufficient length to establish alpha or to allow a detection of the alpha break point. The linear range of multistage amplifiers decreases rapidly with alphas above a certain value. The use of multistage amplifiers with alphas in the vicinity of and above that which give an exponential gain which is one half or less than the midfrequency gain are to be avoided because of this reduction in range of linear output. The primary cause of this effect is saturation of the early stages of the amplifier before the grids of the output stage are driven over their full linear range. This effect is negligible at low alphas, but as alpha increases (with a resultant decrease in stage gain) each stage must put out a correspondingly higher voltage to obtain the same amplifier output.

The schematic diagram of the 418-A Distributed Amplifier is shown in Figure 27. This amplifier has much the same characteristics as the Ivy amplifier; i.e., a voltage gain of 77, a 600 cps to 60 mc bandwidth, and 130 volts output with less than 2% distortion. The sinusoidal response curve of this amplifier is shown in Figure 23.

The single stage shunt-fed amplifier using a 418-A tube connected directly to the vertical deflection plates of type 5XP cathode-ray tube was constructed in accordance with the circuit recommendations developed earlier for optimum amplification of an exponential. The circuit for this Single 418-A Amplifier is shown in Figure 28. It will be noted that this single tube amplifier gave one-fourth as much gain as the 18 tube Ivy Amplifier on an alpha of 2.38×10^8 with good linearity. Furthermore, the Single 418-A Amplifier produced a voltage gain of 5.56 on an alpha of 4.7×10^8 with good linearity while the Ivy Amplifier was so nonlinear that no gain figure was obtained.

4.8 Conclusions

The primary conclusion to be reached is that the conventional pulse amplifier is not at all efficient as an amplifier of constant alpha exponential signals. The design of pulse amplifiers is based on the requirement of maintaining uniform gain and phase shift over as wide a frequency range as possible. On the other hand, optimum amplification of exponential signals is obtained when the gain of the amplifier is maximized over as wide a frequency range as possible (without regard to uniformity of gain). This criteria is most nearly satisfied, with conventional vacuum tubes, by the use of simple shunt-fed stages. Amplifiers of this type show considerable promise for obtaining the maximum gain and output voltage from the minimum number of tubes with good linearity.

The fact that frequency proportional bandpass intervals, spaced geometrically about the angular frequency equal to alpha, make equal contributions to the exponential signal is a new and useful concept. This analysis of the amplitude-frequency spectrum of an exponential has proved to be of value in predicting the performance of networks on exponential signals and in designing amplifiers for optimum gain on this type of signal.

The comparison made between network response on sinusoidal, step function, and exponential signals allows the prediction of the response of a network to one of these signals on the basis of its response to either of the other two. Thus, if the sinusoidal response of an amplifier is known its rise time on a step function and its response to an exponential signal may be determined.

The linearity requirements placed on amplifiers of exponential signals are extremely severe if an accurate measure of alpha is to be obtained. Means for predicting the accuracy

to which alpha can be measured on the basis of the usual pulse linearity data are given in Appendix G.

Tests made on amplifiers and networks with signals from the exponential pulser have shown good agreement with the results predicted by the theoretical calculations. Some preliminary work has been done on designing and testing amplifiers specifically for exponential signals.

SECTION 5 - DISPLAY SYSTEMS AND CATHODE-RAY TUBES

5.1 Introduction

It is the purpose of this section to discuss display systems for recording the exponential signals, with the main emphasis on cathode-ray tube problems. The values of α of interest are in the range from 1×10^8 to 20×10^8. With this value of alpha the total time of the transient is so short, and the rate of rise so fast, that the only practical recording method known at present is to make a photographic record of the signal as it appears on the face of a cathode-ray tube. The value of α is then determined from an analysis of the film record. The problem then is to select the best type of display and the proper cathode-ray tube (CRT). The following types of presentation may be used:

1. Rossi Display
2. Linear Sweep (Type A)
3. Circular Sweep (Type J)
4. X-Y Display
5. Spiral Sweep

5.2 Display Systems

5.2.1 Rossi Display

The classical method of measuring α employs a Rossi type display. In this display the signal is applied to one deflection axis of the CRT and a sinusoidal voltage from a high frequency oscillator is applied to the other axis. The beam of the CRT is biased off, and is unblanked just before the signal reaches the level at which it is desired to record. The display provides its own time calibration and is not critical as to trigger timing. It is especially suited to measuring the rise time of fast rising signals of any type, the only requirement being that the signal should not decrease in value during the display time. If this occurs, the beam will retrace and tend to obscure the desired information.

A number of variations from the basic Rossi display are possible. A modified display can be made by mixing an additional signal with the exponential signal. This may be a portion of the voltage from the timing wave or may be a specially generated modulating voltage. Such displays may provide additional generation coverage on a single cathode-ray tube or may make it possible to record beyond the normal writing speed limitation.

Because of the variation in writing speed required by the Rossi display a means of varying the beam intensity during the trace is desirable. One method of obtaining such dynamic intensification is by applying a portion of the exponential signal to the intensity grid of the cathode-ray tube.

These modified display systems may be useful for special applications. In some cases they exchange accuracy for increased coverage. In general they complicate the recording system and may result in an unusable record if the weapon does not have the predicted alpha.

5.2.2 Linear Sweep Display

The linear sweep is used primarily in measuring time differences between events, as with a radar display. It is most useful for sweep speeds of the order of 0.1 u sec.

and slower. At faster sweep speeds timing problems are most difficult. Other difficulties arise because of the problem of obtaining a time base of the required linearity. The tube must be intensified and the sweep started at a time, between 1/10 and 1/2 of the sweep time, before the signal is displayed and because the sweep is not self calibrating in time it must be calibrated with a timing generator. The linear sweep display does not appear to be generally practical for measuring alpha but may be useful if alpha is very low or is changing.

5.2.3 Circular Sweep Display

A circular sweep display would overcome some of the problems of the linear sweep. In this display the sweep would be obtained by applying a properly phased precision sinusoid in quadrature to the two pairs of deflecting plates, the signal being applied radially by means of a central electrode. This central electrode could be made a traveling wave structure to reduce transit time distortion as well as improve sensitivity. In use the sweep would run continuously and the tube would be intensified just before the signal is displayed so that timing would be much easier than for the linear sweep. Since such a sweep is derived from a sine wave oscillator it is self-calibrating in time. The limitations of the circular sweep have not been determined since a tube of this type has not been developed. It would appear to have some possibilities for alpha measurements because of the extended time base but it is limited by the small field available for the signal.

5.2.4 X-Y Display

For the X-Y display, the signal is divided equally between two transmission lines. In one line the signal is attenuated and applied to one set of deflection plates. The direct signal in the other line is delayed and applied to the other set of plates.

Consider that the signal voltage to be recorded is represented by $Ke^{\alpha t}$. The vertical displacement (produced by the delayed signal) is $S_V = K_1 Ke^{\alpha(t-\tau)}$, where K_1 is a constant which relates signal volts to vertical deflection and τ equals the net delay between the two signals. The horizontal displacement (produced by the attenuated signal) is $S_H = K_1 K_2 Ke^{\alpha t}$, where K_1 is defined as above and K_2 is the voltage ratio of the attenuator and includes any difference in deflection factor of the pairs of plates. The angle between the resulting trace and the horizontal axis can be represented by:

$$\theta = \tan^{-1} \frac{S_V}{S_H} = \tan^{-1} \frac{K_1 Ke^{\alpha(t-\tau)}}{K_1 K_2 Ke^{\alpha t}} \tag{5.1}$$

$$= \tan^{-1} \frac{1}{K_2 e^{\alpha t}}$$

of

$$\alpha = \frac{1}{\tau} \ln \frac{\cot \theta}{K_2}. \tag{5.2}$$

From this it can be seen that if α is constant the trace on the tube face will be a straight line and, provided K_2 and τ are known, the value of α can be determined. The resolution, or accuracy, depends upon the accuracy with which K_2 and τ are known and also upon the rate of change of θ with change of α, which is determined by choice of K_2 and τ. The disadvantage of this system is that the signal must be an exponential with a constant value of α and the value of α must be known beforehand within a factor of approximately 50%. For some purposes it will yield the most accurate results of any system. Although the CRT must be intensified slightly before the signal reaches the deflection plates this delay time is not critical. In this display it is not necessary to time calibrate the indicator. For the ranges of α usually encountered, the delayed signal should have a delay in the order of 10 ns, which is very difficult to measure and calibrate to the required accuracy. One practical method

ot calibration is to apply an exponential signal of known α. Plots of Equation 5.1 showing θ vs α for different values of K_2 and are shown in Figure 29.

From this curve it can be seen that the rate of change of angle (which determines resolution) is greater with larger values of attenuation, but, because of the limit in the signal amplitude which can be obtained from a detector, an attenuation of approximately 20 db. appears to be a maximum practical value.

5.2.5 Spiral Sweep Display

The spiral sweep is similar to the circular sweep. However, in this case the phasing circuits drive amplifiers which are amplitude modulated so that the amplitude decreases linearly with time. This system is most useful for accurately measuring time differences between signals 1 us. to 1000 us. apart in time. The sweep is intensified and the modulator started just before the first signal is applied and signals are displayed radially through the amplifiers. The sweep is self-calibrating but is not useful at very fast rates because of bandwidth limitations of the amplifiers.

5.3 Characteristics of the Rossi Display

A study of the display systems indicates that the Rossi display is the most practical for nearly all applications. In Appendix A the various factors to be considered in designing such a display system are discussed. The main advantages are in simplicity of the system, resulting in increased reliability and in the accuracy of the final record. Using a properly designed system the value of alpha can be determined to within approximately 1 percent over a rather large dynamic range corresponding to a large number of generations. In order to design the Rossi system it is necessary to know not only the characteristics of the signal to be displayed but also the characteristics of available cathode-ray tubes.

5.4 Cathode-Ray Tube Characteristics

In selecting a tube suitable for use as in a Rossi display a number of characteristics are required - high writing speed, large field in trace widths (at least on one axis), small deflection factor (volts/trace width), and small deflector transit time. In meeting these requirements, a tube having a rather large amount of post-deflection acceleration is desirable. The above requirements are approached by a few commercial tubes, as well as the special purpose tubes developed at NRL. Those to be considered are: the DuMont K-1101 (a commercial version of the K-1056), the 5XP11-M, the TW-9, the TW-10, and the proposed TW-11. These have many features in common such as: a five-inch flat face, electrostatic focus and deflection, multi-band post-accelerators, a P-11 screen phosphor with aluminum backing.

The K-1101 has a high writing speed, a large field and a high deflection factor (volts/tw). It uses conventional deflection plates with coaxial deflection plate connectors. The 5XP11-M has a lower writing speed than the K-1101, the same size field on the horizontal axis and a lower deflection factor, especially on the vertical axis. The deflection plates are larger than in the K-1101 and the connectors are not coaxial.

The TW-9 has a high writing speed, a small field on both axis and a low deflection factor. Deflection on both axes is obtained with a traveling wave deflection system resulting in a reduced deflection factor and a reduced transit time distortion. The deflector impedance is 52 ohms, to match standard coaxial cables. The TW-10 is similar to the TW-9 except that normal deflection plates are used on one axis and the 52 ohm distributed deflector is

used on the other. The proposed TW-11 is similar to the TW-10 except that the traveling wave deflection system has been made balanced, each side having an impedance of 125 ohms to ground. The transit time distortion in the distributed deflector will be even less than in the TW-9 or TW-10.

The more important characteristics of each tube have been measured and are listed in Table 5.1. Wherever possible the average characteristics of a large number of tubes of a given type has been taken. However, because only a limited number of tubes were available and because of variations between tubes of the same type, the table cannot be taken as representing all tubes of a type.

Deflection characteristics are given in terms of trace widths since this factor uniquely defines resolution of the record. However, because recorded trace width depends upon many factors, it is subject to considerable variation which means that writing speed, deflection factor and field are a function of the manner in which tracewidth is determined. The characteristics shown in Table 5.1 are representative of those obtainable with good operating conditions at high writing speeds.

To check deflection factor and field a raster type display was applied to each tube from a dc calibrator and the traces photographed. (The traces were photographed with an E G and G Type 3114 camera using an F.1.0 lens with Eastman Tri-X film, developed for 25 minutes in DK-60A developer.) A typical photograph is shown in Figure 30. The dc calibrator applies a series of accurately known centering voltages to the tube and after each new centering voltage is applied the calibrator triggers the time base generator in the indicator which applies a linear sweep to the other axis of the CRT. The entire operation is completely automatic. Accuracy of the calibration is better than ±0.1%.

TABLE 5.1
CATHODE-RAY TUBE CHARACTERISTICS

Type	Max. Writing Speed tw/sec	Vert. Field tw	Vert. D.F. V/tw	Horiz. Field in tw	Horiz. D.F. V/tw	Trace Width (in.)	Transit Time (Sec)
K-1101	2×10^{11}	320	3.1	340	3.1	12×10^{-3}	Horiz. & Vert. 2.9×10^{-10}
TW-9	2×10^{11}	193	0.57	133	0.67	6×10^{-3}	Horiz. & Vert. 1.7×10^{-10}
TW-10	2×10^{11}	133	0.85	445	1.8	9×10^{-3}	Horiz. 6.8×10^{-10} Vert. 1.7×10^{-10}
TW-11 (Proposed)	2×10^{11}	188	1.2	445	1.8	9×10^{-3}	Vert. 0.7×10^{-10} Horiz. 6.8×10^{-10}
5XP11M (4 & 20 KV)	4×10^{10}	124	1.6	250	4.6	15×10^{-3}	Vert. 8.5×10^{-10}
5XP11M (7 & 25 KV)	1×10^{11}	145	2.3	253	6.7	14×10^{-3}	Vert. 6.4×10^{-10}

In determining writing speed characteristics a mercury switch pulse generator was used. Figure 31 shows a block diagram of the circuit. The generator will deliver pulses up to 2 Kv with rise times less than 1 ns. Writing speed is varied by inserting RG-58/U cable in the signal line (which results in longer rise times), by signal attenuators and by varying timing wave amplitude. The exponential pulse generator could also be used, in which case writing speed would vary across the field. This would make it possible to check writing speed over a wide range with a single test. However, this presumes the writing characteristics of the CRT to be constant over the field, which is not the case.

It is quite difficult to define exactly where a CRT stops writing. An attempt was made to define a minimum usable ratio of trace intensity to background by using a recording densitometer. This method has not been found to be satisfactory. The method now used is to view the negative and compare it with one which is considered as a minimum usable picture. Admittedly, this method depends entirely upon the operator's decision. However, it is a fairly accurate method since cathode ray tubes stop writing quite abruptly, because

of film and phosphor characteristics. An example is shown in Figure (32), where all conditions are identical except writing speed. The upper trace is considered minimum usable and shows 3×10^{11} tw/sec. at the last base line crossover; the lower picture shows 4.5×10^{11} tw/sec. at the same point and is not considered not usable. Variation in writing speed from tube to tube of the same type is quite large. A representative average could be taken only if a large number of tubes of the same type were tested. In this study, averages of eight tubes were taken for the 5XP and TW-10. Only three K-1101 tubes were available, which is not enough in view of the considerable difference in characteristics between the tubes tested. A series of pictures were made with each tube to find optimum conditions of intensity and focus. The intensity pulse was adjusted in magnitude to such a value that the CRT control grid would not be driven positive. The writing speeds given in Table 5.1 are near maximum values and are subject to wide variations between tubes. Because of the large variation writing speed should be chosen with a large safety factor. To obtain tubes with sufficient writing speed it is often necessary to select tubes from a particular type by actual test. This is not a good approach but in some cases is the only method of obtaining tubes having the required writing speed.

The 5XP tubes were checked at two different operating conditions - one at DuMont's maximum ratings of 4 and 20 kv, the other at 7 and 25 kv. The higher voltages were used to determine if writing speed would increase. (The gun in the 5XP is similar to that in the K-1101 tube, which operates satisfactorily at the higher voltage.) An improvement of about 2.5 in writing speed was observed but the increased voltage produces stray emission, resulting in "bloom" on the face of some tubes. No figures are available on the effect of increased voltage on tube life.

5.5 Transit Time Distortion

Since the electrons in the beam of the CRT require a finite time to pass through the field between the deflection plates, the deflection of the beam is a function not only of the deflecting voltage but also of this transit time. This leads to a transit time distortion between the signal applied to the deflection plates and the signal displayed on the screen.

The transit time distortion with various driving functions is discussed in Appendix I. It is seen that for a sinusoidal input the effective deflection is reduced by a "sensitivity reduction factor" which is $[(\sin \omega\tau/2)/(\omega\tau/2)]$ where τ is the time required for an electron to travel through the deflector field. The value of this reduction factor is plotted in Figure 33. The response to an exponential signal is reduced by the factor $[(1-e^{-\alpha\tau})/(\alpha\tau)]$. This function is plotted in Figure 34. It is seen that there is a reduction in sensitivity to both the sinusoidal and the exponential signals comprising the Rossi display. The relative response to the exponential for $\alpha = 2 \times 10^8$ and $\tau = 6 \times 10^{-10}$ is 0.94. For a timing wave frequency of 6×10^8 cycles/sec. and $\tau = 6 \times 10^{-10}$ the relative response is about 0.8.

The response to a step function is also analyzed in Appendix I. The effect is to "smear" the rise time to a value equal to the transit time. Thus it is seen that transit time must be small compared to signal rise time if complex signals are to be recorded without distortion.

The preceding discussion has assumed that the voltage is the same on all parts of the deflection plates while under certain conditions with long deflection plates this is not true. Also although parallel plates were assumed, transit time distortion effects are somewhat less when the spacing is tapered.

Using conventional electrostatic deflection plates it is possible to reduce the transit time effect by either reducing the plate length or increasing the beam velocity although either change will result in an increased deflection factor. It is desirable in many applications to have as low a deflection factor as possible. Both decreased deflection factor and decreased transit time can be obtained by making the deflection system a section of transmission line

in which the velocity of propagation of the signal along the line is matched to the velocity of the electron beam. The TW-9, TW-10, and TW-11 tubes have such deflection systems.[10] The traveling wave deflection structure is constructed as a flattened helix in a ground plane housing. A section of each turn of the helix acts as a small deflection plate and the effective transit time is the ratio of the pitch of the helix to the beam velocity. The deflection factor of the system is then inversely proportional to the number of turns in the helix.

5.6 Recording Small Amplitude Signals

So far, little has been said about the limits on signal amplitude. In practice amplitudes are limited because of detector saturation and because alpha is constant over only a limited number of generations of the nuclear reaction. Thus, it is desirable to start recording at the lowest possible level in order to make measurements as complete as possible. This means that the CRT with the smallest deflection factor must be used. If G = 4 and m = 3, discernable recording will start at 10 trace widths; or 10 times the deflection factor gives the signal level in volts (Appendix H). For the TW-9 this minimum recorded level is 5.7 volts; for the TW-10, 8.5 volts, for the 5XP, 16 volts and for the K-1101, 25 volts. It is therefore seen that the TW-9 starts recording at a lower signal level than the others.

It is possible to improve the effective sensitivity of the cathode-ray tube when the deflector impedance is higher than that of the signal line. The simplest case is that in which the transmission line is terminated in only the capacity of the electrostatic deflection plates. The impedance of the plates to the exponential signal is $Z = 1/\alpha C$.[11] Then, if the voltage on the transmission line is $V_0 e^{\alpha t}$, the voltage at the deflection plates will be $V_0 e^{\alpha t} [(2Z_c)/(Z_c + Z_c)]$ where $Z_c = 1/\alpha C$ and Z_c is the transmission line impedance. It should be noted that when balanced deflection is used the effective capacity, C, is higher than when unbalanced deflection is used. In order to reduce deflection defocusing, balanced deflection should be used when possible.

For either 5XP11 or K-1101 tubes the effective deflection plate capacity, for balanced deflection, is about 6×10^{-12} farads and if $\alpha = 2 \times 10^8$ the effective impedance is 833 ohms giving a voltage step-up at the plates of 1.88 from a 52 ohm line. Thus, the minimum effective level can be reduced to 8.5 and 13.3 volts for the 5XP11 and the K-1101 respectively. In the above example, the voltage at the CRT plates can be increased further by using transmission line matching sections of intermediate impedances, although there is a limit to the step-up that can be obtained because of the existing plate capacities. The matching section can be made up of a series of lines of increasing impedance, approaching an exponentially tapered transformer. It should be noted that such a system can only be used with nonrecurrent transients where the signal duration is less than twice the electrical length between line discontinuities. By using a section of 125 ohm line (about the highest practical cable impedance) between the 52 ohm line and the CRT an extra step-up of about 1.4 can be obtained, resulting in a minimum recorded level of 6 volts for the 5XP and 9.5 volts for the K-1101, as referred to the main signal line. An improvement in the deflection factor of the TW-9 and TW-10 distributed deflectors can be obtained by leaving the structures unterminated. The factor will be approximately 2. A similar improvement could be achieved with the proposed TW-11. However, these structures should be terminated for most applications since open circuit operation may affect rise time characteristics.

---

[10] S. T. Smith, R. V. Talbot, and C. H. Smith, "Cathode-Ray Tube for Recording High Speed Transients," Proc. I.R.E., Vol. 40, No. 3, March 1952.

[11] W. H. Weber, "Response of Electrical Circuits to Exponential Driving Forces," LASL Report LA-1323.

In some cases it is desired to record the signal at a lower level than is possible with any arrangement with cathode-ray tubes alone. This requires the use of signal amplifiers (Section 4). Also, some consideration must be given to the cathode-ray tube. Certainly, it is desirable to use a CRT having the smallest deflection factor. Deflector impedance must be considered, since this determines the current required, and furthermore, in order to obtain optimum amplifier linearity it is generally desirable to have balanced deflection. On the basis of deflection factor the TW-9 and 5XP tubes are the best choice. However, when impedance and balanced deflection are considered the 5XP has considerable advantage. Consider the current required for a deflection of 100 tw at an α of 2×10^8. The current for the TW-9 will be $I = (100 \times 0.57)/50 = 1.14$ amps. The 5XP has only the plate to plate capacity of 3.6 uuf to drive, which has an impedance of $1/\alpha C$ or 1390 ohms. Then $I = 160/1390 = 0.115$ amps. Moreover, for the TW-9 the current must be obtained for one unbalanced amplifier while the 5XP would use two amplifiers balanced to ground. Thus the 5XP appears to be the best tube available for use with signal amplifiers, where its writing speed is sufficient. For greater bandwidth and higher writing speed the TW-9 is useful. The proposed TW-11 would give improved performance. Here the current required would be approximately $I = 150/125 = 1.2$ amps total. Since the system is balanced the current from each amplifier would be about 0.6 amps. with improved linearity from the balanced operation.

5.7 Recording Large Amplitude Signals

In some cases a constant α signal from a photocell diode detector may reach a level of about 1000 volts. Much of this signal can be recorded directly on the cathode-ray tube and for this purpose it is desirable to use a tube which utilizes as much signal level as possible and yet gives sufficiently accurate information. A tube having as large a field as possible is usually desired. From Table 5.1 it is seen that the best tubes are the K-1101 and the TW-10, using the horizontal axis.

In these cathode-ray tubes using large deflection voltages it is necessary to use balanced deflection to reduce astigmatism (deflection defocusing) of the spot since the detector output is normally unbalanced to ground. This balancing is accomplished by use of a signal inverter and delay cables. One of these cables is adjustable in length so that the two balanced signals arrive at the CRT at the same time. Due to the impedance mismatch into the inverter, loss in the delay cables, etc., the peak-to-peak amplitude of the signal at the CRT is approximately equal to the unbalanced signal. The signal cables are usually not terminated and are connected directly to the CRT plates. This means that the signal appears at the end of a cable terminated only by the CRT deflection plate capacity, the exponential impedance of the condenser being $1/\alpha C$, so that the signal between plates will be almost twice the signal arriving on the main signal line for exponential impedances considerably greater than the transmission line impedance, as shown in Section 2.6.

5.8 Selection of the Cathode-Ray Tube for a Recording System

In designing a recording system each component should be selected to provide optimum performance. In general, the cathode-ray tube to be used should be selected on the basis of the particular recording requirements involved and where several tubes are equally suitable other factors may be considered, such as cost, availability and reliability.

Consider the case where it is required to record on a single tube at least three generations ($n = 3$)* of a high level exponential signal, having $\alpha = 2 \times 10^8$.

(a) Assuming a practical value for "G" of 4 tw and "m" = 3 the wasted portion at the beginning of the sweep is 10 tw. From Figure 44 the maximum writing speed at 3 generations is found to be 4×10^{10} TW/sec. All tubes give a good safety factor (except the 5XP with 4 and 20 KV; with 7 and 25 KV the 5XP is usable).

*Symbol designations used in this Section and Appendix H are listed at the end of this Section.

(b) All tubes are usable from transit time considerations since the 5XP, with the largest transit time of any of the tubes, has a computed transit time sensitivity reduction factor of 0.63 at 600 mc (m = 3).

(c) Using Figures 45 and 46 it is found that the field of the tube must have at least 220 tw in order to record 3 generations. From Table 5.1 it is seen that either axis of the K-1101 is satisfactory, neither axis on the TW-9, the horizontal field of the TW-10, both axes of the proposed TW-11 and the horizontal field of the 5XP. It appears that the most suitable tube is either the TW-10 or the K-1101. If the requirement were the measurement of α to the highest accuracy, instead of the 3 generation coverage, it is obvious from Appendix H that the tube having the maximum field will be best. The maximum required writing speed will now depend upon the field, being about 8×10^{10} for the K-1101 and 9×10^{10} for the TW-10. Under these conditions the TW-10 becomes the most desirable tube.

Next, consider the case where $\alpha = 10 \times 10^8$, m = 3, and again at least three generations are to be recorded with a high level signal.

(a) From Appendix H maximum required writing speed is about 2×10^{11} tw/sec. This is found to be the maximum writing speed of any of the tubes so that none will provide a safety factor. It will therefore be necessary to carefully select tubes of any type.

(b) At the timing wave frequency of 3000 mc the K-1101 deflection is reduced to approximately 0.14 of its former value because of sensitivity reduction. Hence, it would require a timing wave of 7 times the voltage to give the same deflection. On the other hand, the TW-10 deflection on the distributed deflector is reduced by a factor of 0.64. The most satisfactory tube appears to be the TW-10, with the exponential signal on the parallel plates and the timing wave on the TW structure. It would be desirable in this case to use a lower value of m even though the error in α would be increased.

From the preceding it is seen that with $\alpha = 10 \times 10^8$ the K-1101 or TW-10 will record only to about 220 trace widths due to writing speed limitations so that only a portion of the field is actually used. If even higher values of α are to be measured the usable field will be reduced even further. Under these conditions the TW-9 becomes the most desirable tube since crosstalk and transit time effects are minimized while at the same time best use is made of the available field.

As mentioned previously, for low level signals either the TW-9 or the TW-10 with signal on the TW deflector is best for a direct display. For use with amplifiers the vertical axis of the 5XP11 is suitable for $\alpha = 2 \times 10^8$. It will be noted that the tube will only provide coverage to about 125 trace widths, or about 2.5 generations. However, this is also above the limit of the Ivy amplifier in linear output voltage. The 5XP11 writing speed is satisfactory for this coverage. For higher values of α the proposed TW-11 becomes desirable because of writing speed and crosstalk factors.

The following table tabulates the cathode-ray tubes in terms of α and signal level discussed above. Tubes have been placed only in approximate order of suitability. Final selection must depend upon consideration of the many factors previously mentioned.

	High Level, Direct	Low Level, Direct	Amplified
$\alpha \leqslant 2 \times 10^8$	K-1101 TW-10* TW-11*	TW-9 TW-10**	5XP11 TW-11**
$2 \times 10^8 < \alpha < 10 \times 10^8$	TW-10* K-1101 TW-11*	TW-9 TW-10**	TW-11**
$\alpha > 10 \times 10^8$	TW-9	TW-9	- - -

* Signal in Electrostatic Plates

** Signal on Traveling Wave Structure

5.9 Summary

The Rossi type display is the most suitable method of recording exponential signals. A number of cathode-ray tubes are available which can be used, the actual type employed depending primarily upon the value of α, the signal level and the accuracy required. No one tube is satisfactory for all applications.

Writing speed limitations result in decreased accuracy for measurements of high values of alpha. Even the best available tubes have reduced accuracies at alphas of 10×10^8 sec^{-1} and above. Other limitations encountered are those of sensitivity, transit time distortion and crosstalk. The traveling wave type cathode-ray tubes offer considerable advantages where these problems are encountered.

The accuracy of the α determination is affected by a number of factors. With a well designed system having no signal limitations, such as detector or amplifier non-linearity, the accuracy depends largely upon the number of elements in the useful field of the CRT and upon the selection of the timing frequency.

In order to provide maximum dynamic range and best accuracy the recording system may use several different type tubes, some being used in direct displays and some with signal amplifiers. As improvements are made in nuclear detectors, signal amplifiers and cathode-ray tubes it can be expected that system design will change accordingly.

5.10 List of symbols for Section 5 and Appendix H

1. A = total field of tube (in trace widths)

2. C = number of generations that can be recorded on the CRT

3. D_N = width in trace widths of the Nth cycle, with the Nth peak as the center and given by

$$S_N \, e^{1/2m} - \frac{S_N}{e^{1/2m}}$$

4. d = volts per trace width (deflection factor)

5. f = frequency of the sine wave

6. G = separation of the peaks of a cycle which can just be resolved

7. m = number of cycles of the sine wave per generation

8. n = number of generations ($n = \alpha t$)

9. P_α = error in α

10. $P_{\Delta s}$ = error in Δs

11. P_{S_N} = error in S_N

12. P_y = error in $\ln \Delta s$

13. S_0 = displacement at $t = 0$

14. S_1 = displacement at first peak that can be resolved (wasted part of field)

15. S_2 = displacement from zero to the second peak

16. S_N = displacement from zero to the Nth peak

17. ΔS = displacement between adjacent peaks

18. α = multiplication rate of the exponential signal

19. $1/\alpha$ = time of one generation

SECTION 6 - CONCLUSIONS AND RECOMMENDATIONS

A number of general conclusions can be drawn from this analysis of the measurement of alpha during the period when alpha is constant.

(a) the effect of linear systems is to produce a reduction in the amplitude of the signal. The amount of this reduction is directly related to the "effective bandwidth" of the circuit element.

(b) A reduction in detector response is exhibited at high frequencies, due primarily to the scintillator decay times. Using photodiode detectors the reduction factor (percent of low frequency response) is approximately 70% at $\alpha = 2 \times 10^8$. At higher alphas the relative response decreases, reaching a factor of about 10% at $\alpha = 20 \times 10^8$.

(c) The transmission line used to connect the detector to the recorder causes a signal reduction, the amount depending on the length and quality of the line. For $\alpha = 2 \times 10^8$ and 1000 ft. of 7/8 inch diameter line the reduction factor is about 72%. At $\alpha = 20 \times 10^8$ the relative response drops to 36%. It is obvious that for long lengths of line and/or high values of alpha, high quality (large diameter) lines must be used.

(d) Signal amplifiers permit measurements of the exponential signal several generations earlier than otherwise could be determined. However, if the accuracy is to be comparable to that obtained without amplifiers the requirements on bandwidth and linearity are severe. Distributed amplifiers such as are used for pulse amplification are quite inefficient. For example, although the distributed 18 tube Ivy amplifier has an effective gain of about 40 at $\alpha = 2 \times 10^8$ it becomes so nonlinear at $\alpha = 5 \times 10^8$ that no useful information can be obtained. A much simpler and more efficient amplifier is the shunt-fed uncompensated video amplifier. A single shunt-fed 418-A stage has a gain less than for the distributed amplifier, 10 at $\alpha = 2 \times 10^8$, but it still provides a useful gain of about 5 at $\alpha = 5 \times 10^8$. At higher values of alpha new techniques, such as traveling wave amplifiers, appear to be required.

(e) The most satisfactory display system is, in general, the Rossi display. The cathode-ray tube used must be a high writing speed, high resolution tube designed for use with ultra-high frequencies. For $\alpha = 2 \times 10^8$ a number of tubes are suitable but at higher values of alpha these tubes become less satisfactory until at $\alpha = 20 \times 10^8$ dynamic range coverage and accuracy are very marginal with even the best tubes.

Several recommendations result from the study.

(a) Response characteristics of all system components should be improved if accurate measurements of high alpha signals are desired. These include increased detector resolution, improved amplifier bandwidth and linearity and improved cathode-ray tube writing speed and resolution. High quality transmission lines such as the 3 1/8 inch air dielectric line should be used in all except very short lengths.

(b) Considerable improvement should also be possible in recording values of alpha in the region of 2×10^8. These developments would include: more sensitive detectors to permit recording lower level signals without use of amplifiers; simpler and more efficient amplifiers; cathode-ray tubes with high impedance traveling wave deflectors to make possible certain amplifier improvements as well as to provide increased sensitivity with direct displays.

Finally, it is felt that as new materials and techniques are developed it may be possible to design simple alpha recording systems eliminating amplifiers and cathode-ray tubes for certain applications.

Appendix A

A.1 Detector Response - Case 1, Calculation of $f_1(t)$ for the Case of the Terminated Detector with the Axis Pointing at the Source of Radiation

The purpose of this appendix is to find $f_1(t)$, the response of the detector to a δ-function and to estimate the parameters τ_1 and τ_2 which appear in a simple expression that approximates $f_1(t)$.

For the purpose of this analysis the detector will be considered to have the simplified geometry shown in Figure A.1. The analysis will show that this geometric approximation is sufficiently good.

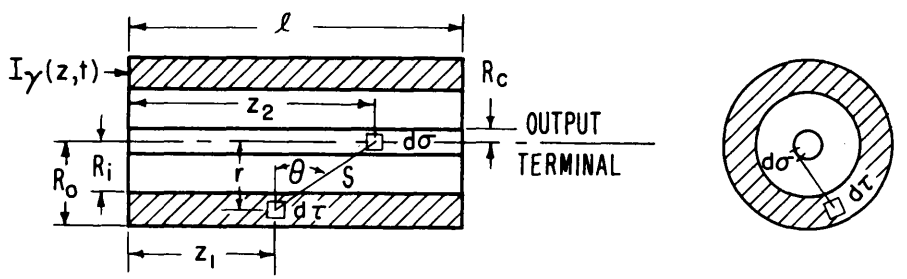

Figure A.1

Coordinates of $d\tau$: r, ϕ, z_1

Coordinates of $d\sigma$: R_c, ϕ_2, z_2

At the volume element $d\tau$ the intensity of the incident γ-ray beam is

$$I_\gamma(z_1,t) = F(t-\frac{z_1}{c})e^{-\beta_1 z_1}$$

where $\beta_1 = \mu_t$ = total γ collision coefficient in cm^{-1}.

The energy per second absorbed from the incident beam in $d\tau$ is proportional to $I_\gamma(z_1,t)$ and $d\tau$; say

$$\mu_a I_\gamma(z_1,t)d\tau = \mu_a F(t-\frac{z_1}{c})e^{-\beta_1 z_1}\, d\tau. \tag{A.1}$$

Part of this energy is then radiated as low energy photons. Assuming the radiation to occur instantaneously and isotropically the energy radiated from $d\tau$ at time t is

$$\xi\, \mu_a F(t-\frac{z_1}{c})e^{-\beta_1 z_1}\, d\tau. \tag{A.2}$$

Part of this energy is absorbed by the element of area (of the cathode) $d\sigma$. In calculating the fraction of the energy absorbed by $d\sigma$ account must be taken of the refraction of the glass interface. The glass itself is ignored and the interface considered a boundary between toluene and vacuum. In what follows the effects of curvature of the glass surface and the attenuation of light in the toluene are also ignored.

For a sufficiently small cathode $d\sigma = 2R_c\, dz_2$; that is, looking from the point at $d\tau$ the cathode appears to be a flat strip of width $2R_c$. With these approximations consideration is given to the effect of refraction at the interface. The notation is that shown in Figure A.2 and A.3.

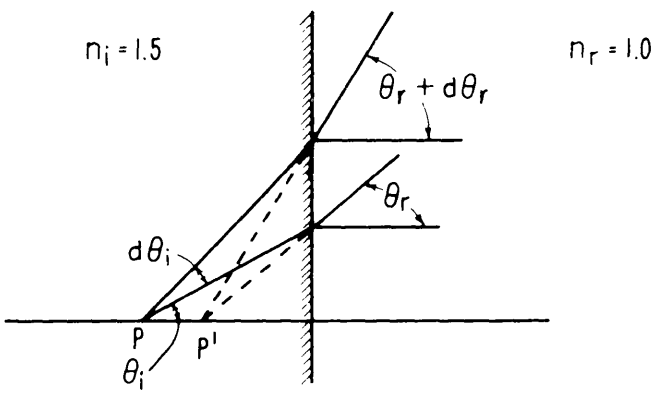

Figure A.2

If E is the energy per unit time emitted by a point source at P, then

$$\frac{E}{4\pi s^2} \cdot 2\pi s \sin\theta_i \cdot s d\theta_i = \frac{1}{2} E \sin\theta_i d\theta_i \tag{A.3}$$

= energy per unit time emitted into region between the cones θi and $\theta_i + d\theta_i$. This energy then flows into the region between the cones θ_r and $\theta_r + d\theta_r$ with apex at P'. (Assuming no reflection at the surface).

Energy per unit time flowing into region between θ_r and $\theta_r + d\theta_r$ is

$$dE(\theta_r) = \frac{1}{2} E \sin\theta_i d\theta_i \tag{A.4}$$

where

$$\sin\theta_i = \frac{1}{n_i}\frac{\cos\theta_r}{\cos\theta_i}\, d\theta_r = \frac{1}{n_i}\frac{\cos\theta_r\, d\theta_r}{\sqrt{1-\frac{1}{n_i^2}\sin^2\theta_r}}$$

$$= \frac{\cos\theta_r d\theta_r}{\sqrt{n_i^2 - \sin^2\theta_r}}.$$

Thus

$$dE(\theta_r) = \frac{1}{2} E \frac{\sin\theta_r}{n_i} \frac{\cos\theta_r d\theta_r}{\sqrt{n_i^2 - \sin^2\theta_r}} \tag{A.5}$$

and because the solid angle between θ_r and $\theta_r + d\theta_r$ is $d\omega = 2\pi \sin\theta_r d\theta_r$

$$\frac{dE(\theta_r)}{d\omega} = \frac{1}{4\pi} E \frac{1}{n_i}\frac{\cos\theta_r}{\sqrt{n_i^2 - \sin^2\theta_r}}.$$

That is

$$dE = \frac{E}{4\pi}\frac{\cos\theta_r}{n_i\sqrt{n_i^2 - \sin^2\theta_r}}\, d\omega \tag{A.6}$$

is the rate at which energy flows into the element of solid angle $d\omega$ centered about the direction θ_r.

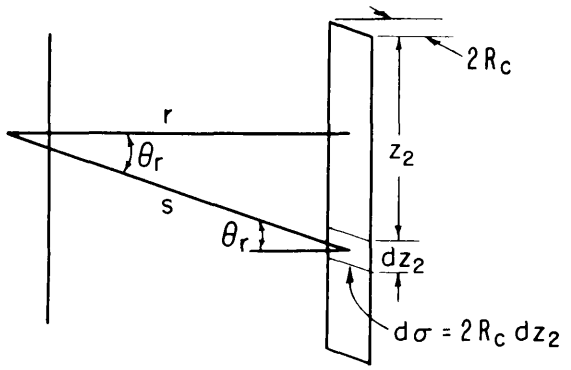

Figure A.3

The solid angle subtended by $d\sigma$ is

$$d\omega = \frac{d\sigma}{s^2} \cos\theta_r = 2\, R_c dz_2 \frac{r}{s^3}. \tag{A.7}$$

Now

$$s = \frac{r}{\cos\theta_r}$$

and

$$dz_2 = \frac{r}{\cos^2\theta_r} d\theta_r$$

$$d\omega = 2R_c\, r \frac{\cos^3\theta_r}{r^3} \frac{r}{\cos^2\theta_r} d\theta_r$$

$$= 2\frac{R_c}{r} \cos\theta_r\, d\theta_r.$$

Thus, energy per unit time falling on $d\sigma$ is

$$\frac{E}{4\pi} \frac{2R_c}{r} \frac{\cos^2\theta_r d\theta_r}{n_i\sqrt{n_i^2 - \sin^2\theta_r}} \tag{A.8}$$

From equations A.2 and A.8 the energy which originates in $d\tau$ and falls on $d\sigma$ at the time t is

$$\frac{\xi\mu_a}{4\mu} \frac{2R_c}{r} F\left(t - \frac{z_1}{c} - \frac{s}{c}\right) e^{-\beta_1 z_1} \frac{\cos^2\theta d\theta}{n_i\sqrt{n_i^2 - \sin^2\theta}} d\tau \tag{A.9}$$

where account is taken of the time delay s/c. The subscript on θ is dropped.

A fraction of this energy (denote the fraction by Q) is absorbed and gives rise to a current pulse dI which travels down the transmission line (within the detector) without attenuation or dispersion. This pulse requires time $(l - z_2)/c$ to reach the output terminal. The current reaching the terminal at time t, due to γ-ray energy absorbed in $d\tau$ and the resultant low energy photons absorbed in $d\sigma$, is

$$dI_o = \frac{Q\xi\mu_a}{4\pi} \frac{2Rc}{r} F\left(t - \frac{z_1}{c} - \frac{s}{c} - \frac{l}{c} + \frac{z_2}{c}\right) e^{-\beta_1 z_1} \frac{\cos^2\theta}{n_i\sqrt{n_i^2 - \sin^2\theta}} d\theta d\tau. \tag{A.10}$$

(Since the detector is terminated the current pulse traveling toward the termination is absorbed. Hence only one-half the energy generated by the detector will appear on the output line.)

Since
$$d\tau = r\,dr\,d\phi_1\,dz_1$$

$$I_o = \frac{Q\,\xi\,\mu_a\,R_c}{2\,\pi\,n_i}\int_{R_i}^{R_o} dr \int_o^{l} dz_1\, e^{-\beta_1 z_1} \int_{\tan^{-1}(-\frac{z_1}{r})}^{\tan^{-1}(\frac{l-z_1}{r})} d\theta\, \frac{\cos^2\theta}{\sqrt{n_i^2 - \sin^2\theta}}$$

$$\cdot F\left(t + \frac{z_2 - z_1}{c} - \frac{s}{c} - \frac{l}{c}\right)\int_o^{2\pi} d\phi_1$$

$$= \frac{Q\,\xi\,\mu_a\,R_c}{n_i}\int_{R_i}^{R_o} dr \int_o^{l} dz_1\, e^{-\beta_1 z_1} \int_{\tan^{-1}(-\frac{z_1}{r})}^{\tan^{-1}(\frac{l-z_1}{r})} d\theta$$

$$\cdot F\left(t + \frac{z_2 - z_1}{c} - \frac{s}{c} - \frac{l}{c}\right) \frac{\cos^2\theta}{\sqrt{n_i^2 - \sin^2\theta}}\,. \tag{A.11}$$

Now
$$s = \frac{r}{\cos\theta} = r\sec\theta$$

$$z_2 - z_1 = r\tan\theta$$

and
$$\frac{\cos^2\theta}{\sqrt{n_i^2 - \sin^2\theta}} \approx \frac{1}{n_i}\cos^2\theta\,.$$

(For $n_i = 1.5$, $\sqrt{n_i^2 - \sin^2\theta}$ ranges from 1.5 at $\theta = 0$ to 1.12 at $\theta = 90°$. This variation will be ignored.)

$$I_o = \frac{Q\,\xi\,\mu_a\,R_c}{n_i^2}\int_{R_i}^{R_o} dr \int_o^{l} dz_1\, e^{-\beta_1 z_1} \int_{\tan^{-1}(-\frac{z_1}{r})}^{\tan^{-1}(\frac{l-z_1}{r})} d\theta \tag{A.12}$$

$$\cdot F\left[t - \frac{1}{c}(l + r\sec\theta - r\tan\theta)\right]\cos^2\theta\,.$$

I_o will now be calculated for $F(t) = \delta(t)$ to give $f_1(t)$.

Let
$$l + r\sec\theta - r\tan\theta = l + s + (z_1 - z_2) \equiv q \tag{A.13}$$

where
$$\cos\theta = \frac{r}{s},\quad s = \sqrt{(z_1 - z_2)^2 + r^2}$$

$$z_2 - z_1 = r\tan\theta$$

(q has the significance of being a total path length from the front face of the detector to the output terminal; that is, γ-ray path + photon path + electrical pulse path.)

A change of variable in the last integral from θ to z_2 gives

$$dz_2 = r \sec^2 \theta d\theta = \frac{r}{\cos^2\theta} d\theta \tag{A.14}$$

$$\cos^2 \theta d\theta = \frac{\cos^4\theta}{r} dz_2 = \frac{r^3}{s^4} dz_2$$

and

$$I_o = K \int_{R_i}^{R_o} r^3 dr \int_o^l e^{-\beta_1 z_1} dz_1 \int_o^l \frac{dz_2}{s^4} F(t-\frac{q}{c}) \tag{A.15}$$

where the factor $(Q\, \xi\mu_a Rc)/ni^2$ has been lumped into the constant K. A change of variable in the last integral from z_2 to q gives the following.

$$q = l + s + (z_1 - z_2) \tag{A.16}$$

and

$$s = \sqrt{(z_1-z_2)^2 + r^2} = q - l - (z_1 - z_2)$$

from which

$$s^2 = (z_1-z_2)^2 + r^2 = (q-l)^2 - 2(q-l)(z_1-z_2) + (z_1-z_2)^2$$

and

$$(z_1-z_2) = \frac{(q-l)^2 - r^2}{2(q-l)}$$

$$= \frac{1}{2}(q-l) - \frac{r^2}{2q-l}$$

giving finally for s

$$s = \sqrt{\frac{[(q-l)^2 - r^2]^2}{4(q-l)^2} + r^2} = \frac{(q-l)^2 + r^2}{2(q-l)} . \tag{A.17}$$

Now

$$-dz_2 = \frac{1}{2} dq - \frac{r^2}{2} \left\{ - \frac{dq}{(q-l)^2} \right\} = \frac{(q-l)^2 + r^2}{2(q-l)^2} dq \tag{A.18}$$

$$\frac{dz_2}{s^4} = - \left[\frac{(q-l)^2 + r^2}{2(q-l)^2} \right] \left[\frac{2(q-l)}{(q-l)^2 + r^2} \right]^4 dq$$

$$= - \frac{8(q-l)^2}{[(q-l)^2 + r^2]^3} dq \tag{A.19}$$

When

$$z_2 = 0,\ q = l + z_1 + \sqrt{z_1^2 + r^2}$$

$$z_2 = l_1\ q = z_1 + \sqrt{(l - z_1)^2 + r^2}$$

$$I_o = 8K \int_{R_i}^{R_o} r^3 dr \int_o^l e^{-\beta_1 z_1}\, dz_1 \int_{z_1 + \sqrt{(l-z_1)^2 + r^2}}^{l + z_1 + \sqrt{z_1^2 + r^2}} dq\ \frac{(q-l)^2}{[(q-l)^2 + r^2]^3}\ \delta(t - \frac{1}{c}q) \tag{A.20}$$

In this expression

$$\int \frac{(q-l)^2}{[(q-l)^2 + r^2]^3}\ \delta(t - \frac{q}{c}) dq$$

$$= \begin{cases} \dfrac{(ct-l)^2}{[(ct-l)^2 + r^2]^3} & \text{If the point } q = ct \text{ is between the limits of integration} \\ 0 & \text{If the point } q = ct \text{ is outside of the limits of integration} \end{cases} \tag{A.21}$$

So

$$I_o = 8K \int_{R_i}^{R_o} r^3 dr \int_{\zeta_1}^{\zeta_2} e^{-\beta_1 z_1}\, dz_1\ \frac{(ct-l)^2}{[(ct-l)^2 + r^2]^3} \tag{A.22}$$

It is noticed that the limits of the z_1 integration are no longer 0 and l but are now ζ_1 and ζ_2. This is because the integration over q gives zero for some values of z_1. ζ_1 and ζ_2 will be determined later from geometric considerations.

Integrating over z_1

$$I_o = \frac{8K}{\beta_1} \left(e^{-\beta_1 \zeta_1}\ e^{-\beta_1 \zeta_2}\right) \int_{R_i}^{R_o} r^3 dr\ \frac{(ct-l)^2}{[(ct-l)^2 + r^2]^3} \tag{A.23}$$

The last integration can be performed in the following way

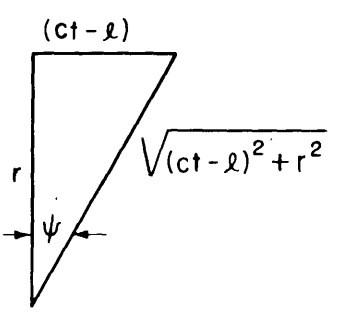

Figure A.4

From Fig. A.4

$$r = (ct-l)\cot\psi = (ct-l)\ \frac{\cos\psi}{\sin\psi} \tag{A.24}$$

giving

$$dr = -(ct-l)\csc^2\psi d\psi = -(ct-l)\frac{1}{\sin^2\psi}\,d\psi$$

$$\sqrt{(ct-l)^2 + r^2} = \frac{(ct-l)}{\sin\psi}$$

and

$$\frac{r^3 dr (ct-l)^2}{[(ct-l)^2 + r^2]^3} = \frac{-(ct-l)^6 \dfrac{\cos^3\psi}{\sin^3\psi}\cdot\dfrac{1}{\sin^2\psi}\,d\psi}{\dfrac{(ct-l)^6}{\sin^6\psi}}$$

$$= -\cos^3\psi \sin\psi\, d\psi\,. \tag{A.25}$$

This can be integrated

$$-\int \cos^3\psi \sin\psi d\psi = +\frac{\cos^4\psi}{4} = \frac{1}{4}\frac{r^4}{[(ct-l)^2 + r^2]^2} \tag{A.26}$$

and thus

$$\int_{Ri}^{Ro} r^3 dr \frac{(ct-l)^2}{[(ct-l)^2 + r^2]^3} = \frac{1}{4}\left\{\frac{R_o^4}{[(ct-l)^2 + R_o^2]^2} - \frac{R_i^4}{[(ct-l)^2 + R_i^2]^2}\right\} \tag{A.27}$$

which gives

$$I_o = \frac{2K}{\beta_1}\left(e^{-\beta_1\zeta_1} - e^{-\beta_1\zeta_2}\right)\left\{\frac{R_o^4}{[(ct-l)^2 + R_o^2]^2} - \frac{R_i^4}{[(ct-l)^2 + R_i^2]^2}\right\}. \tag{A.28}$$

The response to a Dirac Delta function may be plotted from Equation A.28. The above procedure is not strictly correct since ζ_1 and ζ_2 are functions of r and the factor $(e^{-\beta_1\zeta_1} - e^{-\beta_1\zeta_2})$ should have been included in the integration over r. However, this factor is not sensitive to r and r can be replaced by $R_{ave.}$ in this factor. ζ_1 and ζ_2 can now be determined.

From Figure A.5 it is seen that the current begins to arrive at the terminal at $t = (1/c)\sqrt{l^2 + R_{ave.}^2}$

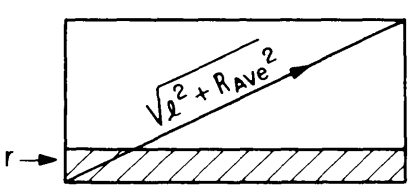

Figure A.5

Then for times slightly greater than this, several paths contribute to the signal, see below

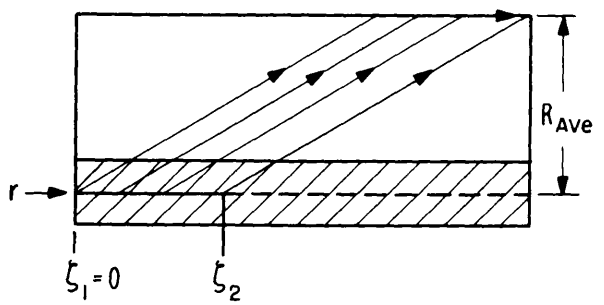

Figure A.6

and also from the figure

$$ct = \zeta_2 + \sqrt{(l-\zeta_2)^2 + R_{ave}^2}$$

$$\zeta_2 = \frac{\left(c^2t^2 - l^2 - R_{ave}^2\right)}{2(ct-l)}. \tag{A.29}$$

So here the limits are

$$\begin{cases} \zeta_1 = 0 \\ \zeta_2 = \dfrac{(c^2t^2 - l^2 - R_{ave}^2)}{2(ct-l)} \end{cases}.$$

The current reaches its maximum value when (approximately) $t = (1/c)(l + R_{ave})$ and the paths are as shown

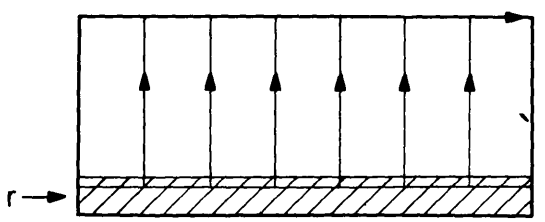

The limits here are

$$\begin{cases} \zeta_1 = 0 \\ \zeta_2 = l \end{cases}$$

Figure A.7

At times greater than this the longer paths begin to contribute

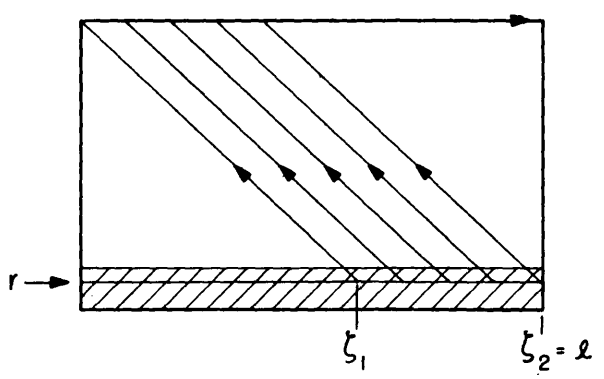

Figure A.8

and

$$ct = \zeta_1 + l + \sqrt{\zeta_1^2 + R_{ave}^2}$$

$$\zeta_1 = \frac{(ct-l)^2 - R_{ave}^2}{2(ct-l)}, \text{ and limits are } \begin{cases} \zeta_1 = \dfrac{(ct-l)^2 - R_{ave}^2}{2(ct-l)} \\ \zeta_2 = l \end{cases}. \tag{A.30}$$

Finally when $t = 1/c\ (l + \sqrt{l^2 + R_{av}^2} + l)$, the current drops to zero.

A plot of I_0 vs t can now be made using equation A.28. The response of the detector is plotted considering its length to be 42 centimeters (the length of the scintillator in the actual detector). Another plot is made for a detector length of 18 centimeters (the length of the photocathode in the actual detector). R_{ave} is 8 cm. in both cases. The curves are plotted in Figure 35. Zero time has been taken as the time when the radiation strikes the leading face of the detector.

It can be seen from the shape of the curves in Figure 35 that the shape is only slightly affected by the length of the detector. The amplitude of the response does, of course, depend on the detector length since the longer detector will have a larger sensitive volume of scintillator; however, since the response to $Ce^{\alpha t}$ is ultimately expressed in terms of the response to a constant unit γ-ray intensity which is an experimentally measurable quantity, it is only the shape of the curves that need consideration.

It should be noted that the curves are very narrow (the half width is about 0.3×10^{-9} sec.). This indicates that most of the light which is collected is that which takes the shortest path from the point of scintillation to the cathode. This fact is the basis for an approximation which will be used in the next two sections. In the preceding analysis the attenuation of the fluorescent radiation in the scintillator and the reflection at the glass interface has been neglected. Qualitative considerations indicate that these two effects would further reduce the width of the response.

For simplicity an approximation to $f_1(t)$ is used in the calculation of the sensitivity reduction factor in Section 2. A plot of this function

$$A\left[e^{-\frac{1}{\tau_1}(t-a)} - e^{-\frac{1}{\tau_2}(t-a)}\right] \tag{A.31}$$

is also given in Figure 35 where

$$\tau_1 = 0.137 \times 10^{-9} \text{ sec.}$$

$$\tau_2 = 0.130 \times 10^{-9} \text{ sec.}$$

The factors A and α have been chosen so that the above function approximates $f_1(t)$ for $l = 42$ cm. The numerical values of A and α are not significant since the sensitivity reduction factor depends only on τ_1 and τ_2, and these are the same for $l = 42$ cm and 18 cm.

A.2 Detector Response - Case 2, Calculation of $f_1(t)$ for the Case of the Open Circuited Detector with the Axis Pointing at the Source of Radiation.

In the last section it was assumed that the end of the detector nearest the source of radiation was terminated in its characteristic impedance so that no reflection occurs from this end. These results will now be extended to the case in which the end of the detector is open circuited so that complete reflection occurs.

$f_1(t)$ may be divided into the two parts $R_1(t)$ and $R_2(t)$, where $R_1(t)$ is the response already found (i.e., for a detector terminated in its characteristic impedance) and $R_2(t)$ is that part of the response due to reflection from the open circuited end. The approximate function

$$A\left[e^{-\frac{1}{\tau_1}(t-a)} - e^{-\frac{1}{\tau_2}(t-a)}\right] \tag{A.32}$$

found in the last section will be used for $R_1(t)$. In calculating $R_2(t)$ the approximation is made that only those light paths which strike the cathode perpendicularly contribute appreciably to the response. The results of the last section indicate that this approximation is a fairly good one. Such a path is shown below in Fig. A.9. Also r is replaced by the average value R_{ave}.

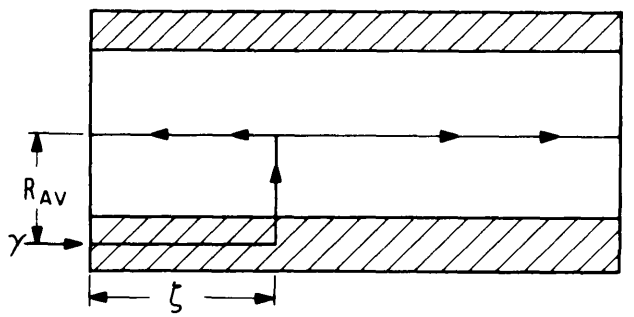

Figure A.9

From Figure A.9 it is seen that $R_2(t) = 0$ for $t < 1/c\ (l + R_{av}) = a'$ and also $R_2(t) = 0$ for $t > 1/c\ (3\,l + R_{av}) = b$. The pulse that travels over the path shown will arrive at the output terminal at the time

$$t = \frac{1}{c}(2\zeta + R_{av} + l).$$

Due to absorption of the gamma rays in the scintillator the pulse will be reduced in intensity by the factor

$$e^{-\beta_1 \zeta} = e^{-\beta_1 \frac{c}{2}[t - \frac{1}{c}(l + R_{av})]}$$

and $R_2(t)$ may be written as

$$R_2(t) = \begin{cases} 0 & t < a' \\ Ke^{-\beta_1 \frac{c}{2}(t-a')} & a' < t < b \\ 0 & t > b \end{cases} . \tag{A.33}$$

The total response to a δ-function is then

$$F_1(t) = R_1(t) + R_2(t)$$

where $R_2(t)$ is given above and $R_1(t)$ is

$$R_1(t) = \begin{cases} 0 & t < a \\ A\left[e^{-\frac{1}{\tau_1}(t-a)} - e^{-\frac{1}{\tau_2}(t-a)}\right] \end{cases} \tag{A.34}$$

Since as much current flows toward the open circuited end as flows toward the output terminal, the areas under $R_1(t)$ and $R_2(t)$ must be equal. It is convenient to set each of these areas equal to 1/2 so that the area under $f_1(t)$ is normalized to unity. This determines the constants A and K. Thus, from

$$\int_0^\infty R_1(t)dt = A(\tau_1 - \tau_2) = \frac{1}{2} \tag{A.35}$$

$$A = \frac{1}{2(\tau_1 - \tau_2)}$$

and from

$$\int_0^\infty R_2(t)dt = K \cdot \frac{2}{\beta_1 c}\left[1 - e^{-\frac{\beta_1 c}{2}(b-a')}\right] = \frac{1}{2} \tag{A.36}$$

$$K = \frac{\beta c}{4\left[1-\epsilon^{-\frac{\beta_1 c}{2}(b-a')}\right]} .$$

In using this function to calculate the sensitivity reduction factor the small difference between a and a′ has been ignored.

A.3 Detector Response - Case 3, Calculation of $f_1(t)$ for the Case of the Open Circuited Detector with the Radiation Entering from the Side.

As in the last section we will divide $f_1(t)$ into the two parts $R_1(t)$ and $R_2(t)$; only those light paths which strike the cathode perpendicularly are considered; r is replaced by R_{ave}. In addition absorption in the scintillator is neglected. The coordinates to be used are shown in Figure A.10.

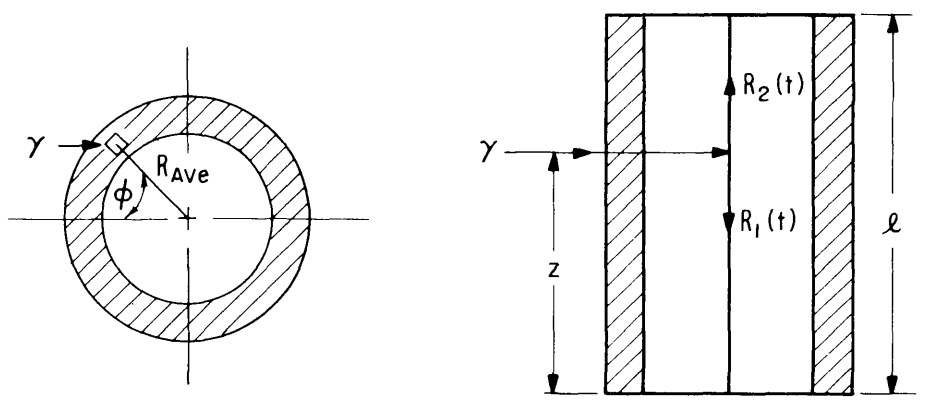

Figure A. 10

Consider first $R_1(t)$. If the γ-ray intensity is referred to the axis of the detector, it is seen from Figure 10 that the length of the path shown is

$$q_1 = R_{ave}(1-\cos\phi) + z_1 .$$

The response to a δ-function is found by adding up the contributions due to each of the paths. Therefore

$$R_1(t) = 2\int_0^l dz \int_0^\pi d\phi\,\delta(ct-q_1) . \tag{A.37}$$

It is helpful at this point to form a physical picture of what is happening. At a given time t there will be a set of paths in the detector which contribute to $R_1(t)$ (all other paths contribute to $R_1(t)$ at some other time). This set of paths is specified by the locus of points in the scintillator at which the γ-rays are absorbed, which yields a q_1, the path length in the detector, equal to ct. That is

$$R_{ave}(1-\cos\phi) + z = ct \tag{A.38}$$

and for a given value of t this relation between ϕ and z specifies the locus of points in the scintillator. The loci for several values of t are sketched in Fig. A.11.

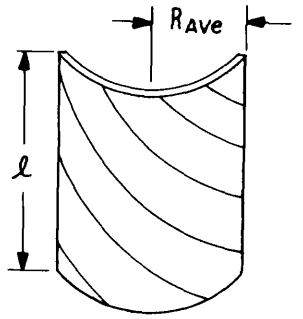

Figure A.11

Figure A.12 shows the half cylinder developed onto a plane surface with $X = R_{ave}$ $(1 - \cos\phi)$ so that $q_1 = x + z$.

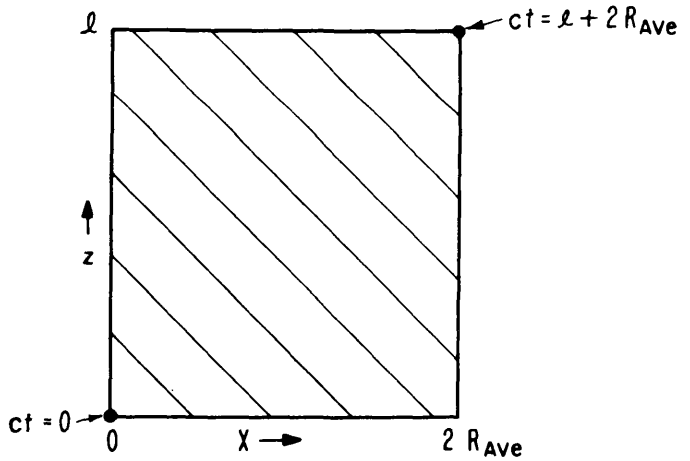

Figure A.12

Each diagonal corresponds to a value of ct between 0 and $l + 2R_{ave}$. Such a diagram is used later to determine the limits of the z integration. Now going back to the expression for $R_1(t)$

$$R_1(t) = 2\int_0^l dz \int_0^\pi d\phi\,\delta(ct-x-z)$$

In the last integral the variable of integration is changed from ϕ to x,

$$x = R_{ave}(1-\cos\phi)$$

$$dx = R_{ave}\sin\phi\, d\phi$$

$$d\phi = \frac{1}{R_{ave}\sin\phi}\, dx = \frac{dx}{\sqrt{2R_{ave}x-x^2}}$$

and

$$\int d\phi\ \delta(ct-x-z) = \int \frac{dx}{\sqrt{2R_{ave}x-x^2}}\ \delta(ct-x-z)$$

$$= \begin{cases} 0 & \text{If } x=ct-z \text{ is not between the limits of integration} \\ \dfrac{1}{\sqrt{2\,R_{ave}(ct-z)-(ct-z)^2}} & \text{If } x=ct-z \text{ is between the limits of integration.} \end{cases} \tag{A.39}$$

Therefore

$$R_1(t) = 2\int_{\zeta_1}^{\zeta_2} dz \frac{1}{\sqrt{2\,R_{ave}(ct-z)-(ct-z)^2}} \tag{A.40}$$

$$R_1(t) = 2\left[\sin^{-1}\left(1+\frac{\zeta_2}{R_{av}}-\frac{ct}{R_{ave}}\right)-\sin^{-1}\left(1+\frac{\zeta_1}{R_{ave}}-\frac{ct}{R_{ave}}\right)\right] \tag{A.41}$$

ζ_1 and ζ_2 are to be determined by solving the equation

$$ct = x + z$$

for z when x is given the values 0 and $2R_{ave}$. This is subject to the restriction that ζ_1 and ζ_2 must lie between 0 and l. An example will perhaps clarify this. Take l = 18 CM and $2R_{ave}$ = 16 CM then

$$ct = 9 = x + z$$

and substituting

$$x = 0$$

$$9 = 0+\zeta_2$$

$$\zeta_2 = 9.$$

Substituting

$$x = 2\,R_{ave} = 16$$

$$9 = 16 + \zeta_1$$

$$\zeta_1 = -7.$$

But this corresponds to a point below the bottom of the detector so ζ_1 must be taken as zero. (ζ_1 and ζ_2 may also be found by taking the limits of z of the diagonal lines in Figure 12.)

By taking a number of values of t, the corresponding values of ζ_1 and ζ_2 may be determined and a curve of $R_1(t)$ may be plotted.

Consideration is now given to $R_2(t)$.

$$R_2(t) = 2\int_0^{l} dz \int_0^{\pi} d\phi\ \delta(ct-q_2) \tag{A.42}$$

where

$$q_2 = R_{ave}(1-\cos\phi)+ z + 2(l-z)$$

$$= \text{Path length for the reflected pulse.}$$

Letting

$$x = R_{ave}(1-\cos\phi).$$

Then

$$\delta(ct-q_2) = \delta\left[c(t-\frac{l}{c}) - x - (l-z)\right].$$

Define

$$t' \equiv t - \frac{l}{c}$$

$$z' \equiv l - z \ .$$

If now the variable of integration is changed from z to z', $R_2(t)$ becomes

$$R_2(t) = 2\int_0^l dz' \int_0^\pi d\phi \ \delta(ct'-x-z'). \tag{A.43}$$

This is the same integral we had before for $R_1(t)$, but now the whole curve is shifted to the right by l/c due to the transformation from t to t'.

In Figure 36 the curve of

$$F_1(t) = R_1(t) + R_2(t)$$

is plotted. The ordinate scale is arbitrary since constant factors cancel out of the sensitivity reduction factor. It is seen that the curve may be roughly approximated by

$$F_1(t) = \begin{cases} 0 & t < 0 \\ \frac{t}{a} & 0 < t < a \\ 1 & a < t < b \\ \frac{c-t}{c-b} & b < t < c \\ 0 & t > c \end{cases}$$

with

$$a = 0.53 \times 10^{-9} \text{ sec.}$$

$$b = 1.2 \times 10^{-9} \text{ sec.}$$

$$c = 1.73 \times 10^{-9} \text{ sec.}$$

Appendix B
Transmission Line Response Consideration

It has been shown in Section 3 that the response of a transmission line having negligible shunt conductance can be analyzed for the sinusoidal, impulse, exponential and step function input. The response to other functions may be obtained indirectly by a graphical evaluation of the superposition integral. This has been done (12) by expressing Equation 3.20 as a Stieltjes integral (13). Figures 37, 38, and 39 show the response to a ramp, a cosine squared and a triangular driving function respectively.

These response functions have been plotted somewhat differently since the response is a function not only of time, t, and line constant, τ, but also of the rise time of the driving function, T. Thus the time scale has been expressed in terms of the rise time (t/T). Curve 0 in each case represents the input function. Curve 1 then represents the response of a line of arbitrary length chosen such that its time constant, τ, is 1/400 of the rise time, T. Curve 2 is the response of a line whose length is twice that of Curve 1 and so on. (Since τ is proportional to z^2, where z is line length, the time constant of the line for Curve 2 is four times that of Curve 1.) Thus the curve numbers represent multiples of the unit length. The unit length depends upon the cable characteristics and is given in the table for three standard air dielectric lines. The first column shows unit lengths for a unit time constant of 1/400 ns, the second column for 10/400 and the third for 100/400 ns.

Unit Transmission Line Lengths (meters)

Unit Time	1/400 ns	10/400 ns	100/400 ns
3 1/8 inch dia.	159	503	1590
1 5/8 inch dia.	80	253	800
7/8 inch dia.	41	130	410

Lengths shown are based on the conductivity of copper being approximately 5.8×10^7 Mho/meter. In practice the conductivity is somewhat poorer due to the presence of impurities. An approximate correction for this can be made by taking unit lengths as 10% shorter than those listed.

As a typical example consider the response of 1200 ft. of 7/8 inch line to a function rising in 1 ns. This length, about 370 meters, is 10% shorter than that shown for a unit time of 100/400 ns. The number of unit lengths is then $\sqrt{100/1} = 10$ and the response is curve 10, the time scale being in 1 ns units. If the rise time of the function had been 4 ns the number of unit lengths would have been $\sqrt{100/4} = 5$ and the response would be curve 5, the time scale being in 4 ns units.

[12] "Greenhouse Final Report," NRL Report 3978, Vol. V

[13] Nerken, Electrical Engineering, 56, (1937) pp. 768-9

Appendix C
Response of Electrical Networks to Exponential Driving Functions

Consider a series RLC circuit subjected to an exponential driving voltage of the form $Ee^{\alpha t}$;

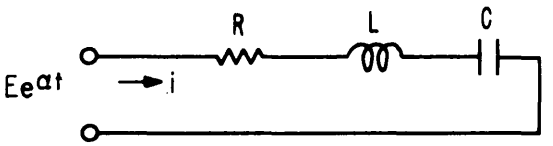

Figure C.1

The differential equation for this circuit in terms of the quantity of charge (q) is;

$$L\frac{d^2q}{dt^2} + R\frac{dq}{dt} + \frac{q}{c} = Ee^{\alpha t}. \tag{C.1}$$

Assume a solution for q of

$$q = AEe^{\alpha t}.$$

Substituting this assumed solution into the original differential equation yields

$$LAE\,\alpha^2 e^{\alpha t} + RAE\,\alpha\, e^{\alpha t} + \frac{AEe^{\alpha t}}{c} = Ee^{\alpha t}$$

$$AE\,e^{\alpha t}\left(\alpha^2 L + \alpha R + \frac{1}{c}\right) = Ee^{\alpha t}$$

$$A = \frac{1}{\alpha R + \alpha^2 L + \frac{1}{\alpha c}}$$

$$\therefore q = \frac{Ee^{\alpha t}}{\alpha R + \alpha^2 L + \frac{1}{c}}. \tag{C.2}$$

Since

$$i = \frac{dq}{dt}$$

$$i = \frac{d}{dt}\left[\frac{Ee^{\alpha t}}{\alpha R + \alpha^2 L + \frac{1}{c}}\right]$$

$$i = \frac{Ee^{\alpha t}}{R + \alpha L + \frac{1}{\alpha c}}. \tag{C.3}$$

Thus the equivalent exponential impedance (Z_e) on an exponential driving function is;

$$Z_e = R + \alpha L + 1/\alpha C.$$

The impedance of a resistance of R ohms on an exponential is a real positive value of R ohms magnitude. The impedance of an inductance of L henries on an exponential is a real positive value of α L ohms magnitude. The impedance of a capacitor of C farads on an exponential is a real positive value of $1/\alpha$ C ohms magnitude. Therefore the transformation

from sinusoidal impedance to exponential impedance is accomplished by substituting α for $j\omega$ of the sinusoidal case.

Using these impedance relationships allows circuits to be analyzed on an exponential in the same manner as sinusoidal circuit operation. Furthermore in the exponential case all impedances are real positive values which makes for extremely simple analysis. Since there are no negative terms there can be no resonance phenomena in these circuits on exponential signals.

In the solution of the differential equation for the RLC circuit on an exponential voltage the assumption is made that the voltage has existed since negative infinity in time. If the exponential starts at some finite time the exact solution would require an additional transient term to account for the step voltage E appearing at zero time. In practice, the exponential is first detected and measured several generations after zero time so that this original step transient has died out and can be neglected.

Appendix D
Comparison of Amplifier Response to Sinusoidal, Step Function and Exponential Signals

D.1 Introduction

It is often useful to be able to predict the response of an amplifier to one type of signal on the basis of its response to one or more other types of signals. The two most common means of specifying amplifier performance are on the basis of the 3 db bandpass of sinusoidal signals and on the basis of the rise time (10% to 90%) on a step function.

This appendix develops the relationship between the basic circuit parameters and the circuit response to sinusoidal, step function, and exponential signals with constant positive exponents. Furthermore, relationships are developed so that the response to one type may be predicted on the basis of the response to either of the other two.

D.2 Circuit Analysis

The basic circuit used in this analysis is a single RC-coupled vacuum tube stage. For purposes of this analysis only the high frequency limitations will be considered since this is usually the limiting condition on exponential signals in practice. The equivalent circuit for a single vacuum tube amplifier stage at high frequencies is:

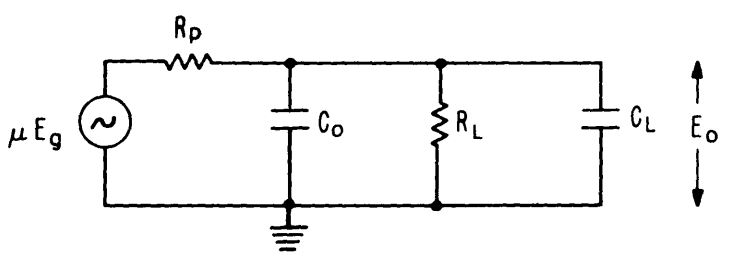

Figure D.1

Where μ = Amplification factor of the tube.

R_p = Dynamic plate resistance of the tube.

R_L = Plate load resistance.

C_o = Output capacity of the tube.

C_L = Input capacity of next stage plus strays.

E_g = Input voltage.

This circuit may be reduced to the following:

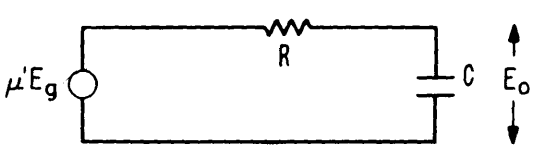

Figure D.2

Where

$$\mu' = \mu \frac{R_L}{R_p + R_L}$$

$$R = \frac{R_p R_L}{R_p + R_L}$$

$$C = C_o + C_L .$$

Thus, at high frequencies each vacuum tube stage acts like a constant voltage source feeding an RC network in which the output voltage appears across C.

D.3 Response of Cascaded Vacuum Tube Stages to a Sinusoidal Function

Using the equivalent circuit derived above for the case in which

$$E_g = E \text{ Sin } \omega t$$

$$E_o = \mu' E \text{ Sin } \omega t \left(\frac{1}{1 + jR\omega C}\right). \tag{D.1}$$

The 3 db cutoff for an RC network of this type occurs when $R = X_C$. (In all cases in this appendix, cutoff refers to the 3 db down response point.) Letting ω_H be that angular frequency for which $R = X_C$ gives

$$R = \frac{1}{\omega_H C} .$$

Substituting this in the equation above for E_O gives

$$E_o = \mu' E \text{ Sin } \omega t \left(\frac{1}{1 + j\frac{\omega}{\omega_H}}\right) \tag{D.2}$$

and the response for n such vacuum tube stages in cascade is

$$E_o = (\mu')^n E \text{ Sin } \omega t \left(\frac{1}{1+j\frac{\omega}{\omega_H}}\right)^n . \tag{D.3}$$

There are two quantities in this expression which describe the frequency dependent parameters of the amplifier. These are: ω_H which is the 3 db cutoff angular frequency for a single RC stage and n which is the number of such cascaded RC stages. Both of these quantities can be determined from a cw sinusoidal response curve of the amplifier. The quantity n is one sixth of the slope of the high frequency rolloff in db per octave and ω_H (the cutoff angular frequency of each stage) is that angular frequency for which the over-all amplifier response is down from the midfrequency gain by 3n db.

D.4 Response of Cascaded Vacuum Tube Stages to a Step Function

Using the equivalent circuit derived in Section D.2 for the case

$$E_g = \begin{Bmatrix} 0 & t < 0 \\ E & t > 0 \end{Bmatrix}$$

gives

$$E_o = \mu' E \left(1 - e^{-\frac{t}{RC}}\right) = E \left(1 - e^{-\omega_H t}\right) \tag{D.4}$$

where

$$\omega_H = \frac{1}{RC} \quad \text{as in Section D.3}$$

For n such vacuum tube stages in cascade

$$E_o = (\mu')^n E \left[1 - e^{-\omega_H t} \sum_{n=1}^{n=n} \frac{(\omega_H t)^{n-1}}{(n-1)!}\right]. \tag{D.5}$$

A plot of this equation for n from one to ten is shown on page 66 of Radiation Laboratory Series No. 18, "Vacuum Tube Amplifiers." It is ordinarily quite difficult to determine which of these curves one is working with when pulse testing an amplifier. For that reason it is usually convenient to use the curve for n = 1 and to get an equivalent amplifier time-constant $1/\omega_A$ on that basis.

Column 3 of Table D.1 lists the number of RC time constants required for a pulse to rise from 10% to 90% for values of n from one to ten. This data is taken from the Radiation Laboratory curves noted above.

Column 4 of Table D.1 gives the RC time constant required in each stage of Column 3 to maintain an over-all amplifier rise time of 10 ns while the corresponding angular cutoff frequency of each stage is shown in Column 5 (i.e., $\omega_{H-} = 1/RC$). Column 6 is the calculated stage cutoff angular frequency required in each case to maintain an over-all amplifier cutoff of 220 x 10^6 radians per second.

It will be noted that Columns 5 and 6 are very nearly identical for each value of n. There is actually a ±4% variation in them but this is very probably due to reading errors in taking the data from the Radiation Laboratory curves. This close agreement between Columns 5 and 6 indicates that amplifier rise time is dependent solely on the over-all amplifier cutoff frequency and is independent of the slope of the sinusoidal response rolloff. Also it means that it makes no difference in amplifier analysis which value of n is used (at least between 1 and 10) as long as the same value of n is selected in both the step function case and the sinusoidal case.

TABLE D.1

1	2	3	4	5	6
n	Rise Time $t_{(10-90\%)}$	RC Time Constants to go from 10% to 90%	RC Time Constant of Each Stage (10^{-9})	Stage Cutoff Angular Freq. (10^6)	Stage Cutoff Freq. for Constant $\omega_A = 220 \times 10^6$ (10^6)
1	10 x 10^{-9}	2.2	4.54	220	220
2	10 x 10^{-9}	3.4	2.94	340	345
3	10 x 10^{-9}	4.2	2.38	420	434
4	10 x 10^{-9}	5.0	2.0	500	493
5	10 x 10^{-9}	5.6	1.785	560	572
6	10 x 10^{-9}	6.1	1.64	610	629
7	10 x 10^{-9}	6.6	1.515	660	680
8	10 x 10^{-9}	7.05	1.42	705	733
9	10 x 10^{-9}	7.6	1.317	760	777
10	10 x 10^{-9}	8.0	1.25	800	821

For example, if the rise time of an amplifier is known but the proper value of n to use is not known, any value of n may be selected to obtain a value for stage time constant from the Radiation Laboratory curves. The stage time constant is then converted to stage cutoff frequency which will be identical to over-all amplifier 3 db cutoff frequency.

Referring again to Table D.1 it is seen that a three stage amplifier having a stage cutoff frequency of 420 x 10^6 radians per second is exactly the same, on the basis of the 10-90% rise time and 3 db sinusoidal cutoff, as a single stage amplifier having a stage cutoff frequency of 220 x 10^6 or a ten stage amplifier having a stage cutoff frequency of 800 x 10^6 radians per second. In all of these cases the cutoff frequency for the over-all amplifier is 220 x 10^6 radians per second and the rise time of the amplifier is 10 ns. For this reason there is no point in using a value of n other than unity when converting from amplifier rise time to amplifier sinusoidal response or vice versa.

Since it takes 2.2 RC (n = 1) for a signal to rise from 10-90% on a step function the following expression holds

$$t_{10\text{-}90\%} = 2.2\ RC \quad \text{for } n = 1 \tag{D.6}$$

and by definition

$$\omega_H = \frac{1}{RC}.$$

Where the 3 db cutoff angular frequency point for each stage occurs at ω_H, the relationship between the rise time of a single RC stage and ω_H $(= 2\pi f_H)$ is

$$t_{10\text{-}90\%} = \frac{2.2}{\omega_H} = \frac{.35}{f_H} \quad \text{for } n = 1. \tag{D.7}$$

In the preceding paragraphs it was shown that the same relationship between the 3 db amplifier cutoff angular frequency, ω_A, and rise time holds for all values of n as holds for n = 1. Therefore:

$$t_{10\text{-}90\%} = \frac{2.2}{\omega_A} = \frac{.35}{f_A} \tag{D.8}$$

where the over-all 3 db amplifier cutoff angular frequency is ω_A $(= 2\pi f_A)$.

D.5 Response of Cascaded Vacuum Tube Stages to an Exponential Function

Using the equivalent circuit derived in Section D.2 for the case where

$$E_g = Ee^{\alpha t}$$

gives

$$E_o = \mu' Ee^{\alpha t} \left(\frac{1}{1 + \frac{\alpha}{\omega_H}} \right)$$

where

$$\omega_H = \frac{1}{RC} \quad \text{as in Section D.2.}$$

For n such stages in cascade the expression for E_O becomes

$$E_o = (\mu')^n Fe^{\alpha t} \left(\frac{1}{1 + \frac{\alpha}{\omega_H}} \right)^n. \tag{D.9}$$

Here again n and ω_H are the significant amplifier parameters. The last term in this expression is referred to as the gain reduction factor (GRF).

D.6 Comparison of Sinusoidal, Step Function and Exponential Response

Equations D.3, D.5, and D.9 are the pertinent equations for relating the performance on sinusoidal, step function and exponential signals. These equations are shown in Table D.2.

TABLE D.2

Sinusoidal:

1. $E_O = (\mu')^n \; E \; \text{Sin}\, \omega t \left(\frac{1}{1+j\frac{\omega}{\omega_H}}\right)^n$

2. n = Number of cascaded stages. = One sixth the slope of the sinusoidal rolloff in db/octave

3. $\omega_H = \frac{1}{RC}$ = 3 db cutoff angular frequency of each stage, or the angular frequency for which the response of the over-all amplifier is down from the midfrequency response by 3n db.

Step Function:

1. $E_O = (\mu')^n \; E \left[1 - e^{-\omega_H t} \sum_{n=1}^{n=n} \frac{(\omega_H t)^{n-1}}{(n-1)!}\right]$

2. $t_{10-90\%} = \frac{2.2}{\omega_A} = \frac{.35}{f_A}$

3. $\omega_A = 2\pi f_A$ = Over-all amplifier cutoff angular frequency for which the amplifier response is down by 3 db from the midfrequency gain.

Exponential:

1. $E_O = (\mu')^n \; Ee^{\alpha t} \left(\frac{1}{1+\frac{\alpha}{\omega_H}}\right)^n$

2. $GRF = \left(\frac{1}{1+\frac{\alpha}{\omega_H}}\right)^n$

In all cases:

$\omega_H = \frac{1}{RC}$ = 3 db cutoff angular frequency of each stage.

n = Number of cascaded stages.

The rise time of an amplifier versus the amplifier cutoff frequency, f_A, is shown in Figure 40. In addition the GRF for several values of alpha and for n = 1 versus f_A are also shown.

Comparison of step function and exponential signal performance leads to an interesting conclusion. It was shown in Section D.4 (Equation D.8) that it is necessary to know only the cutoff frequency of the amplifier in order to calculate its rise time. It is not necessary to know the value of n, which is another way of saying that it is not necessary to know the slope of the sinusoidal rolloff curve. On the other hand, Equation D.9 indicates clearly that both ω_H and n must be known in order to calculate the GRF on an exponential signal.

Table D.3 shows the manner in which the GRF varies with n for an alpha of 2.5×10^8 and a constant over-all amplifier cutoff frequency, f_A, of 100 mc (corresponding to an amplifier rise time of 3.5 ns.)

TABLE D.3

n	Alpha	f_A Complete Amp.	f_H Ea. Stage	GRF
1	2.5×10^8	100 mc	100 mc	.716
2	2.5×10^8	100 mc	157 mc	.636
3	2.5×10^8	100 mc	197 mc	.574
4	2.5×10^8	100 mc	224 mc	.517
5	2.5×10^8	100 mc	260 mc	.49
6	2.5×10^8	100 mc	286 mc	.456
7	2.5×10^8	100 mc	309 mc	.432
8	2.5×10^8	100 mc	333 mc	.405
9	2.5×10^8	100 mc	353 mc	.38
10	2.5×10^8	100 mc	373 mc	.36

It will be noted that the GRF varies by 2:1 over the range of n from one to ten for the same over-all amplifier cutoff frequency (100 mc) and rise time (3.5 ns). This shows that in order to predict the GRF on an exponential signal that both ω_H and n must be known. Usually this can be determined only from the sinusoidal response data. It should be noted also that the stage cutoff frequency for n = 10 must be 3.73 times that for n = 1 in order to maintain the 100 mc over-all cutoff frequency. It would be necessary to use a stage cutoff frequency of 1170 mc for n = 10 in order to obtain the same GRF (0.716) as that for a single stage with a 100 mc cutoff frequency.

Appendix E
Spectrum Analysis of Exponential Signals

E.1 General

In Appendix C the response of various circuits to exponential signals was investigated using conventional transient analysis. Another approach to the problem involves the use of the Fourier transform of the exponential signal and the combination of the Fourier transform with the sinusoidal response characteristics of the network under test to obtain the Fourier integral. The Fourier integral describes the response of the network to the exponential driving function. An extension of this method yields a simplified network analysis based on the use of equivalent RC networks.

This appendix is concerned with developing convenient means of evaluating amplifier performance on exponential driving functions through utilization of the frequency-amplitude spectrum of the exponential by a simple graphical analysis. This method does not yield an exact solution, but is very helpful in setting up system requirements for specific alphas.

E.2 Network Analysis with the Fourier Transform

If the driving function, f(t), is such that

$$f(t) = \begin{Bmatrix} e^{\alpha t} & t < \Delta \\ 0 & t > \Delta \end{Bmatrix} \tag{E.1}$$

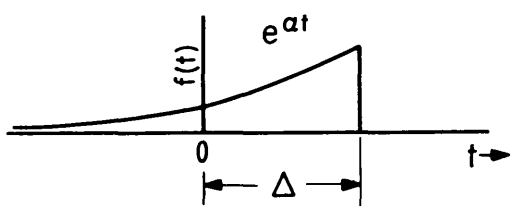

Figure E.1

the Fourier transform, f (ω), of this function is given by:

$$f(\omega) = \frac{1}{\sqrt{2\pi}} \int_{-\infty}^{\Delta} e^{-j\omega t} \; e^{\alpha t} \, dt$$

$$= \frac{1}{\sqrt{2\pi}} \int_{-\infty}^{\Delta} e^{(\alpha - j\omega)t} \, dt$$

$$= \frac{1}{\sqrt{2\pi}} \; \frac{1}{\alpha - j\omega} \left[e^{(\alpha - j\omega)\Delta} - 0 \right]$$

$$= \frac{1}{\sqrt{2\pi}} \; \frac{1}{\alpha - j\omega} \; e^{\alpha\Delta} \, e^{-j\omega\Delta} \tag{E.2}$$

This Fourier transform (E.2) may be used to determine the response of electrical networks to exponential signals of this type by means of the Fourier integral. The Fourier integral, f(t), is defined by the following expression in terms of the Fourier transform, $f(\omega)$, and the sinusoidal response of the network, $A(\omega)$

$$f(t) = \frac{1}{\sqrt{2\pi}} \int_{-\infty}^{\infty} e^{j\omega t} \, [f(\omega)] \, [A(\omega)] \, d\omega. \tag{E.3}$$

For example, the sinusoidal response of single low pass RC network is given by the expression

$$A(\omega) = \frac{\omega_H}{\omega_H + j\omega} \tag{E.4}$$

where

$$\omega_H = \frac{1}{RC}.$$

The response of this low pass RC network to the exponential is then given by the Fourier integral

$$f(t) = \frac{1}{\sqrt{2\pi}} \int_{-\infty}^{\infty} \left[e^{j\omega t}\right] \left[\frac{e^{(\alpha - j\omega)\Delta}}{\sqrt{2\pi}(\alpha - j\omega)}\right] \left[\frac{\omega_H}{\omega_H + j\omega}\right] d\omega$$

$$= \left\{ \begin{array}{ll} e^{\alpha t} \dfrac{\omega_H}{\alpha + \omega_H} = e^{\alpha t} \dfrac{1}{1 + \dfrac{\alpha}{\omega_H}} & \text{for } t < \Delta \\[2ex] e^{\alpha\Delta} e^{-\omega_H (t - \Delta)} \dfrac{1}{1 + \dfrac{\alpha}{\omega_H}} & \text{for } t > \Delta \end{array} \right\}. \tag{E.5}$$

Considering only the period $t < \Delta$ it is seen that the result is the same as the GRF portion of Equation 4.5, which is discussed in Section 4.3.

The above case for a single RC network may be extended to that for n cascaded networks

$$A_n(\omega) = \frac{\omega_H^n}{(\omega_H + j\omega)^n}$$

$$A_n(\omega) = \frac{\omega_H^n (-1)^{n-1}}{(n-1)!} \frac{d^{n-1}}{d\,\omega_H^{n-1}} \frac{1}{\omega_H + j\omega}$$

$$A_n(\omega) = \frac{(-1)^{n-1}}{(n-1)!} \omega_H^n \frac{d^{n-1}}{d\omega_H^{n-1}} \frac{A_{(n-1)}(\omega)}{\omega_H}$$

hence

$$f_n(t) = \frac{(-1)^{n-1}}{(n-1)!} \omega_H^n \frac{d^{n-1}}{d\,\omega_H^{n-1}} \frac{f_{(n-1)}(t)}{\omega_H}$$

$$= \frac{(-1)^{n-1}}{(n-1)!} \omega_H^n \frac{d^{n-1}}{d\,\omega_H^{n-1}} \left[\frac{e^{\alpha t}}{\alpha + \omega_H}\right] \text{for } t < \Delta$$

$$= e^{\alpha t} \left[\frac{\omega_H}{\alpha + \omega_H}\right]^n$$

$$= e^{\alpha t} \left[\frac{1}{1 + \dfrac{\alpha}{\omega_H}}\right]^n. \tag{E.6}$$

This same technique may be used to determine the response of n cascaded high pass RC networks to an exponential, thus

$$f_n(t) = e^{\alpha t} \left[\frac{1}{1 + \frac{\omega_L}{\alpha}} \right]^n \tag{E.7}$$

where

$$\omega_L = \frac{1}{RC}.$$

This method of determining the performance of electrical networks by taking the Fourier integral of the combination of their sinusoidal characteristics and the Fourier transform of the input exponential voltage works quite nicely for the simple RC networks which have been considered. The sinusoidal characteristic of more intricate networks involving R, L, and C in various combinations are much more complicated, and obtaining the Fourier integral of these is often difficult. For that reason it is desirable to use a method of analysis based on the principle that if two networks have identical sinusoidal response characteristics they will have identical exponential characteristics (See Equation E.3). The technique is to replace the complicated R, L, C network with a cascaded RC network which matches the sinusoidal response of the original as closely as possible. This is done most easily by determining the number of equivalent cascaded RC stages, n, from the sinusoidal response curve of the original network

$$n = \frac{\text{Slope of the rolloff in db per octave}}{6} \tag{E.8}$$

and either ω_H or ω_L (or both) which correspond to the angular frequency at which the sinusoidal response of the original network is 3n db below the midfrequency response. Once n, ω_H, and/or ω_L have been determined the response of the equivalent RC network (and therefore the approximate response of the original network) to an exponential are determined by using Equation E.6 or E.7 or the product of them if it applies. This method of analysis, based on the use of equivalent cascaded RC networks, has proven to be quite accurate on a number of distributed amplifiers and line filters tested with exponential signals. It appears that if there is little or no cw response overshoot this method gives an accurate exponential gain figure for the network.

E.3 Spectrum Analysis

Investigation of the Fourier transform of the exponential (E.2) for the relative amplitudes of the sinusoidal components of the exponential is of value in designing and evaluating network performance on this type of signal. It is apparent from Equation E.2 that the amplitude of the spectrum is increasing at an exponential rate proportional to $e^{\alpha t}$ but that the relative amplitude-frequency spectrum at any instant ($t < \Delta$) is proportional to

$$f(\omega) \sim \frac{1}{\alpha - j\omega}. \tag{E.9}$$

A plot of Equation E.9 showing the normalized voltage magnitude and the phase angle versus ω/α is shown in Figure 8, Curves A and B, respectively. Investigation of Equation E.9 shows that the maximum occurs at an angular frequency, ω, equal to zero; that the magnitude of the voltage is 0.707 of the maximum at an angular frequency equal to alpha; and that the voltage decreases at a rate approaching 20 db per decade beyond this point.

From the preceding analysis it appears that in a system designed to pass exponential signals, the response in the frequency range between $\omega = 0$ and $\omega = \alpha$ is of primary importance and that the range above $\omega = \alpha$ is of lesser importance. However, Equations E.2 and E.9 represent the amplitude of each individual frequency in the spectrum. In general the response characteristics of most networks are approximately frequency proportional.

For example, the response rolloff rates of simple RC networks are frequency proportional since they are expressed as so many db per decade or octave and not on the basis of db for a fixed number of cycles. Furthermore, the degree of difficulty of building bandpass electrical networks is not determined by a fixed bandpass interval of so many cycles but is a function of the number of decades or octaves which are passed. For a spectrum of steady-state sinusoidal voltages the resultant voltage of the components in the bandpass interval is the rms sum of the component voltages. If the bandpass interval has been chosen to be frequency proportional the number of cycles in each interval will be proportional to a midfrequency ω_0. Thus the amplitude of the resultant voltage, as a function of the midfrequency ω_0, will be proportional to $\sqrt{\omega_0}$.

For the exponential signal the frequency components are not in a steady state condition and the rms sum of the component voltages has no direct meaning. However, from practical experience with bandpass devices, it is found that this concept is still useful.

Then the magnitude of the rms sum of the sinusoidal components in an exponential, as a function of the midfrequency of a frequency proportional interval, is

$$|f(\omega_0)| \sim \sqrt{\frac{\omega_0}{\alpha^2 + \omega_0^2}} \, . \tag{E.10}$$

A plot of Equation E.10 showing the relative voltage in each decade is shown in Curve C in Figure 8, with the results normalized so that the maximum equals unity. Investigation of this equation (E.10) for the relative voltage in each frequency proportional interval discloses that the maximum occurs at an angular frequency equal to alpha; that the interval voltage is 0.707 of maximum at $\omega = 3.7\alpha$ and $\omega = \alpha/3.7$; that the spectrum decreases symmetrically (on a logarithmic plot) both sides of $\omega = \alpha$ and approaches a rolloff rate of 10 db per decade. This curve clearly shows that intervals geometrically spaced about $\omega = \alpha$ make equal contributions to the exponential.

The type of bandpass device to use for optimum efficiency in amplifying an exponential can immediately be inferred from this Curve C. Assume, for example, that a conventional bandpass device is to be used having a region of uniform gain and a symmetrical rolling off of response at the low and high frequencies. The maximum output for this bandpass device would be obtained when the geometric mean of its angular frequency bandpass, $\sqrt{\omega_H \omega_L}$, was made to coincide with alpha.

The use of a low pass device such as a simple RC network will serve as another example in applying this spectral distribution information. Assume that the high frequency 3 db response point of a low pass network occurs at an angular frequency equal to alpha. The effect of changing the slope of the rolloff curve is now apparent in that varying amounts of the higher frequency contributions are passed. The advantage of slow rolloff in networks for exponential signals is readily apparent.

It should be noted that Curves A and C of Figure 8 represent the relative rms voltage. The phase characteristics of the exponential signal have not been considered. Furthermore, in the two examples noted above the phase characteristics of the bandpass devices have been ignored and only the relative amplitude response information used in each case. Since the phase characteristics of both the signal and the bandpass device is ignored in this type of analysis it can yield only an approximate solution. Hence, this concept should only be used where its limitations are known.

Appendix F
Response of Simple Shunt Fed Amplifier to Exponential Signals

In Appendix E it is shown that maximum gain is obtained from an amplifier which is adjusted to give as much gain over as wide a frequency range as possible (without regard to uniformity of gain). A simple shunt fed capacity coupled amplifier circuit most nearly satisfies this condition using conventional vacuum tubes. Consider the equivalent circuit for one pentode stage of such an amplifier;

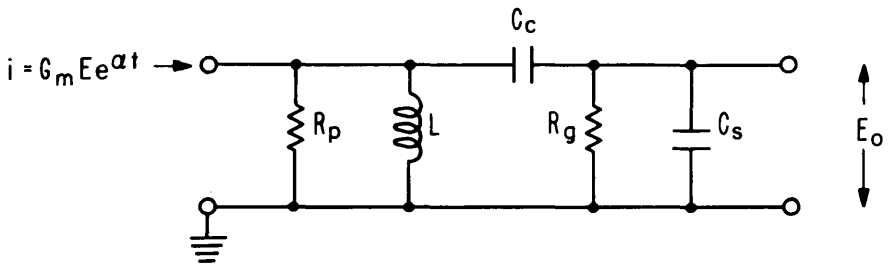

Figure F.1

It is obvious from the above circuit that the shunt impedance loading to ground should be minimized in order to achieve maximum gain. Practically, this means making L of such a value that its exponential impedance, α L, is much larger than the exponential impedance of the shunt capacity to ground, $1/\alpha$ C_S (C_S is equal to the sum of the output capacity of the stage, the input capacity of the next stage, plus the stray circuit capacities).

As pointed out in the Section 4.4 the voltage level in a decade three decades either side of the angular frequency equal to alpha is less than 5% of the voltage contribution in the decade geometrically centered over alpha. Therefore, there is little to be gained by passing the frequency range beyond these limits. From this a lower limit is placed on L for α L to be large compared to the other shunt components in the desired passband range.

In practice the gain is almost solely a function of $1/\alpha C_S$ because with the usual alpha values this term is considerably smaller (in the band pass and frequency range necessary for that particular exponential) than the other shunt impedances. It is also larger than the impedance of the coupling capacitor ($1/\alpha C_c$). The equivalent circuit in this case reduces to;

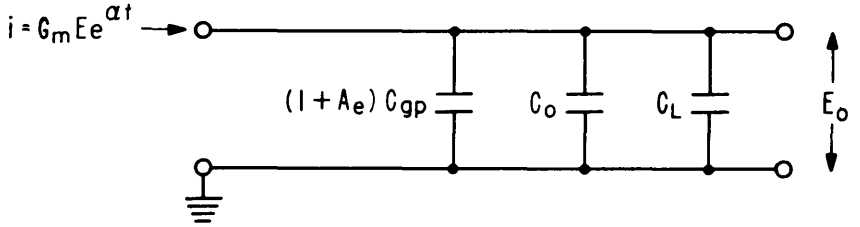

Figure F.2

$Ee^{\alpha t}$ = Input voltage to grid of tube.

G_m = Transconductance of tube.

C_L = Input capacity of next stage or deflection plates of cathode-ray tube, and strays.

C_o = Plate to screen, cathode, and heater capacity.

C_{gp} = Plate to grid capacity.

A_e = Exponential gain = $G_m/\alpha C_s$.

C_s = $C_o + (1 + A_e) C_{gp} + C_L$.

From this

$$A_e = G_m/\alpha C_s = \frac{G_m}{\alpha[C_L + C_o + (1 + A_e) C_{gp}]} \tag{F.1}$$

giving for the exponential gain

$$A_e = \frac{-\left[\frac{C_o + C_L + C_{gp}}{C_{gp}}\right] \pm \sqrt{\left[\frac{C_o + C_L + C_{gp}}{C_{gp}}\right]^2 + \frac{4\, G_m}{\alpha\, C_{gp}}}}{2} \tag{F.2}$$

Equation F.1 shows that the exponential gain is very nearly inversely proportional to alpha for large values of alpha (i.e., when $[(1+A_e)C_{gp}] << [C_o+C_L]$). As alpha is reduced the exponential gain increases, and when $[(1+A_e)C_{gp}]$ is comparable in magnitude to $[C_o+C_L]$ the gain begins to vary approximately as the inverse of the square root of alpha. This deviation from inverse proportionality is caused by the onset of the Miller effect which is accounted for by the $(1+A_e)$ term. A plot of alpha vs. the gain obtainable from a single 418-A stage having a G_m of 24,000 micromhos, a C_o of 2.7 $\mu\mu$f, a C_{gp} of .05 $\mu\mu$f and working into device having a shunt capacity of 6.6 $\mu\mu$f is shown on Figure 41. In addition, the gain obtainable under the same operating conditions but neglecting Miller effect is shown on the same figure.

Appendix G
Amplifier Linearity Considerations

The gain-input voltage relationships of most amplifiers may be expressed as

$$A' = A \frac{1}{1 + \left[\frac{E_{in}}{E_L}\right]^m} \tag{G.1}$$

where

A' = Actual voltage gain.

A = Voltage gain in the linear region.

E_{in} = Amplifier input voltage.

E_L = Input voltage for which the actual gain (A') is 50% of the gain in the linear region (A).

m = The exponent of the E_{in}/E_L ratio which makes this expression match as closely as possible the gain-input voltage relationship of the specific amplifier under consideration.

In order to write this equation for any particular amplifier it is necessary to use a curve fitting technique. The input voltage, E_L, for which the A'/A ratio is 0.5 is determined from the measured linearity data and a plot is made of the measured A'/A versus E_{in}/E_L for the amplifier. Various values of m are then substituted into Equation G.1 until the resulting calculated curve agrees as closely as possible with the measured curve.

Consider an input signal, E_{in}, to the amplifier of $Ee^{\alpha t}$. The output voltage, E_o, will be

$$E_o = A'E_{in} = A'Ee^{\alpha t} = AEe^{\alpha t} \frac{1}{1 + \left[\frac{E_{in}}{E_L}\right]^m} . \tag{G.2}$$

Since E_{in} is $Ee^{\alpha t}$, then E_L will equal $Ee^{\alpha t_L}$, where t_L is the time at which the amplifier gain is 50% of the linear gain.

$$E_o = AEe^{\alpha t} \frac{1}{1 + \left[\frac{Ee^{\alpha t}}{Ee^{\alpha t_L}}\right]^m} = AEe^{\alpha t} \frac{1}{1 + e^{m\alpha(t - t_L)}} .$$

Taking the logarithm of this equation yields,

$$ln\ E_o = \alpha t + ln\ AE - ln \left[1 + e^{m\alpha(t - t_L)}\right]$$

and differentiating this expression with respect to time gives

$$\frac{d\ ln\ E_o}{dt} = \alpha - \frac{m\ \alpha\ e^{m\alpha(t - t_L)}}{1 + e^{m\alpha(t - t_L)}}$$

$$= \alpha \left[1 - \frac{me^{m\alpha(t - t_L)}}{1 + e^{m\alpha(t - t_L)}}\right] \tag{G.3}$$

Substituting

$E_{in} = Ee^{\alpha t}$ and $E_L = Ee^{\alpha t_L}$ into Equation G.1 gives

$$A' = A\left[\frac{1}{1 + e^{m\alpha(t-t_L)}}\right] \tag{G.4}$$

from which

$$e^{m\alpha(t-t_L)} = \frac{A - A'}{A'}. \tag{G.5}$$

Combining Equations G.5 and G.3 yields

$$\frac{d\ ln\ E_o}{dt} = \alpha\left[1 - (m)\left(\frac{A - A'}{A'}\right)\left(\frac{A'}{A}\right)\right] = \alpha\left[1 - m\left(\frac{A - A'}{A'}\right)\right]. \tag{G.6}$$

Now in this report the percentage amplitude nonlinearity of an amplifier will be as defined by

$$\%\ \text{Amplitude Nonlinearity} = \frac{A - A'}{A}\ 100 \tag{G.7}$$

which combined with Equation G.1 gives

$$\%\ \text{Amplitude Nonlinearity} = \frac{100}{1 + \left[\frac{E_L}{E_{in}}\right]^m}. \tag{G.8}$$

Therefore Equation G.6 becomes

$$\frac{d\ ln\ E_o}{dt} = \alpha\left[1 - m\ \frac{(\%\ \text{Nonlinearity})}{100}\right] \tag{G.9}$$

or

$$\frac{d\ ln\ E_o}{dt} = \alpha\left[1 - \frac{m}{1 + \left[\frac{E_L}{E_{in}}\right]^m}\right]. \tag{G.10}$$

Equations G.9 and G.10 represent the apparent instantaneous alpha (α_a) at the output of the amplifier. Equation G.9 indicates that the rate of change of the apparent alpha is proportional to both the percentage nonlinearity of the amplifier and to the rate of change of nonlinearity as represented by m.

As an example of some of the above items consider a typical Ivy amplifier with the following amplitude linearity characteristics

E_L = 2.5 volts

m = 4.

From this the expression for the ratio of the apparent gain (A′) to the linear gain (A) is

$$\frac{A'}{A} = \frac{1}{1 + \left[\frac{E_{in}}{2.5}\right]^4}. \tag{G.11}$$

The curve of A′/A for various E_{in}/E_L ratios is plotted in Figure 42. A plot of the percentage amplitude nonlinearity and the ratio of the apparent alpha (α_a) to the true alpha (α) are also shown in this figure. It will be noted that (a) percentage-wise, the apparent alpha is dropping at approximately four times the rate at which the percentage nonlinearity is

increasing; (b) the apparent alpha has dropped to zero at an E_{in}/E_L ratio of 0.76, corresponding to 25% amplitude nonlinearity; and (c) the apparent alpha equals $(-\alpha)$ at the E_{in}/E_L ratio of unity, corresponding to 50% amplitude nonlinearity.

This method of analysis should be used only if it is not possible to test the amplifier with an exponential signal of the type under consideration. Furthermore, this method of analysis applies only if alpha is of such value that the amplifier is operating with an exponential gain near the midfrequency sinusoidal gain (i.e., with a gain reduction factor near unity).

A further reduction in the linear output range of multistage amplifiers is encountered with exponential signals having values of alpha such that the GRF of the amplifier is in the vicinity of, or below, one-half. This is due primarily to the overloading of early stages before the final stages have reached normal output. This effect has been measured using the exponential pulser.

The net result of amplifier nonlinearity is a reduction in the useful field of the cathode-ray tube. The Ivy amplifier is rated at 125 volts output with less than 2% nonlinearity on a step function signal. This 125 volts corresponds to only about 70% of the useful field of the type 5XP cathode-ray tube. Any further reduction in the range of linear output produces in an additional reduction in the useful field on the cathode-ray tube resulting in a further decrease in the accuracy of the alpha measurement.

Appendix H
Parameters of the Rossi Display

H.1 General

In order to obtain optimum results with the Rossi display several factors must be considered; the determination of writing speed requirements, the number of generations ($n = \alpha t$) that can be recorded and the choice of the frequency of the sinusoidal timing wave.

The general expression for the voltage of an exponential signal is $V_0 (e^{\alpha t} - 1)$, but after several generations the expression $V_0 e^{\alpha t}$ will differ from the general expression by only a negligible amount. For example, after 10 generations the difference is less than 0.005%. Since the signal does not reach a recordable level until nearly 20 generations the simplified expression will be used. The signal voltage to be recorded is applied to a deflection system and it produces a displacement of the electron beam on the face of the CRT. The displacement, S, of the beam is related to voltage by a constant and can be represented as

$$S = S_o e^{\alpha t}. \tag{H.1}$$

H.2 Unresolved Displacement at Start of the Sweep

Referring to Figure (43), it can be seen that, since the signal is an exponential, the displacement must exceed a certain value, S_1*, before the cycles of the sine wave can be resolved. All displacements less than this can not be resolved, therefore this portion of the field is wasted. In order to determine the number of generations that can be recorded and the accuracy of the alpha measurement it is necessary to know the amount of unresolved displacement, or wasted field. If $t = 0$ at the time of the first peak of the first cycle that can be resolved, then the value of S_1 is

$$S_1 = S_o. \tag{H.2}$$

At t_2 (time of the second peak)

$$S_2 = S_1 e^{\alpha t_2} = S_1 e^{\frac{1}{m}} \tag{H.3}$$

where m is the number of cycles per generation. Then G, the displacement between the peaks of the first resolved cycle, is

$$G = S_1 e^{\frac{1}{m}} - S_1 = S_1 \left(e^{\frac{1}{m}} - 1\right) \tag{H.4}$$

giving

$$S_1 = \frac{G}{e^{\frac{1}{m}} - 1}. \tag{H.5}$$

Thus, in order to determine the actual values of S_1, it is necessary to know a value for G. Based on the analysis of a number of pictures, a practical value has been found to be 4 trace widths. A table of S_1 vs. m is given below for G = 4.

*Symbol designations used in this appendix are listed at the end of Section 5.

m	S_1
1 (cycles/gen)	2.3 Trace widths
2 (cycles/gen)	6.2 Trace widths
3 (cycles/gen)	10.2 Trace widths
4 (cycles/gen)	14.3 Trace widths
5 (cycles/gen)	18.2 Trace widths
6 (cycles/gen)	23.5 Trace widths
8 (cycles/gen)	30.8 Trace widths
10 (cycles/gen)	38.0 Trace widths
20 (cycles/gen)	78.0 Trace widths

H.3 Writing Speed Requirements

Permanent records of many exponential signals of interest are obtained by photographic methods. In order to obtain a satisfactory film exposure there must be a certain minimum amount of light per unit area in the trace which means that for a given beam current there is a maximum writing speed (spot velocity) at which this amount of light is obtained.

The rate of change of displacement on the face of the cathode-ray tube (writing speed) is continually increasing with an exponential signal. It is therefore necessary to express this writing speed in terms of α and time. Using the displacement, S_1, found above, the displacement at any time later can be found from the general equation:

$$S = S_1 e^{\alpha t}.$$

The derivative of this equation gives the horizontal component of the writing speed, V_H, at any time (assuming the signal to be displayed on the horizontal axis).

$$V_H = \frac{dS}{dt}$$

$$= S_1 \alpha e^{\alpha t} = \alpha S$$

or

$$V_H = S_1 \alpha e^n \text{ tw/sec} \tag{H.6}$$

where n is the number of recorded generations and S_1 is in trace widths. Figure 44 shows the function plotted for a value of S_1 equal to 10 (which assumes a value of G = 4 and m = 3).

Since writing speed is proportional to displacement it is obvious that the maximum speed will occur at the maximum possible horizontal displacement. Thus in order to obtain optimum results with a given CRT it should have sufficient writing speed to write over the entire horizontal field and the maximum possible writing speed required is

$$V_{H_{max}} = \alpha A \text{ tw/sec} \tag{H.7}$$

where A = horizontal field in trace widths.

The preceding analysis of the writing speed considers only the effect of the exponential signal on one deflection axis. In the actual display the timing voltage on the other axis also affects the spot velocity. The vertical displacement due to the timing voltage is $S_V = B \sin \omega t$ where B = one half the peak to peak displacement and ω = angular timing frequency. The vertical velocity is $V_V = B \omega \cos \omega t$ and the maximum vertical velocity is

$$V_{v\ max} = B\omega \text{ or } V_{v\ max} = 2\pi mB\alpha \tag{H.8}$$

Then the maximum net spot velocity (which occurs at the far edge of the horizontal field just as the spot crosses the base line) is

$$V_{max} = \sqrt{(\alpha A)^2 + (2\pi mB\alpha)^2}$$

$$= \alpha \sqrt{A^2 + (2\pi mB)^2} = \alpha A \sqrt{1 + \left(\frac{2\pi mB}{A}\right)^2} . \qquad \text{(H.9)}$$

In a typical case A = 400 tw, B = 25 tw and m = 3 giving $V_{max} = \alpha A \sqrt{1 + 1.18} = 1.55\,\alpha A = 622\,\alpha$.

It is seen that the maximum required writing speed is approximately 50% more for reading at the base line than for reading the peaks. The variation in writing speed between the peaks of the rf cycles and the base line crossings becomes increasingly larger near the start of the signal. Thus, at 100 trace widths of horizontal displacement the variation is 2.4/1 and at 25 is 4.5/1. However, if only the peaks are to be read the effect of the timing wave can be neglected.

H.4 Number of Generations that can be Recorded

Consideration is given here to the number of generations that can be recorded on the face of the tube. From Figure 43 it is seen that

$$A = S_1 e^C \quad \text{where C is the number of generations recorded.} \qquad \text{(H.10)}$$

Solving for C

$$C = \ln\left(\frac{A}{S_1}\right).$$

Substituting the value of S_1 obtained in Equation 3.

$$C = \ln \frac{A}{G} + \ln\left(e^{\frac{1}{m}} - 1\right). \qquad \text{(H.11)}$$

The value of ln A/G shown in Figure 45 is a constant for any given CRT. The value of $\ln(e^{1/m} - 1)$ is found in Figure 46. Note that if m is greater than 1.5 the value of $\ln(e^{1/m} - 1)$ is negative.

In order to obtain an experimental check of the effects of a variation of "m" a series of pictures taken with "m" having values from 1 to 8 are shown in Figs. 47 through 50. Also included is a linear sweep with a 1000 mc. timing wave for comparison in Figure 51. The value of alpha was 3.75×10^8 in all cases. A comparison of the actual number of recorded generations with the calculated number for G = 4 and A = 445 (TW-10) is given below.

Fig. No.	m	C (calculated)	C (measured)
47	1.07	5.1 gen.	4.9 gen.
48	2.13	4.2 gen.	4.6 gen.
49	2.66	3.9 gen.	3.8 gen.
50	8.00	2.7 gen.	2.7 gen.

It is seen that the assumed values of G and A give quite accurate results.

H.5 Determining Alpha from the Rossi Display

From Equation H.6

$$S_N = S_1 e^{\alpha t_N} \tag{H.12}$$

where S_N is the displacement at the Nth cycle from the origin and t_N is the time for N cycles giving

$$\alpha = \frac{1}{t_N} \ln \frac{S_N}{S_1} = N f \ln \frac{S_N}{S_1} \tag{H.13}$$

The values of displacement in this equation are measured from the point of zero displacement. In practice it is impossible to determine the location of this zero point accurately because of over-exposure of the film at the start of the trace. To overcome this difficulty the value of alpha can be determined by another method that does not require knowledge of the zero, namely, from the relative location of three adjacent peaks of the timing wave.

$$S_N - S_{(N-1)} = S_1 e^{\frac{N}{m}} - S_1 e^{\frac{N-1}{m}} \tag{H.14}$$

and

$$S_{(N-1)} - S_{(N-2)} = S_1 e^{\frac{(N-1)}{m}} - S_1 e^{\frac{N-2}{m}}. \tag{H.15}$$

Dividing H.14 by H.15 gives

$$\frac{S_N - S_{(N-1)}}{S_{(N-1)} - S_{(N-2)}} = e^{\frac{1}{m}} \tag{H.16}$$

and substituting f/α for m yields an expression for α

$$\alpha = f \ln \frac{\left(S_N - S\right)_{(N-1)}}{\left(S_{(N-1)} - S_{(N-2)}\right)}. \tag{H.17}$$

This result utilizes the displacement between only three peaks of the timing wave. The record generally has more peaks than this and the accuracy of the results can be improved by including all peaks that can be accurately located. The alpha determination is accomplished most simply by making a semilogarithmic plot of the displacement between adjacent peaks against an arbitrary time scale. The value of α is given by the slope of a line drawn through all the points. That this is a straight line can be shown by taking the logarithmic of expressions for the displacements of the peaks.

$$\ln S_N = \ln S_1 + \alpha t_N$$

and

$$\ln S_{(N-1)} = \ln S_1 + \alpha t_{(N-1)}. \tag{H.18}$$

From these relations

$$\ln S_N - \ln S_{(N-1)} = \alpha t_N - \alpha t_{(N-1)}$$

or

$$\ln (\Delta S) = \alpha (\Delta t) \tag{H.19}$$

where ΔS = displacement between adjacent peaks

and Δt = time between peaks.

On a semilog plot this is the equation of a straight line with a slope of α.

H.6 Error in Measuring Alpha by a Rossi Display

It is possible to determine the approximate error to be expected in alpha when measured by a Rossi display. A number of factors contribute to the error in the measurement. These include: accuracy of oscillator frequency, harmonic content of oscillator, orthogonality of deflection plates and reading accuracy in locating points on the record. The oscillator frequency can be measured very accurately and is constant with good oscillator design. Harmonic content can be reduced by good oscillator design and by the use of harmonic filters although if only peaks either above or below the baseline are used in the measurement harmonic content has no effect. Any non-orthogonality of the deflection plates can be accounted for by making a calibration of the field of the CRT. The remaining factor is reading error. This can be reduced by proper reading techniques but still is the largest factor in the error. Reading error can be reduced by using both positive and negative peaks, zero or base line crossings, or other points on the cycle at known times. However, the use of these points requires a knowledge of harmonic content and plate orthogonality and in addition recording points other than peaks requires increased writing speed. As a result, as long as the number of peaks either above or below the base line is fairly large, the small increase in accuracy obtained by reading other points usually does not justify the increased effort.

Since the value of α is found by drawing the "best-fit" straight line through a group of points, the value of α can be calculated by the least squares method.[14,15] Using the short method with an odd number of time differences it can be shown that

$$\alpha = \frac{\Sigma XY}{\Sigma X^2} \tag{H.20}$$

where X = time interval number with the origin at the middle of the series of points

$$Y = \ln \Delta S$$

and

$$\alpha \pm P_\alpha = \frac{\Sigma X \ (Y + P_y)}{\Sigma X^2} \qquad \begin{array}{l} P_\alpha = \text{error in } \alpha \\ P_y = \text{error in } Y \end{array} . \tag{H.21}$$

Combining these expressions gives

$$\pm P_\alpha = \frac{\Sigma X \ (Y + P_y)}{\Sigma X^2} - \frac{\Sigma XY}{\Sigma X^2} \tag{H.22}$$

and the percent error in α is

$$P_\alpha = \pm \frac{\Sigma X \ P_y \times 100}{\Sigma X^2} . \tag{H.23}$$

Because the sine wave frequency may be chosen at will it is important to know how the error "P_α" varies with "m" (cycles/generation). However, before actual values can be found it is necessary to evaluate P_y as shown in the next paragraph.

The uncertainty in S_N, the displacement with respect to zero of the Nth peak, can be expressed as

$$P_{S_N} = KD_N + C \tag{H.24}$$

[14] W.A. Neiswanger, "Elementary Statistical Methods," Macmillan Co. 1943

[15] Owen L. Davies, "Statistical Methods in Research and Production," Oliver and Boyd, 1949

where D_N is the width in trace widths of the Nth cycle, with the Nth cycle as the reference center, and K and C are constants.

(Uncertainties increase with increasing D_N because of a broadening of the peaks and the resulting inability to locate accurately this centers.)

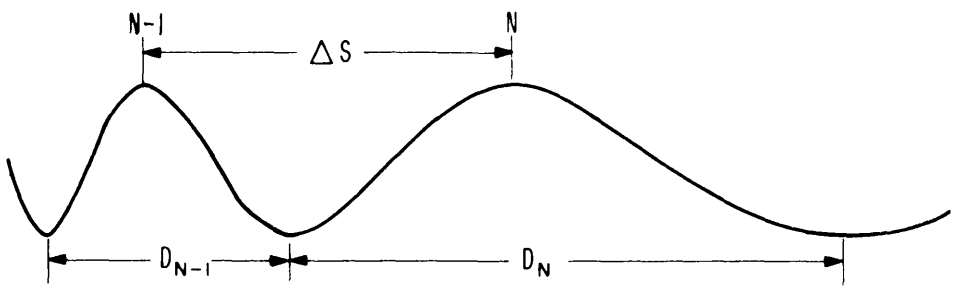

Figure H.1

In order to evaluate P_y, it is necessary to find values of $P_{\Delta S}$ (errors in ΔS) in terms of P_{S_N}. $P_{\Delta S}$ is equal to the RMS average of the errors in S_N

$$P_{\Delta S} = \sqrt{(KD_N + C)^2 + (KD_{N-1} + C)^2} \tag{H.25}$$

ΔS can be substituted for D_N and D_{N-1}. This is a good approximation because ΔS is approximately the geometric mean of D_N and D_{N-1}. Therefore

$$P_{\Delta S} = \sqrt{2}\ (K\Delta S + C) \text{ or } \sqrt{2}(.02\Delta S + 0.5).$$

The value P_y can now be found by taking the difference between $\ln \Delta S + \sqrt{2}(\Delta S + C)$ and $\ln \Delta S - \sqrt{2}(\Delta S + C)$ and P_α can be determined.

Values of P_α vs. "m" have been computed for three different values of A (total field of CRT) 100, 200, and 400 t.w. (Figure 52). It is seen from the curves that the error decreases rapidly between m = 1 and m = 3. For values of m larger than 3 the error decreases at a slow rate, reaching a minimum value where only three peaks are resolved. Any further increase in m will not give sufficient information to determine the value of α since three peaks are the minimum number that can be used to determine α (assuming the use of only the difference between peaks). The curves in Fig. 52 are for values of K = 0.02 and C = 0.5. Since these constants entirely define P_y and its change with m, the actual shape of the curve will be changed if their values change. The curves will, however, remain almost flat thru a large range of m even if the constants are changed.

In practice a number of factors must be considered in the selection of the optimum value for the sine wave frequency. Certainly the frequency of minimum error should not be used because it allows no safety factor in α. Moreover, because of the transit time sensitivity reduction with increasing timing frequency, the voltage to maintain a constant deflection increases, producing increased crosstalk between tube elements. Also, this increased voltage at the higher frequencies becomes more difficult to generate and transmit to the deflection system. Therefore, it is desirable to use the lowest frequency possible consistent with the necessary accuracy. As suggested previously, a good value for m is approximately 3.

Appendix I
Transit Time Effects of Deflection Plates

For low frequency signals the deflection of the electron beam of a CRT can be assumed to be proportional to the voltage on the deflection plates at any instant. However, this assumption cannot be made when the voltage is changing rapidly because the electrons take a finite time to travel through the deflecting field.

For non-relativistic beam velocities the displacement of the beam at the screen can be determined easily. Thus, for vertical displacements the vertical velocity of the electron may be found from

$$m \frac{d}{dt} v = \frac{V(t)}{S} e \tag{I.1}$$

and the velocity when the electron emerges from the deflection system is

$$v_y = \frac{e}{ms} \int_{t-T-\tau}^{t-T} V(t)\, dt \tag{I.2}$$

giving for the vertical displacement on the screen

$$y(t) = v_y T \tag{I.3}$$

where m = mass of electron

e = charge of electron

v_y = vertical velocity when electron emerges from deflection plates

S = deflection plate spacing

τ = transit time through deflecting field

T = electron travel time from plates to CRT screen

$y(t)$ = displacement at screen

$V(t)$ = driving voltage on deflection plates

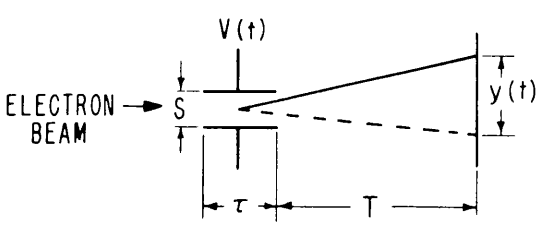

Figure I.1

Time T represents a delay time during which the electrons are outside the deflecting field and are traveling to the screen. Thus T is measured from the edge of the deflection plates to the screen.

If T is measured from a point along the plates, such as the center, the electrons continue to be deflected until they reach the edge of the field. Time T then includes a time during which the electrons are being deflected and cannot be considered as simply a signal delay.

If V(t) = 1 volt and is constant

$$y(t) = \frac{e\,T}{ms} = k, \text{ the sensitivity factor} \tag{I.4}$$

and the displacement can be written as

$$Y(t) = \frac{k}{\tau}\int_{(t-T-\tau)}^{(t-T)} V(t)dt. \tag{I.5}$$

For V(t) = δ(t), the Dirac impulse function, the response is

$$Y_I(t) = \frac{k}{\tau}\int_{(t-T-\tau)}^{(t-T)} \delta(t)dt \tag{I.6}$$

giving

$$Y_I(t) = \frac{k}{\tau} \text{ if } T + \tau > t > T \tag{I.7}$$

and

$$Y_I(t) = 0 \text{ if } T>t \text{ or } t>T+\tau \tag{I.8}$$

Thus the response to the δ function is seen to be a pulse of amplitude k/τ and duration τ, delayed by time T, as shown below.

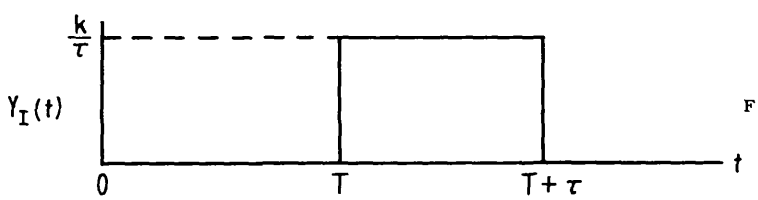

Figure I.2

The response to any other driving function V(t) is

$$Y(t) = \int_0^\infty V(t-\lambda)\, Y_I(\lambda)\, d\lambda \tag{I.9}$$

or

$$Y(t) = \int_{-\infty}^{t} V(\lambda)\, Y_I\,(t-\lambda)\, d\lambda \tag{I.10}$$

where $Y_I(t)$ is the response to the δ function just derived.

For example, if

$$V(t) = e^{i\omega t}$$

then

$$V(t-\lambda) = e^{i\omega t}\; e^{-i\omega\lambda}$$

and

$$Y(t) = e^{i\omega t}\int_0^\infty e^{i\omega\lambda}\; Y_I(\lambda)\, d\lambda \tag{I.11}$$

from which

$$Y(t) = e^{i\omega t} \frac{k}{\tau} \int_T^{T+\tau} e^{-i\omega\lambda} \, d\lambda \tag{I.12}$$

since $Y_I(\lambda) = k/\tau$ between the limits $\lambda = T$ and $\lambda = T + \tau$ and is zero at all other values of λ. Then

$$Y(t) = \frac{k}{\tau} e^{i\omega t} \left[\frac{e^{-i\omega T} - e^{-i\omega(T+\tau)}}{i\omega}\right] \tag{I.13}$$

giving

$$Y(t) = \frac{k}{\tau} e^{i\omega(t-T)} \left[\frac{1-e^{-i\omega\tau}}{i\omega}\right]. \tag{I.14}$$

It is seen that the response is delayed by T and reduced in amplitude. The absolute value is

$$\left|Y(t)\right| = \frac{k \sin \omega\tau/2}{\omega\tau/2}. \tag{I.15}$$

Thus for a sinusoidal input there is a sensitivity reduction factor of $\sin(\omega\tau/2)/(\omega\tau/2)$. In the case of an exponential signal input where

$$V(t) = e^{\alpha t}$$

$$Y(t) = \frac{k}{\tau} e^{\alpha(t-T)} \left[\frac{1-e^{\alpha t}}{\alpha}\right] \tag{I.16}$$

by substituting $\alpha = i\omega$ in Eq. I.14 and it is seen that the sensitivity reduction factor is $(1 - e^{-\alpha\tau})/(\alpha\tau)$.

The response to a step function input can be obtained from Equation I.9 where

$$V(t-\lambda) = 0 \text{ for } \lambda > t$$

and

$$V(t-\lambda) = 1 \text{ for } \lambda < t.$$

Then

$$Y(t) = \int_0^t Y_I(\lambda) d\lambda \tag{I.17}$$

from which results

$$Y(t) = \int_0^t 0 \, d\lambda = 0 \text{ for } t < T \tag{I.18}$$

$$Y(t) = \int_0^T 0 \, d\lambda + \int_T^t \frac{k}{\tau} d\lambda = \frac{k}{\tau}(t-T) \text{ for } T<t<T+\tau$$

$$Y(t) = \int_0^T 0 \, d\lambda + \int_T^{T+t} \frac{k}{\tau} d\lambda + \int_{T+\tau}^t 0 \, d\lambda = k \text{ for } t>T+\tau$$

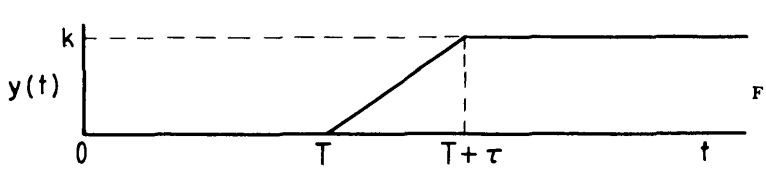

Figure I.3

The response to the step function is seen to be delayed by a time T and to rise in a time τ to the steady state. Thus, the trace deflection records the step function with correct amplitude but with a rise time of τ.

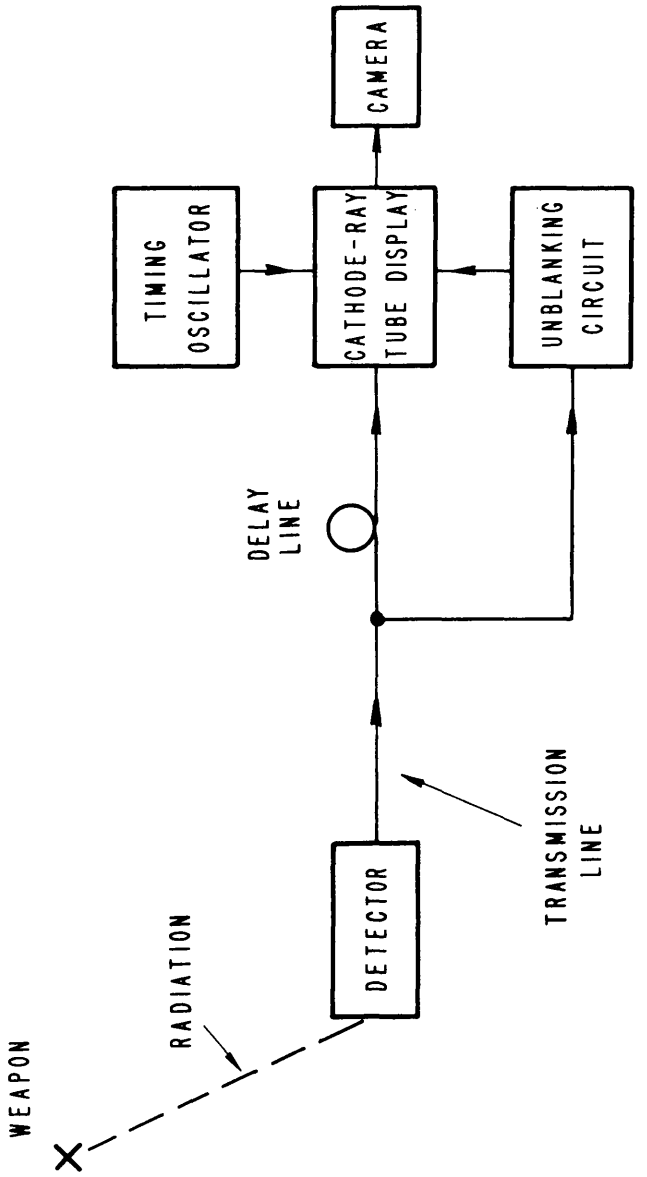

Figure 1 - Basic recording system block diagram

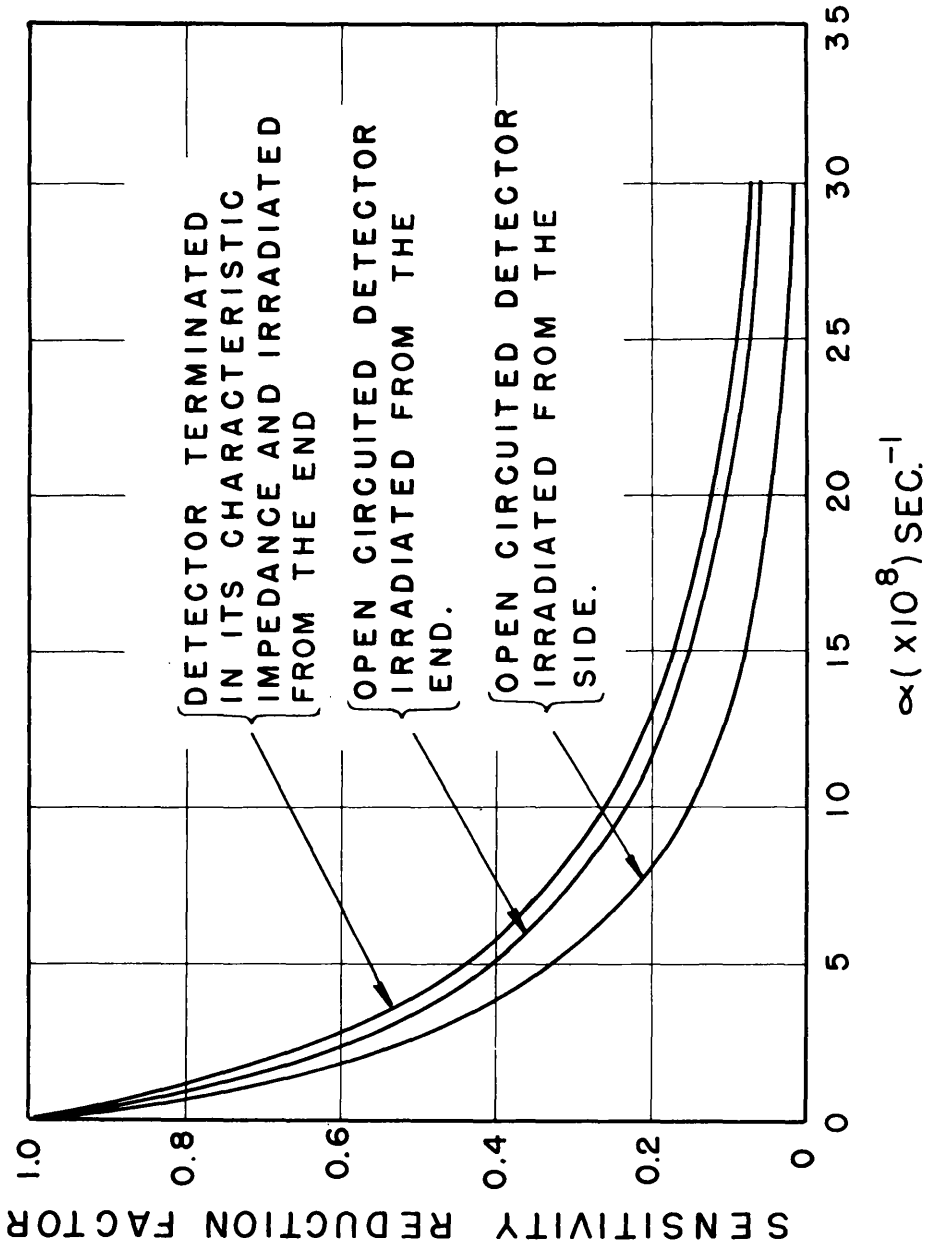

Figure 2 - Sensitivity reduction factors for the coaxial photocell

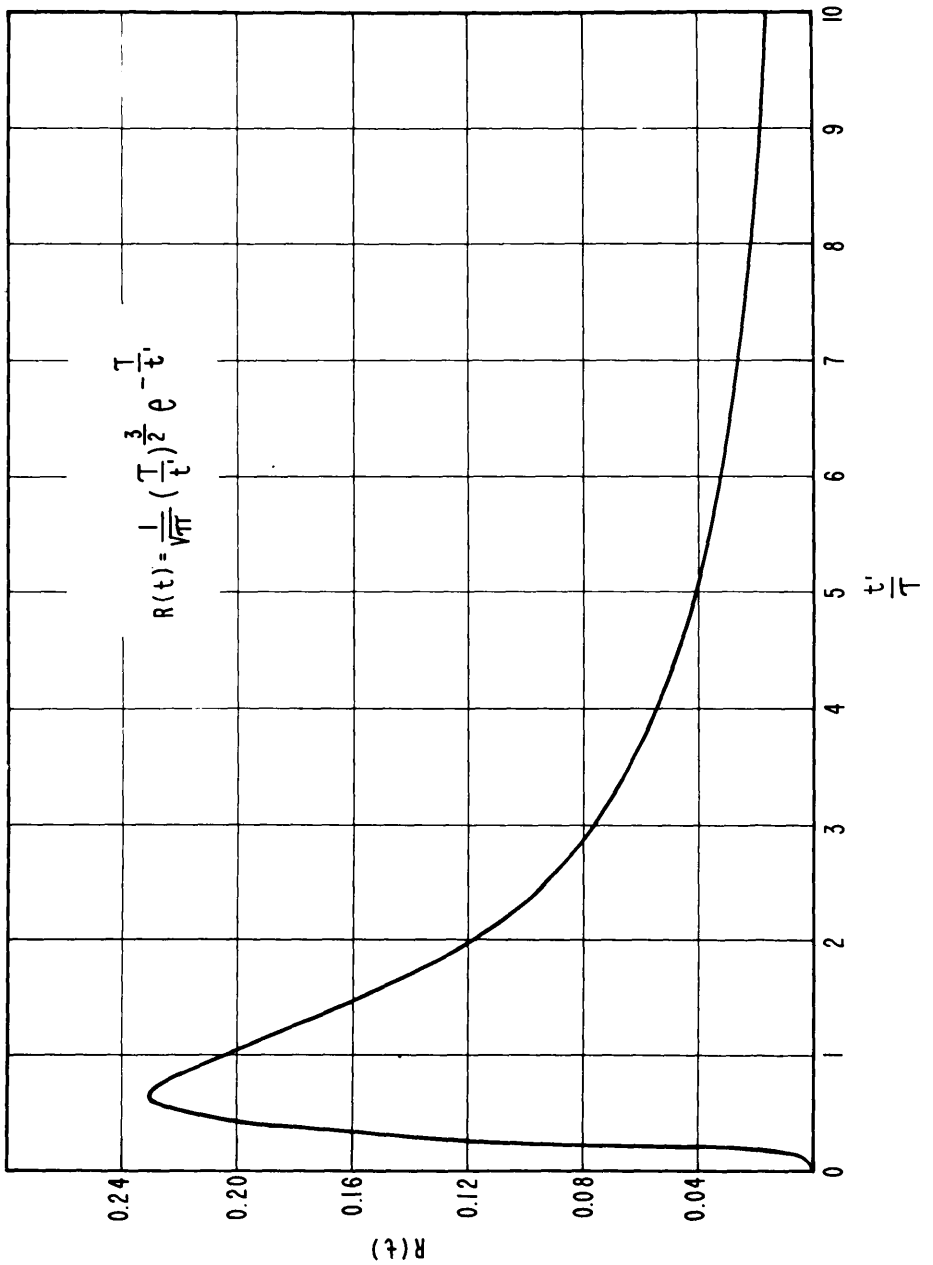

Figure 3 - Response of transmission line to delta function input

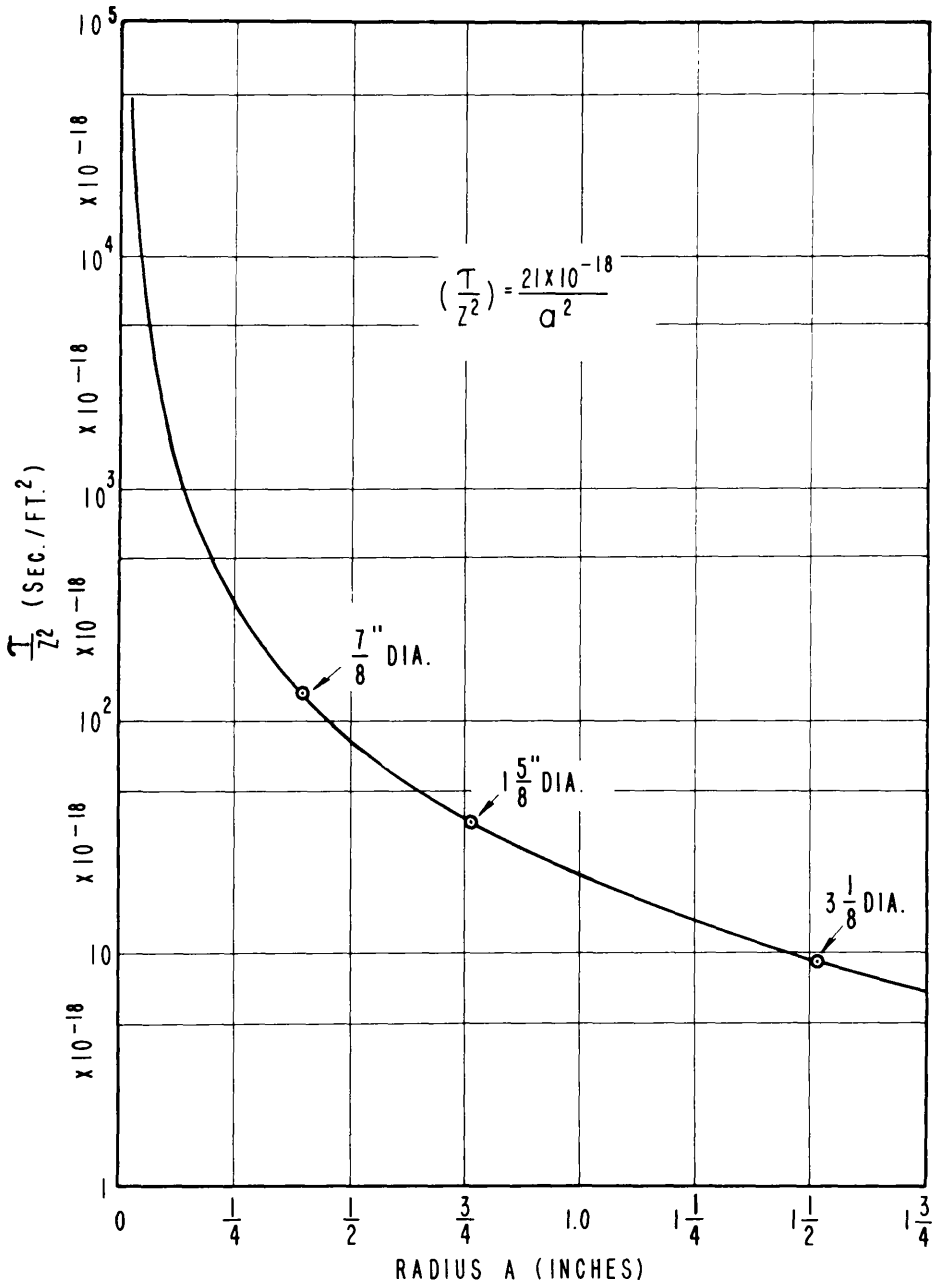

Figure 4 - Transmission line time constant

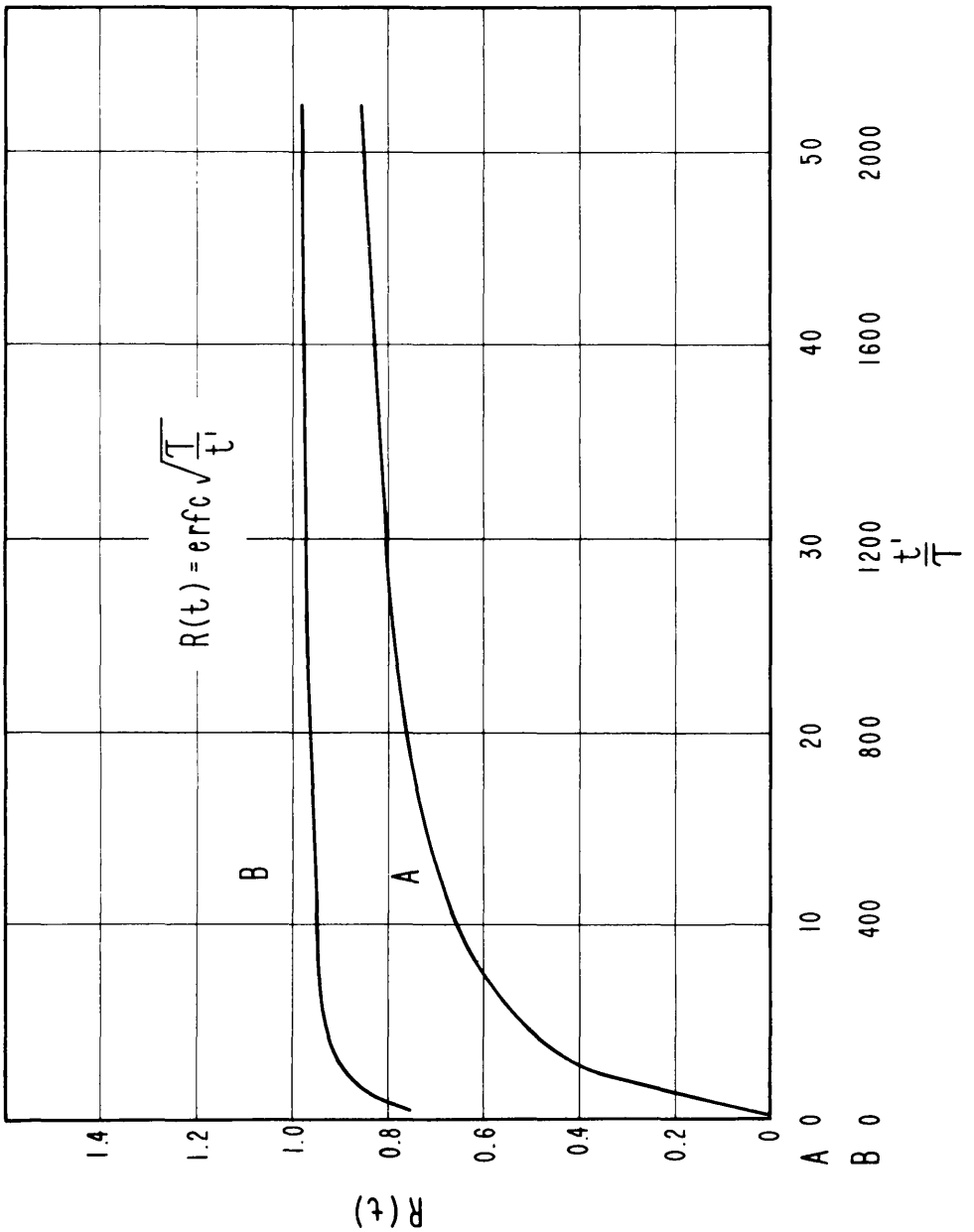

Figure 5 - Response of transmission line to step function input

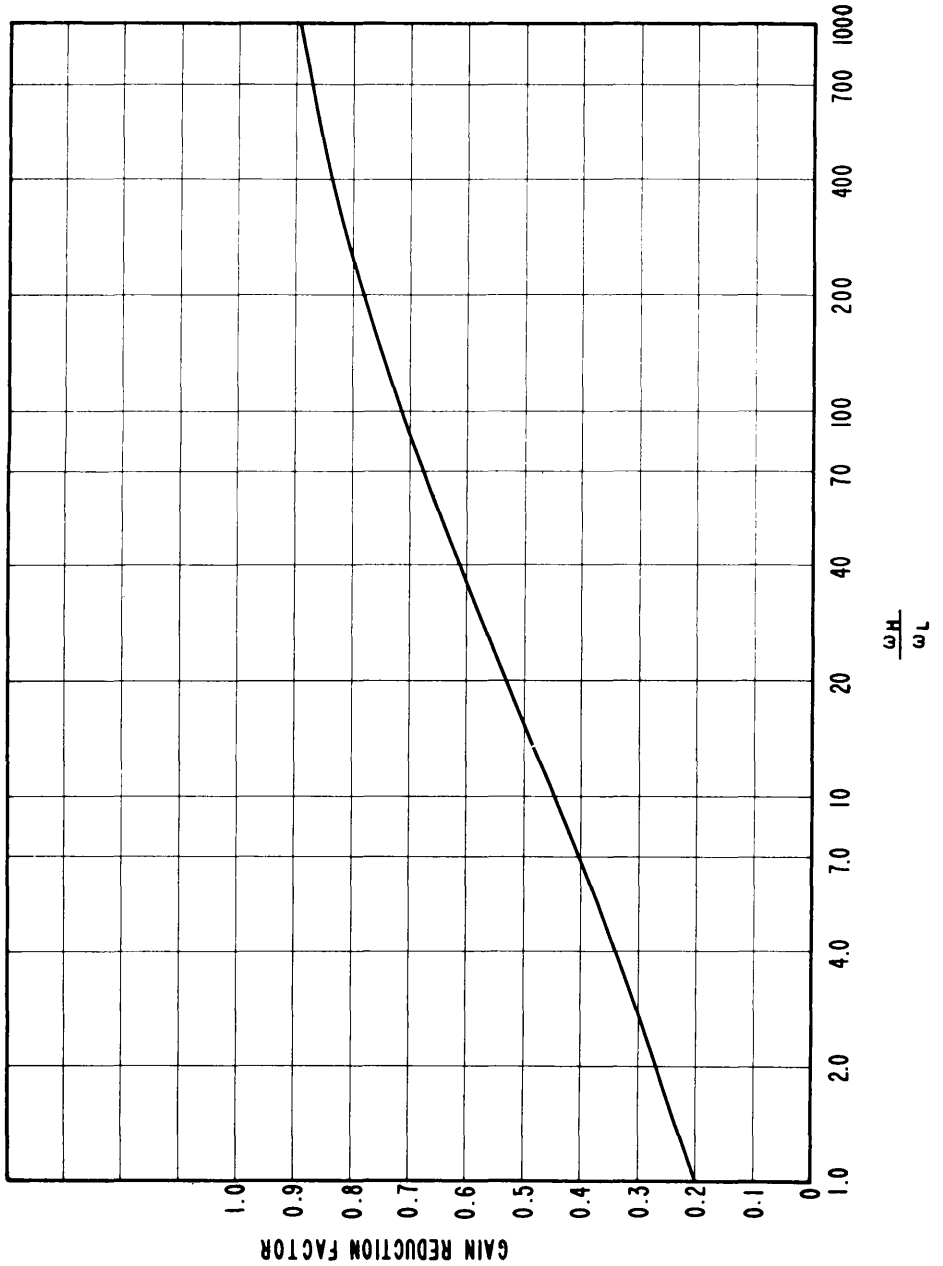

Figure 6 - Optimum GRF vs. (ω_H/ω_L)

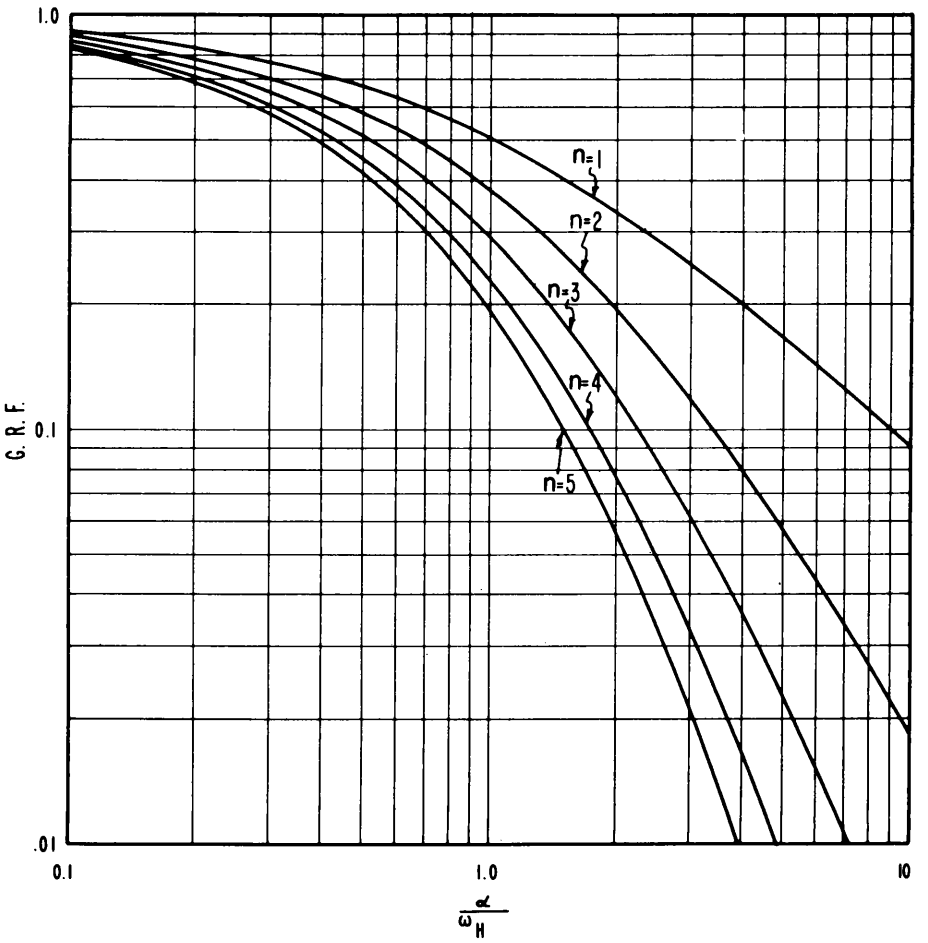

Figure 7 - Universal GRF curves for n=1 to n=5

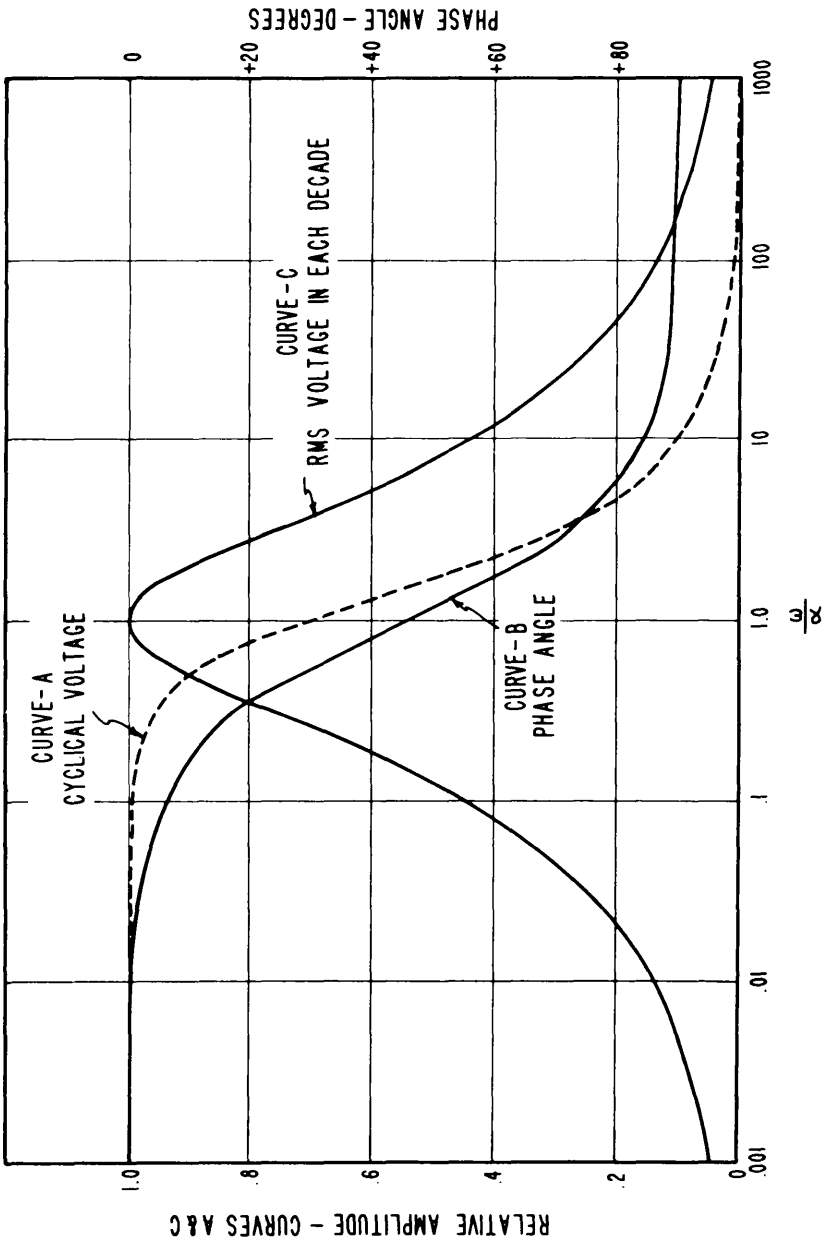

Figure 8 - Magnitude and phase angle of the sinusoidal components of an exponential signal vs. ω/α

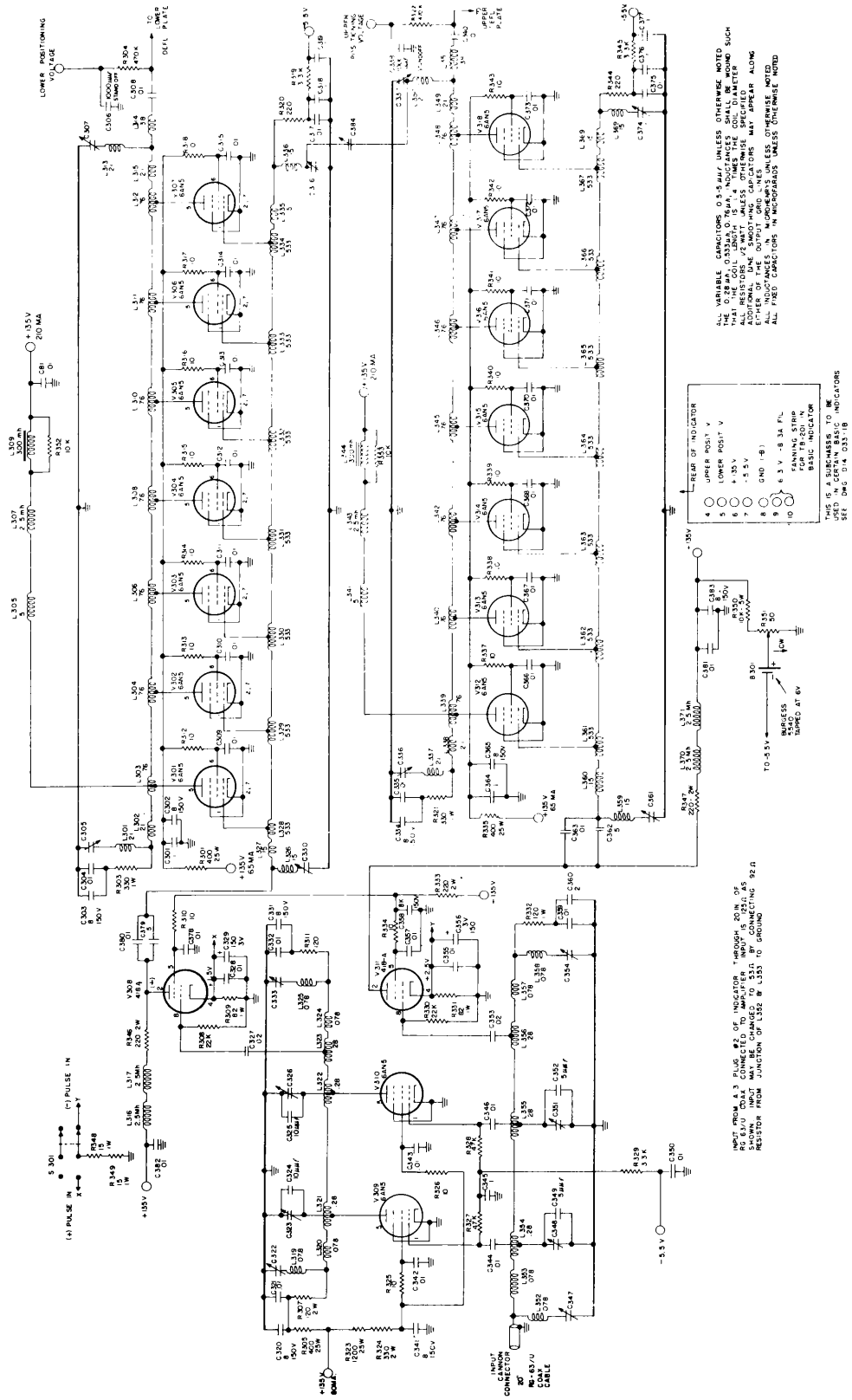

Figure 9 - Ivy amplifier circuit diagram

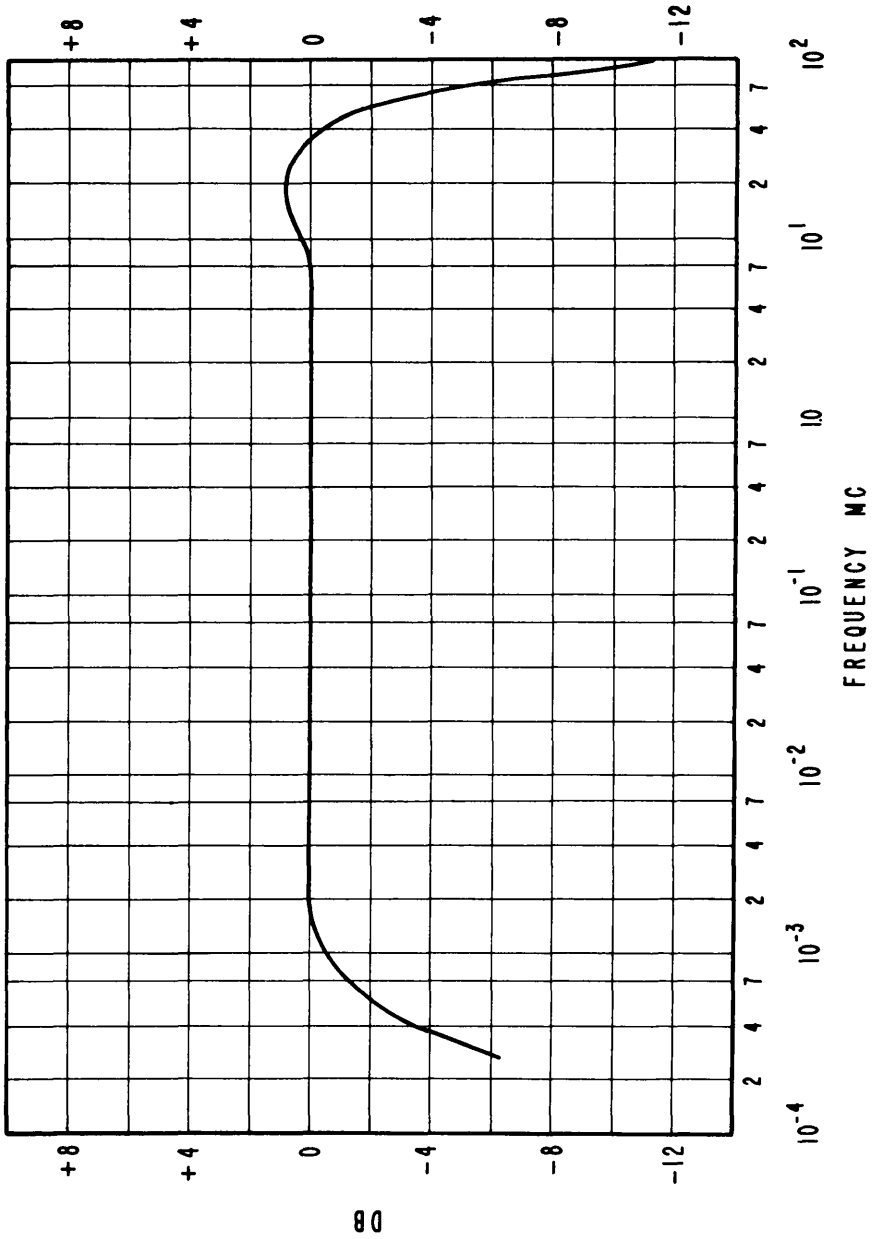

Figure 10 - Ivy amplifier frequency response

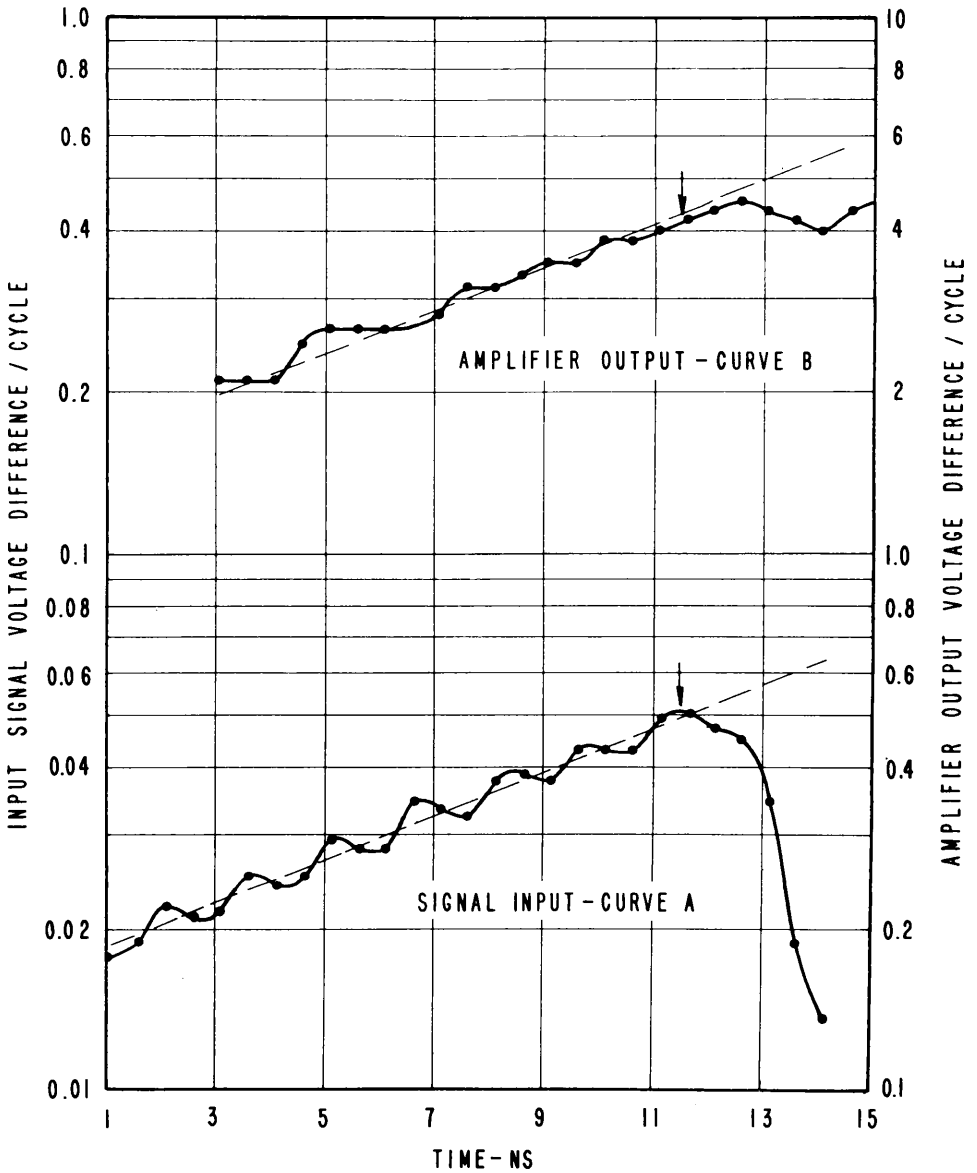

Figure 11 - Ivy amplifier exponential response

(α=0.925×10^8)

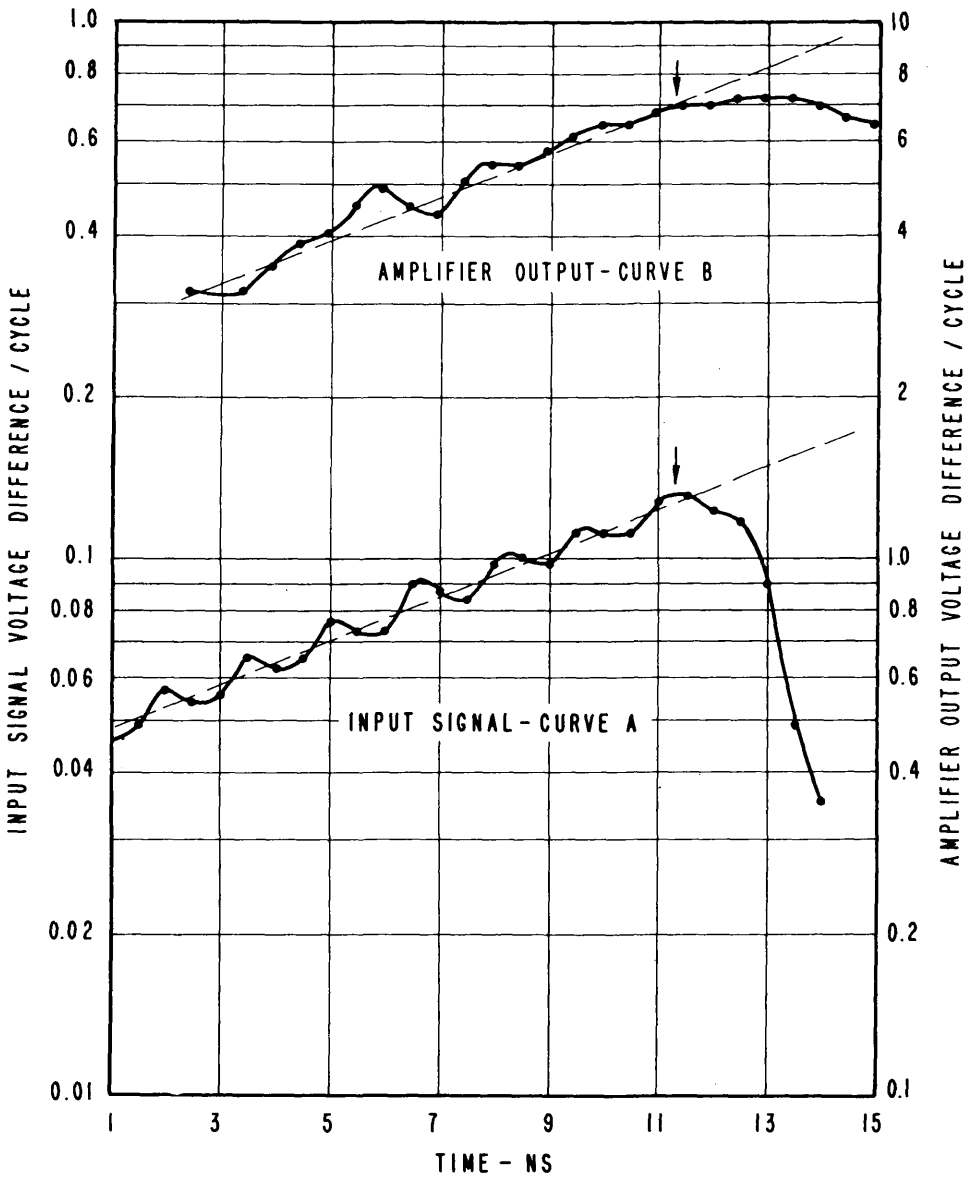

Figure 12 - 418-A distributed amplifier exponential response

(α=0.925×10^8)

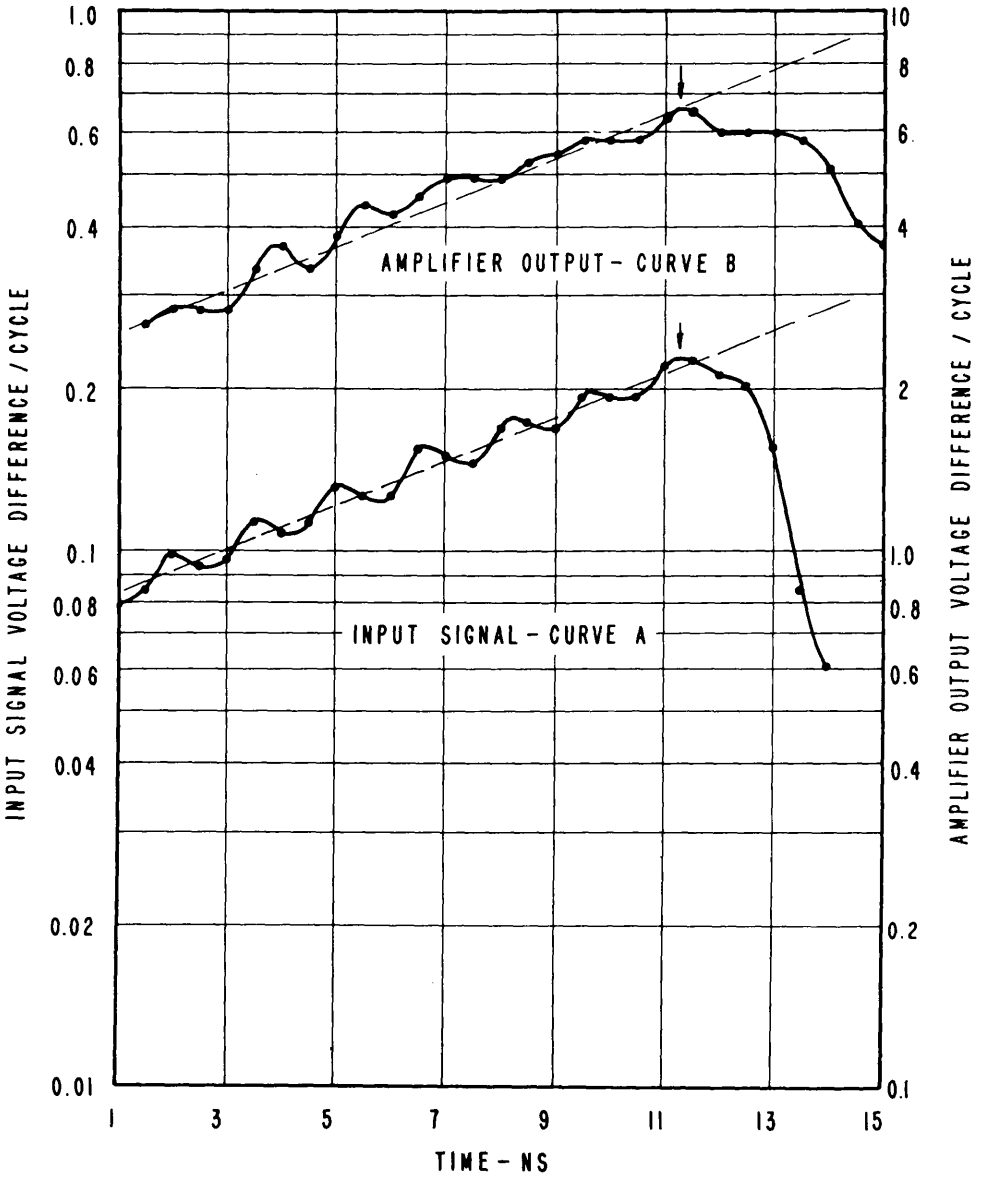

Figure 13 - Single 418-A amplifier exponential response

(α=0.925×10^8)

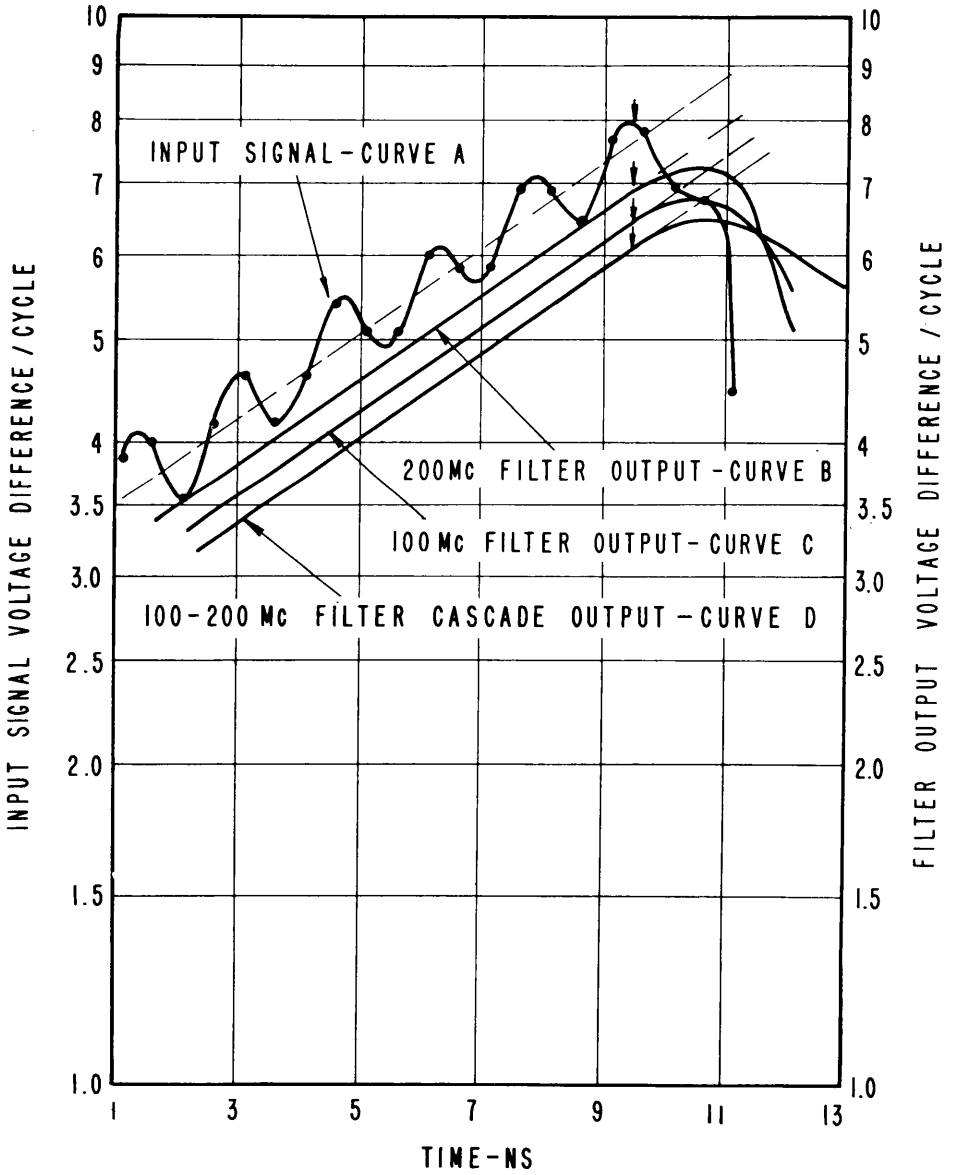

Figure 14 - 100 Mc & 200 Mc filters-exponential response

(a=0.925×10^8)

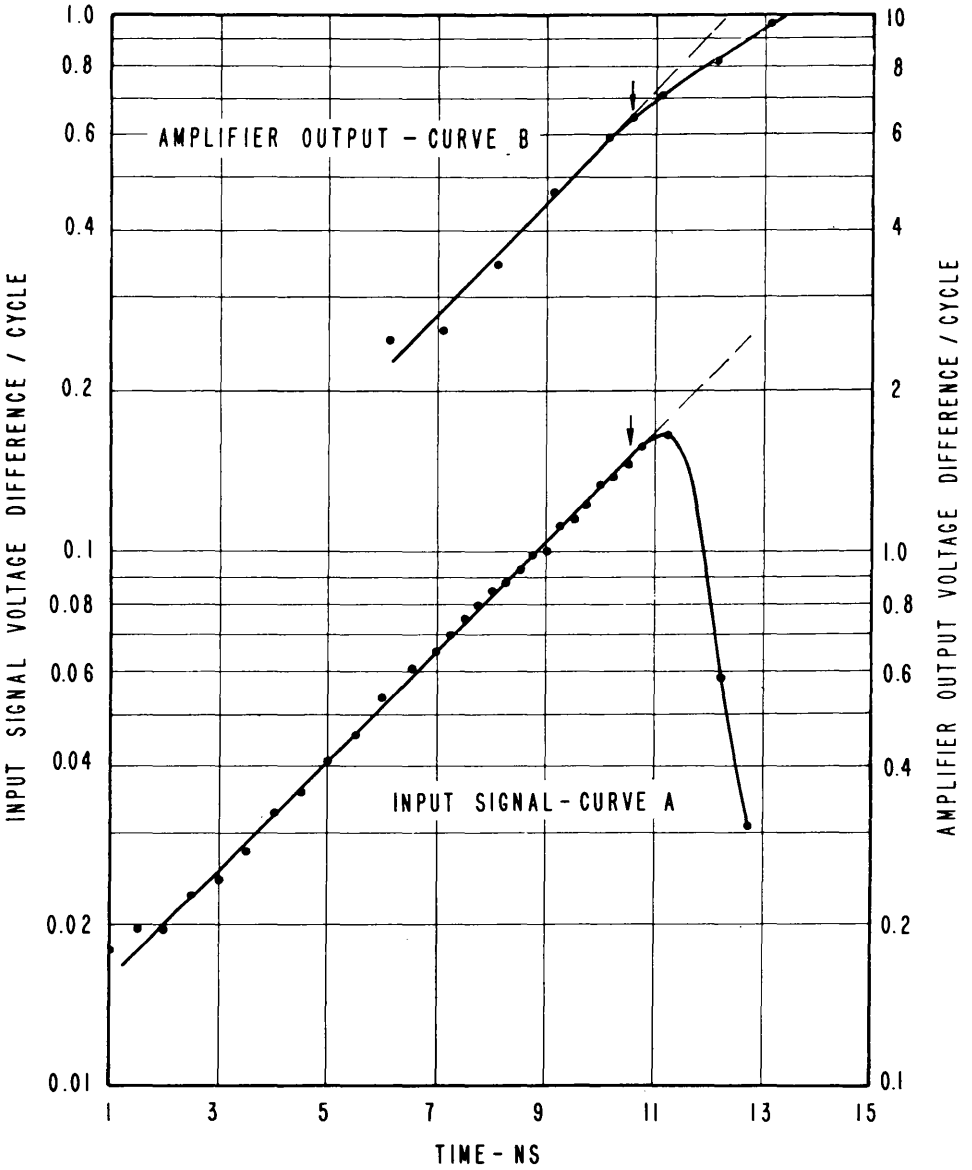

Figure 15 - Ivy amplifier exponential response

(a=2.38×10^8)

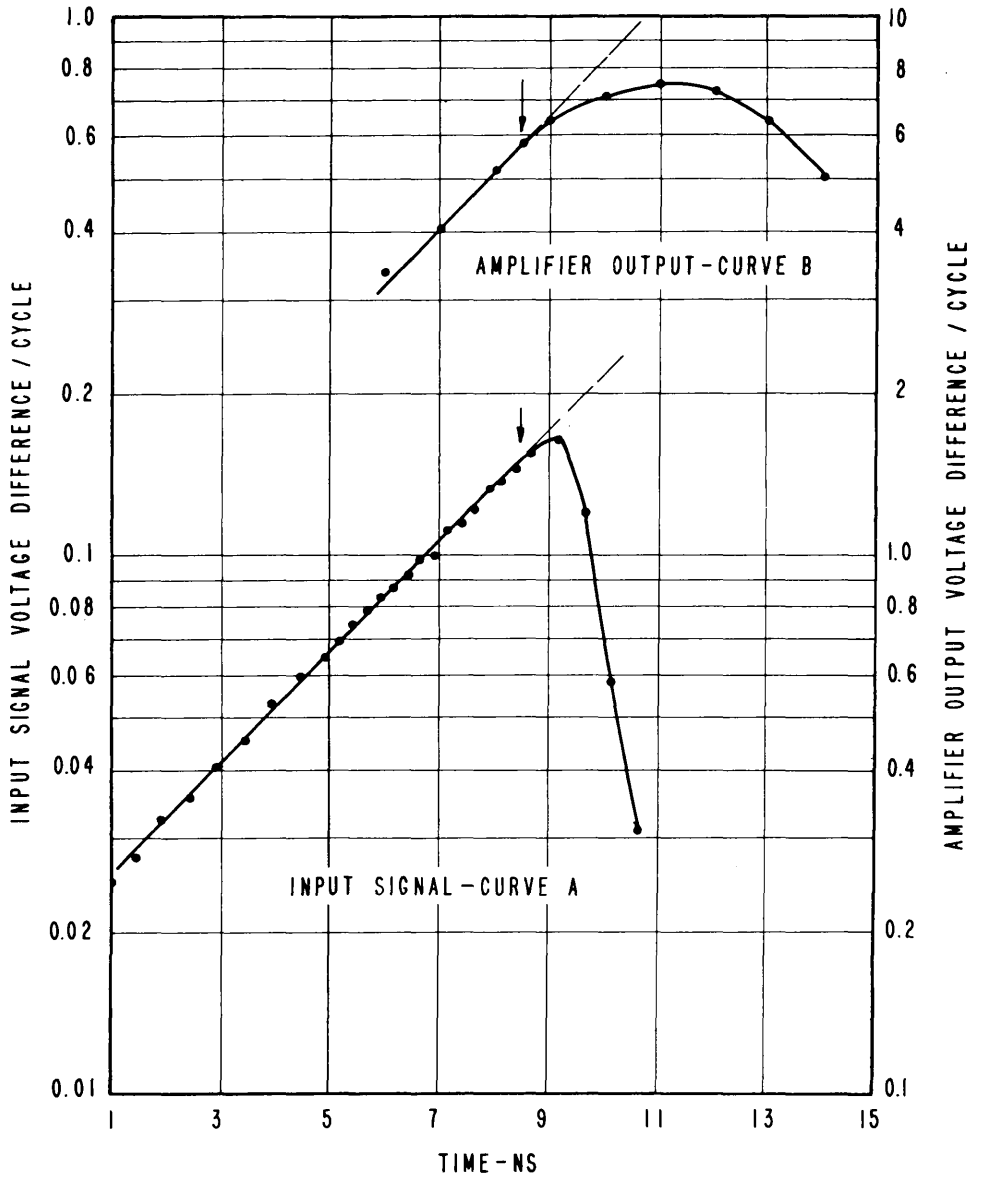

Figure 16 - 418-A distributed amplifier exponential response

(a=2.38×10^8)

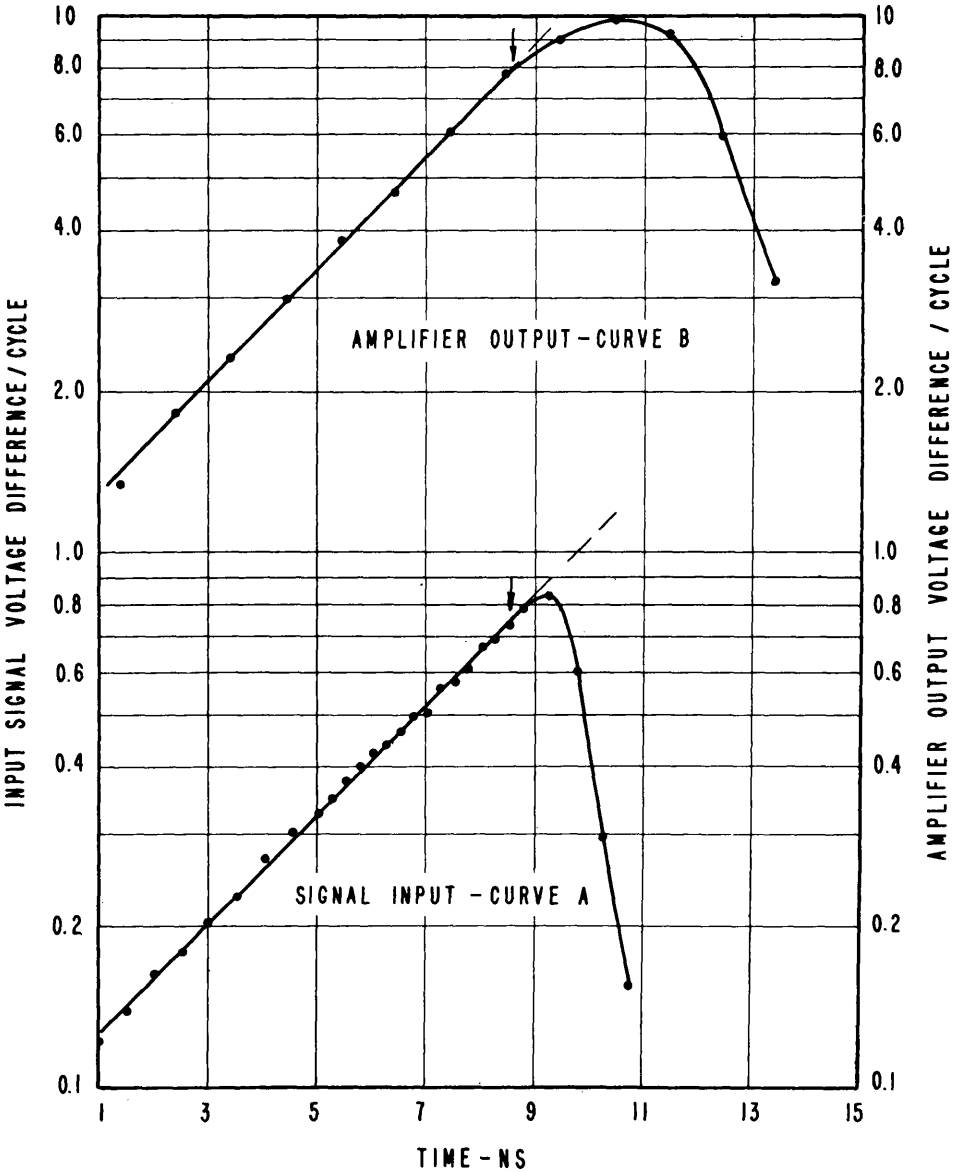

Figure 17 - Single 418-A amplifier exponential response

(α=2.38×10^8)

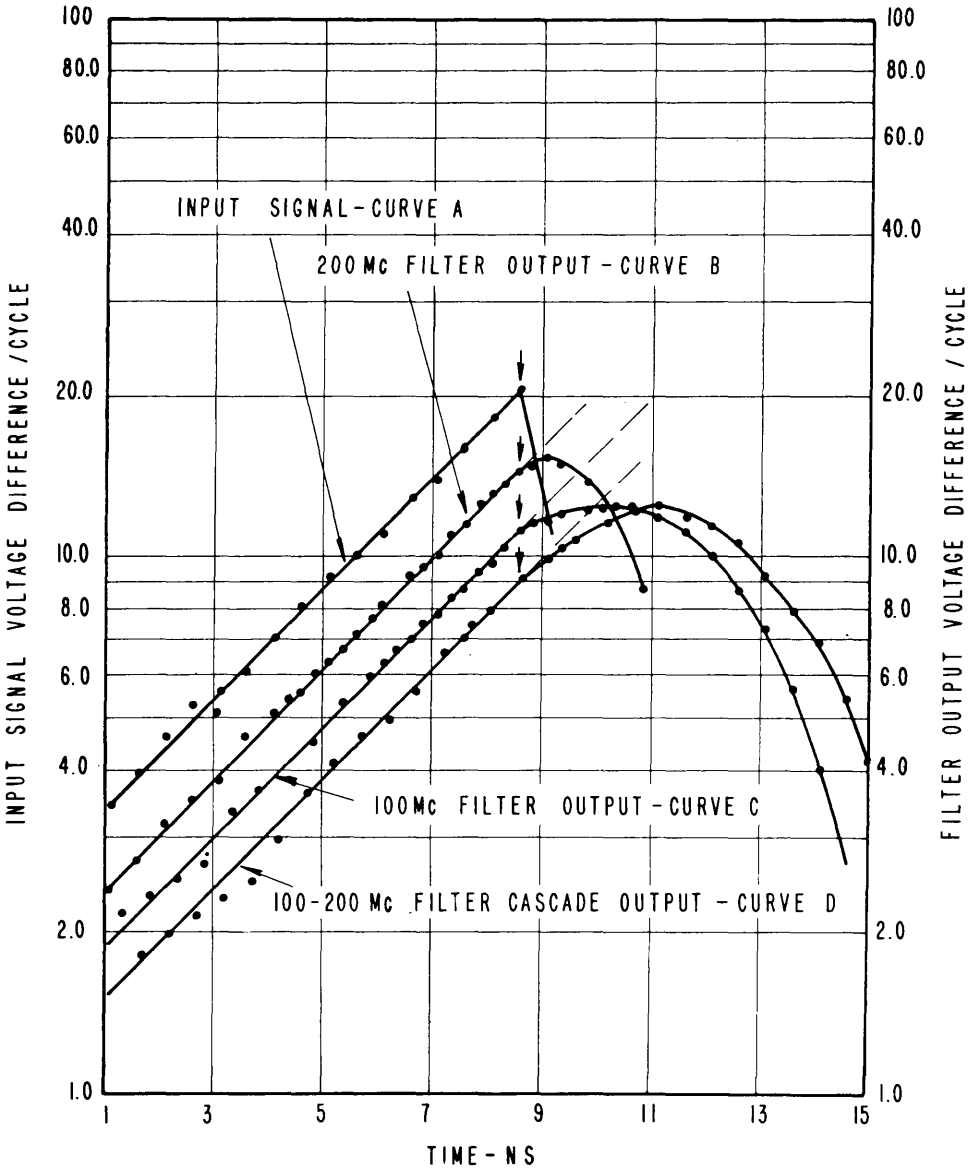

Figure 18 - 100 Mc & 200 Mc filters exponential response

($\alpha = 2.38 \times 10^8$)

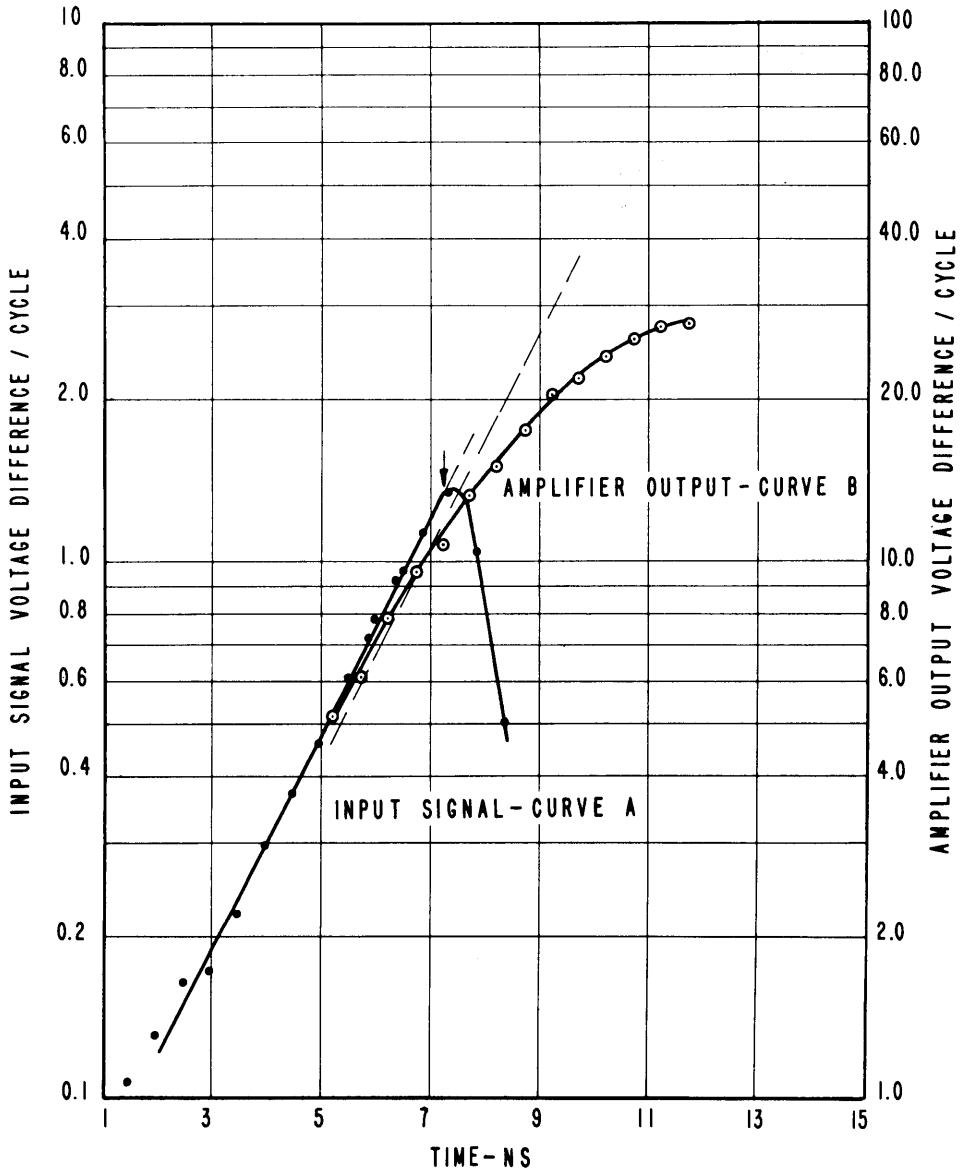

Figure 19 - Ivy amplifier exponential response

(α=4.7×10^8)

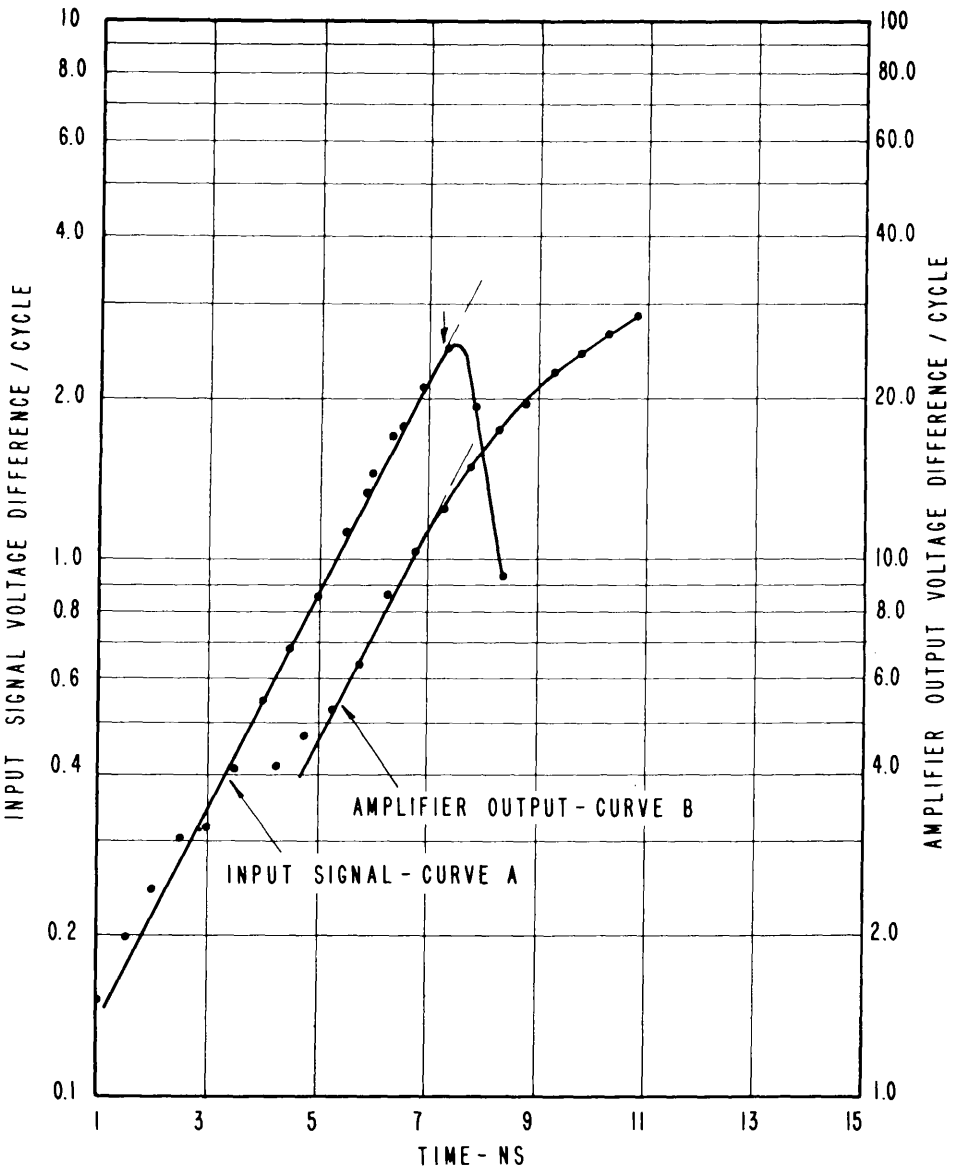

Figure 20 - 418-A distributed amplifier exponential response

(α=4.7×10^8)

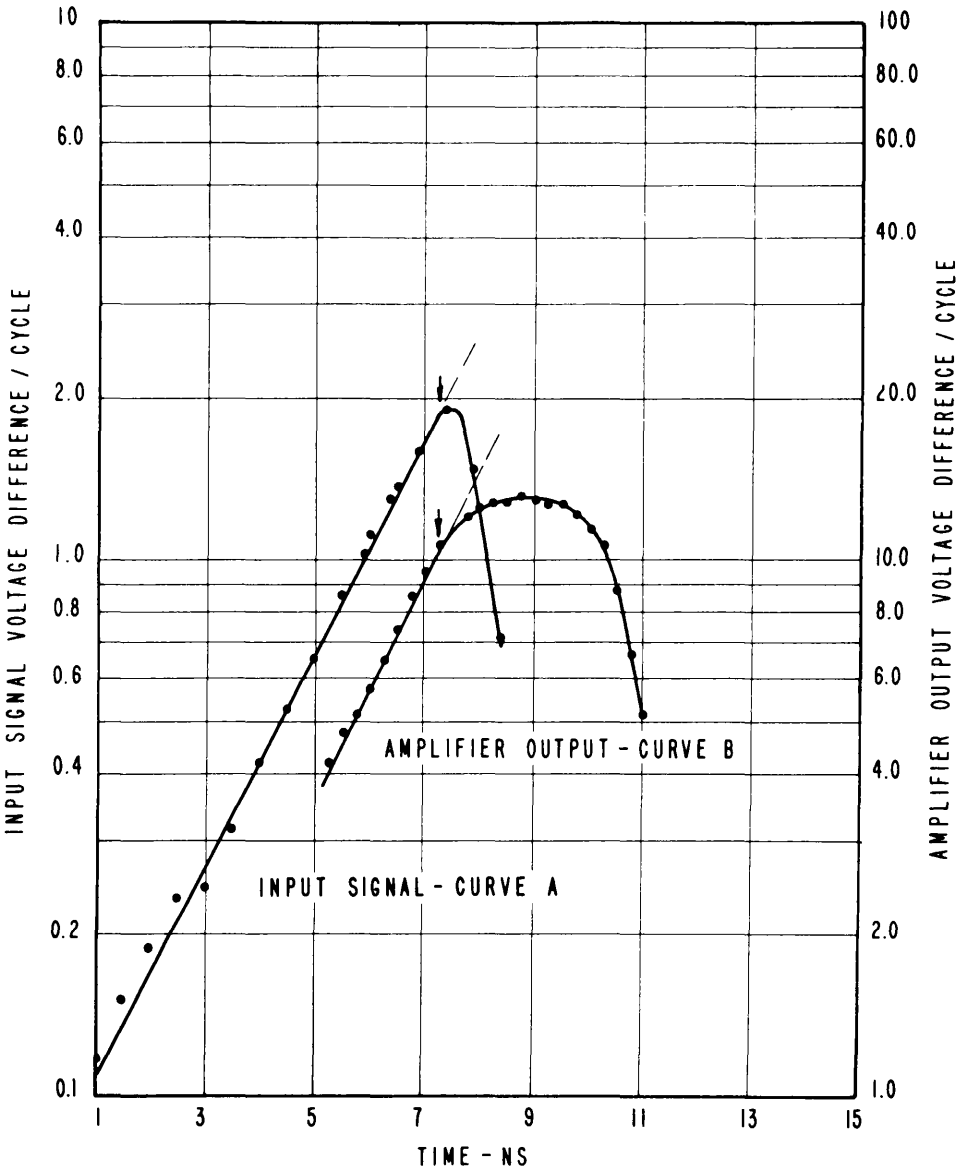

Figure 21 - Single 418-A amplifier exponential response

(α=4.7×10^8)

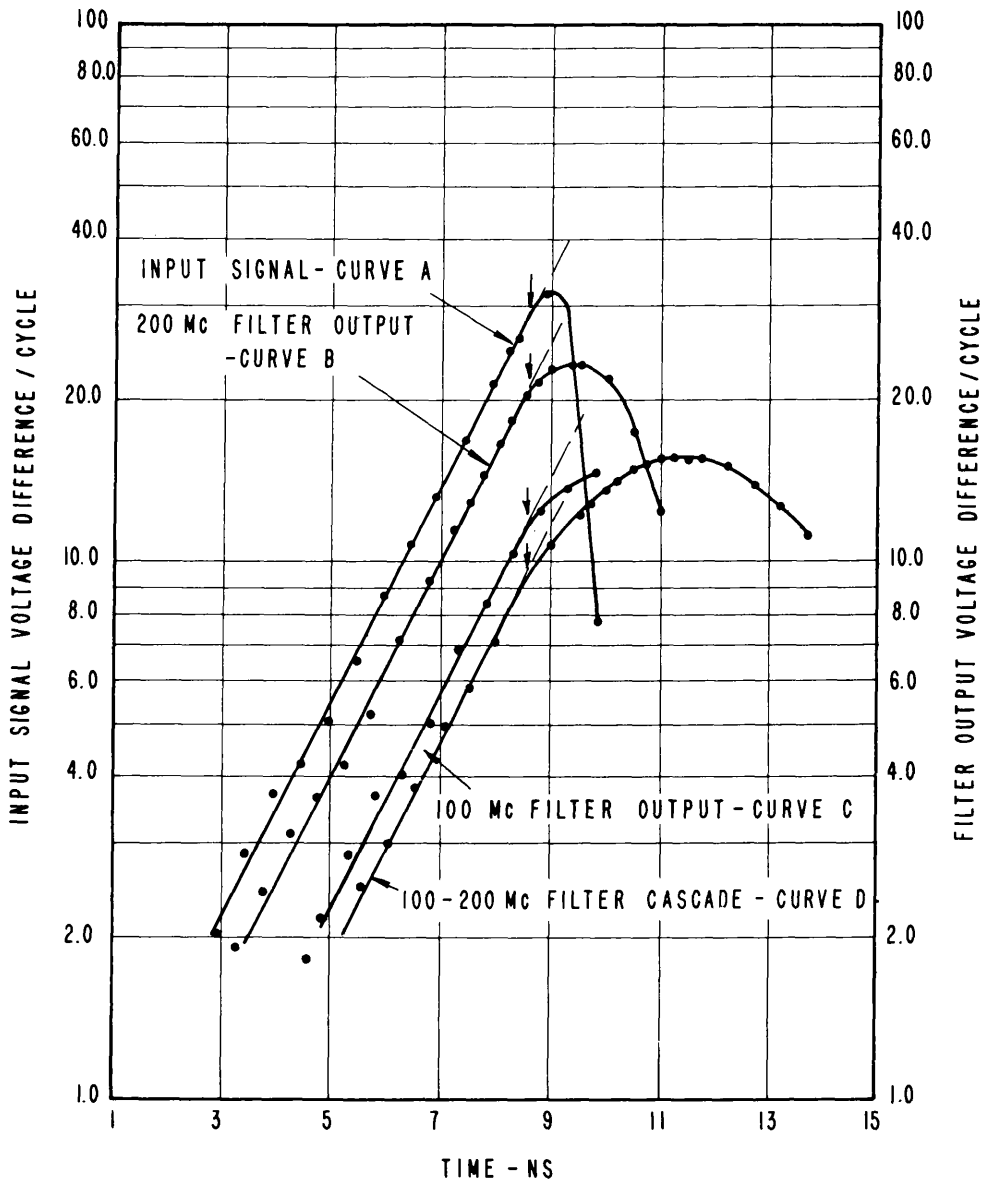

Figure 22 - 100 Mc and 200 Mc filters exponential response

(a=4.7×10^8)

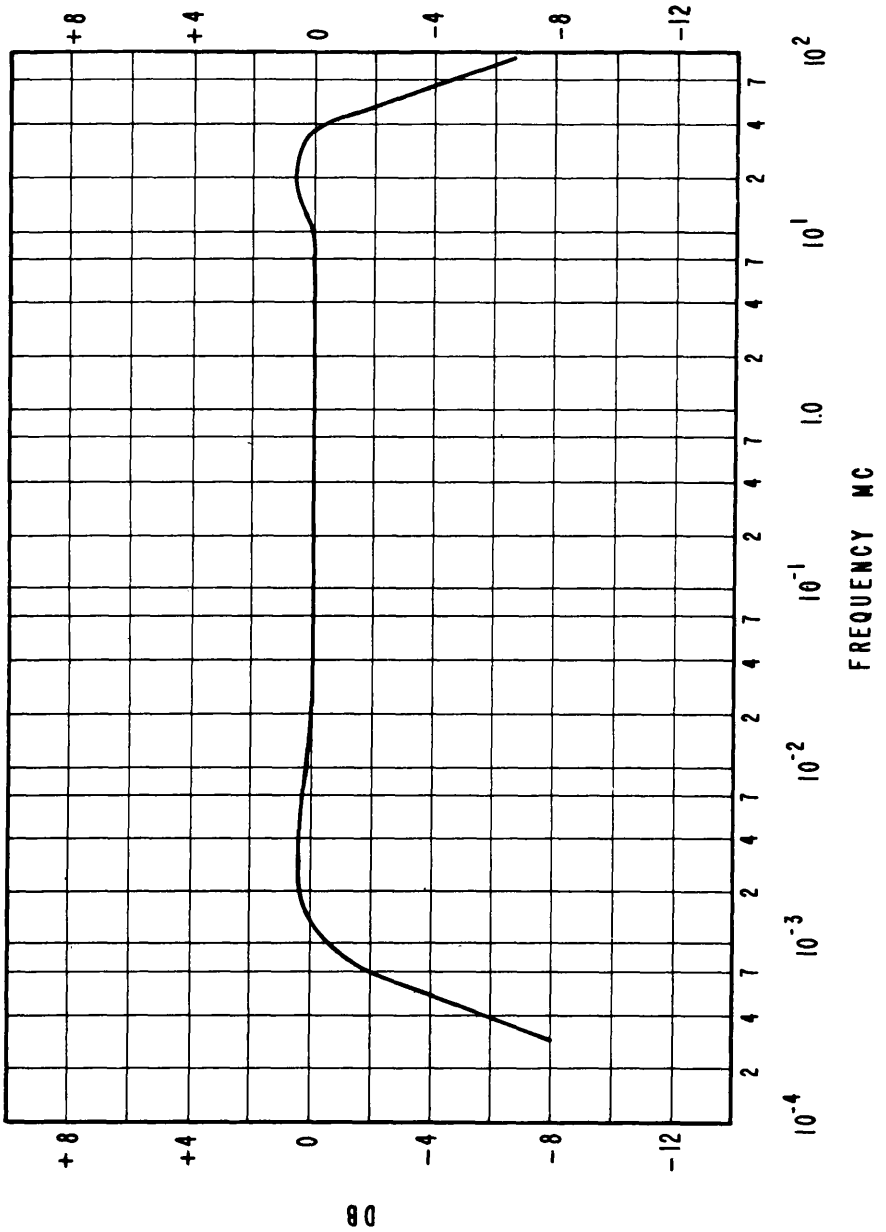

Figure 23 - 418-A distributed amplifier frequency response (V.G. at 0 DB = 77)

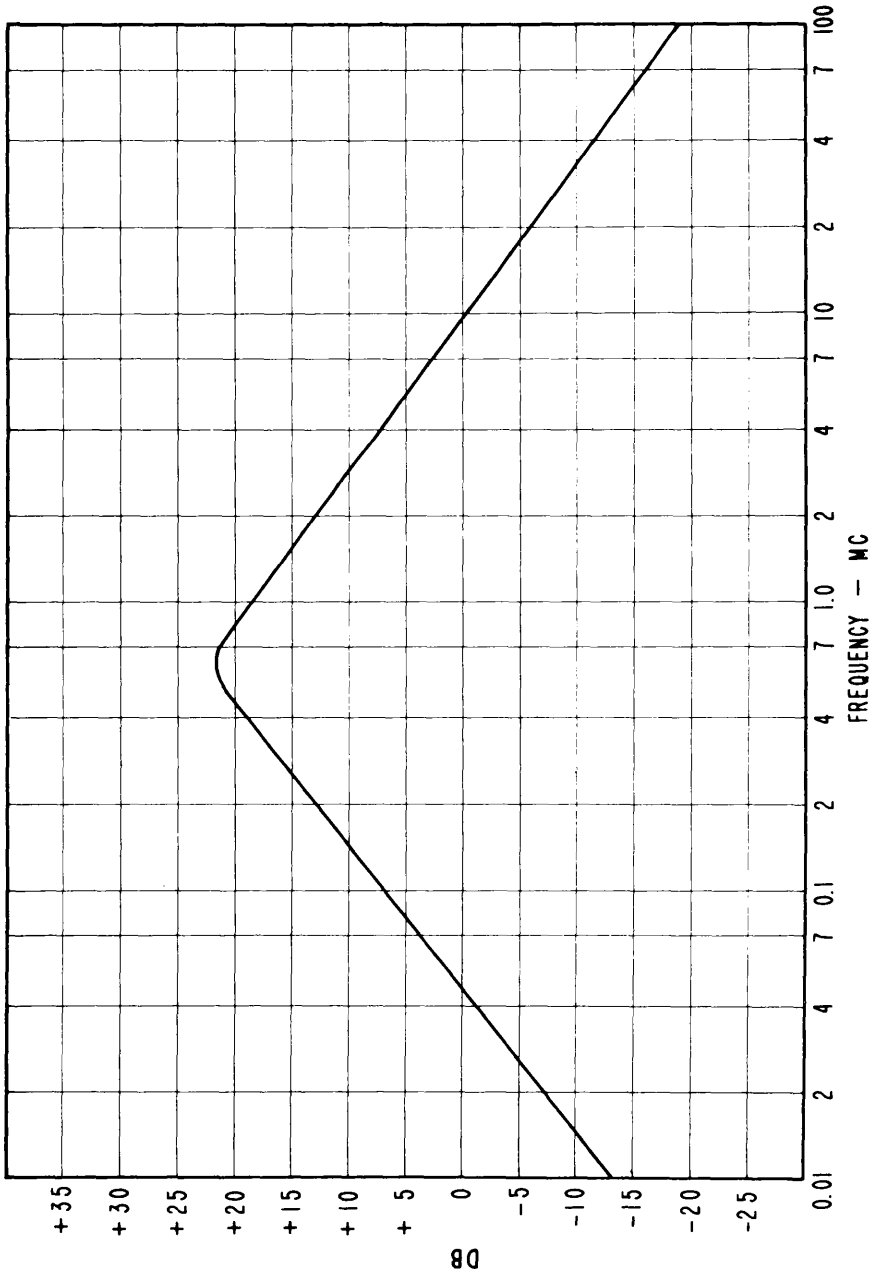

Figure 24 - Single 418-A amplifier frequency response
(V.G. at O DB = 37.5)

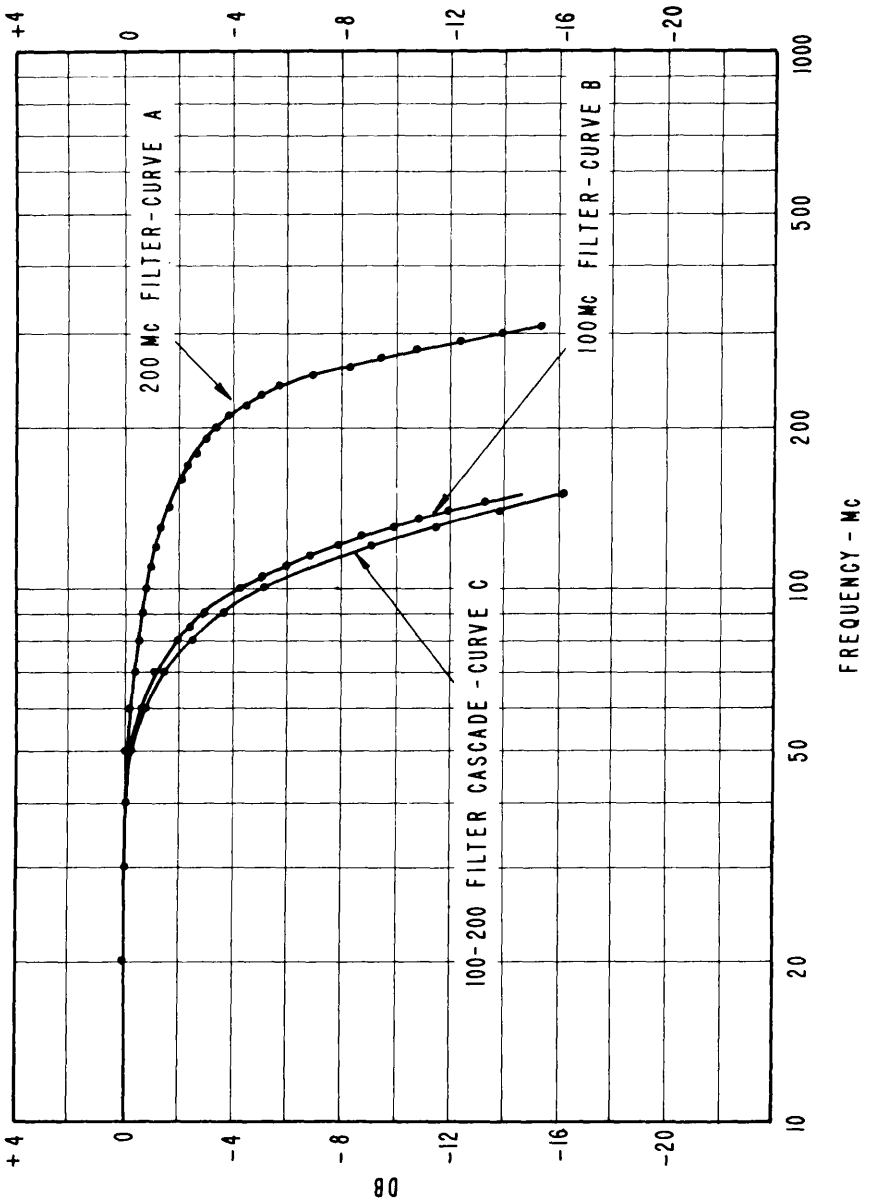

Figure 25 - 100 Mc & 200 Mc filters frequency response

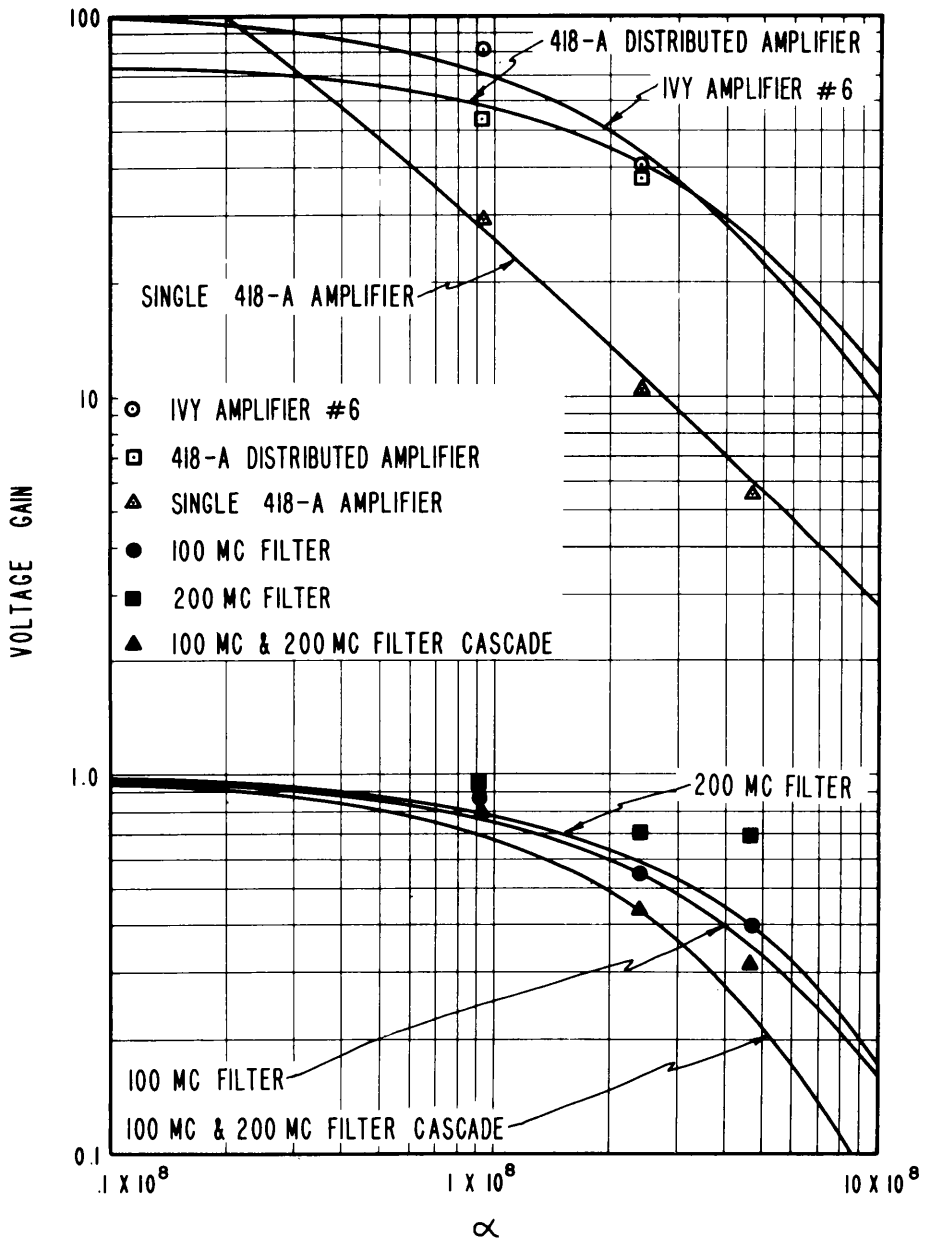

Figure 26 - Measured & calculated gain versus α

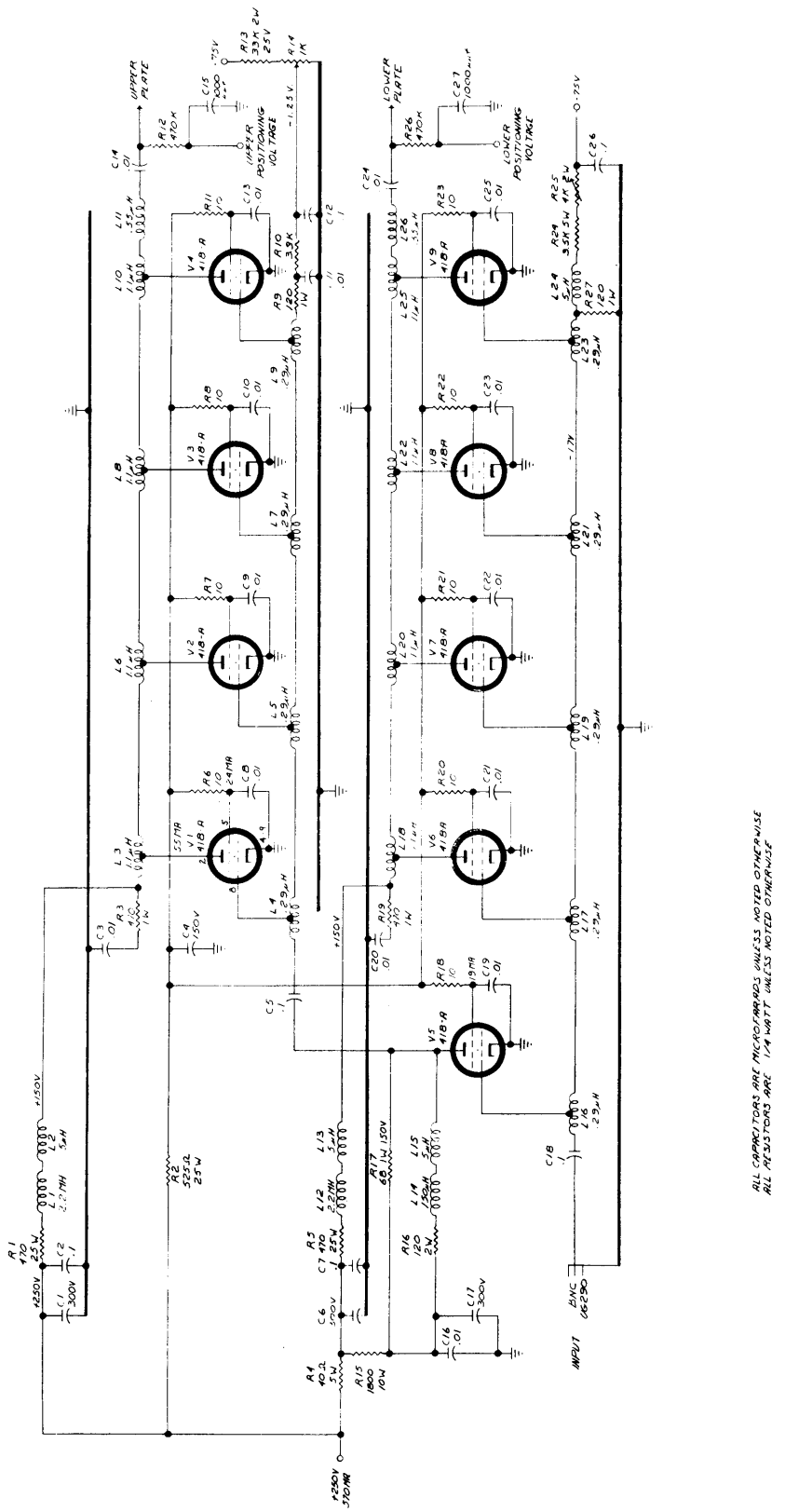

Figure 27 - 418-A distributed amplifier circuit diagram

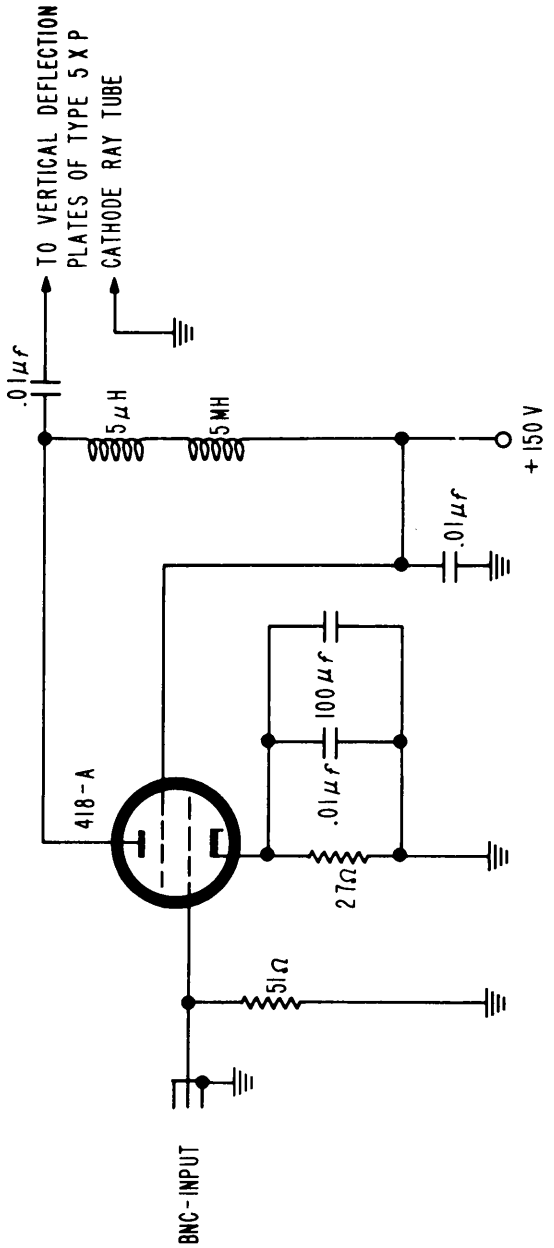

Figure 28 - Single 418-A amplifier circuit diagram

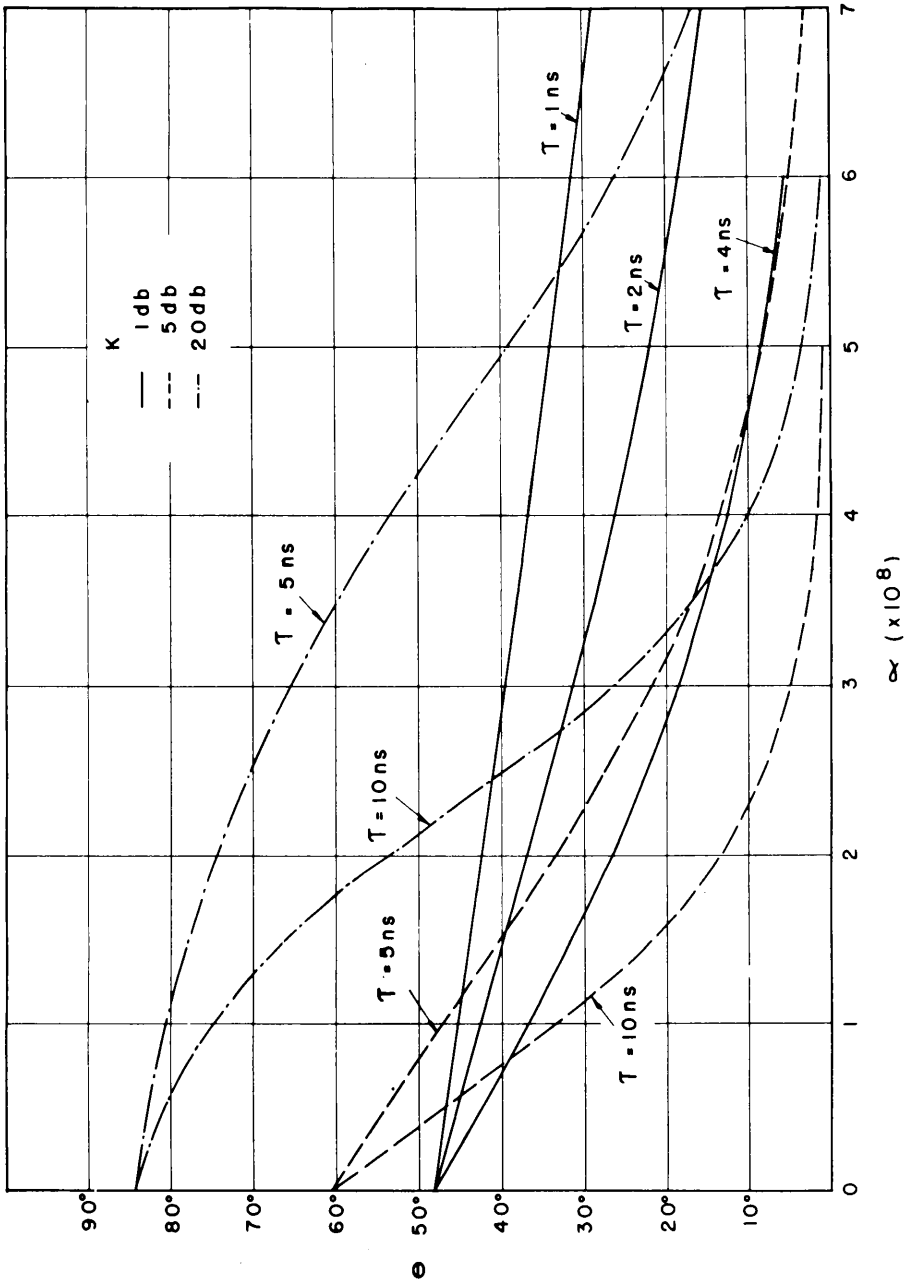

Figure 29 - Variation of X-Y angle vs. alpha

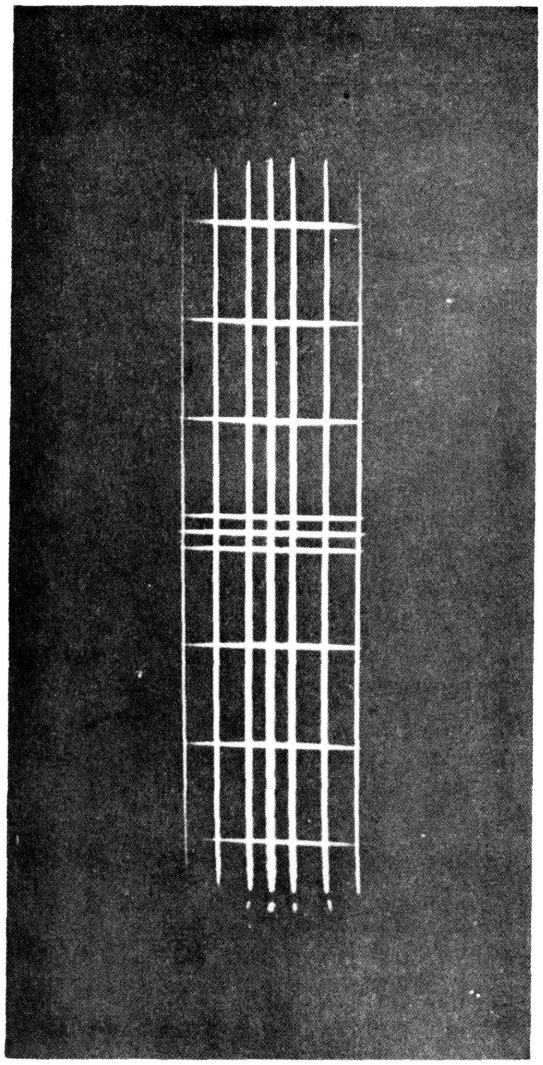

Figure 30 - D.C. calibration raster

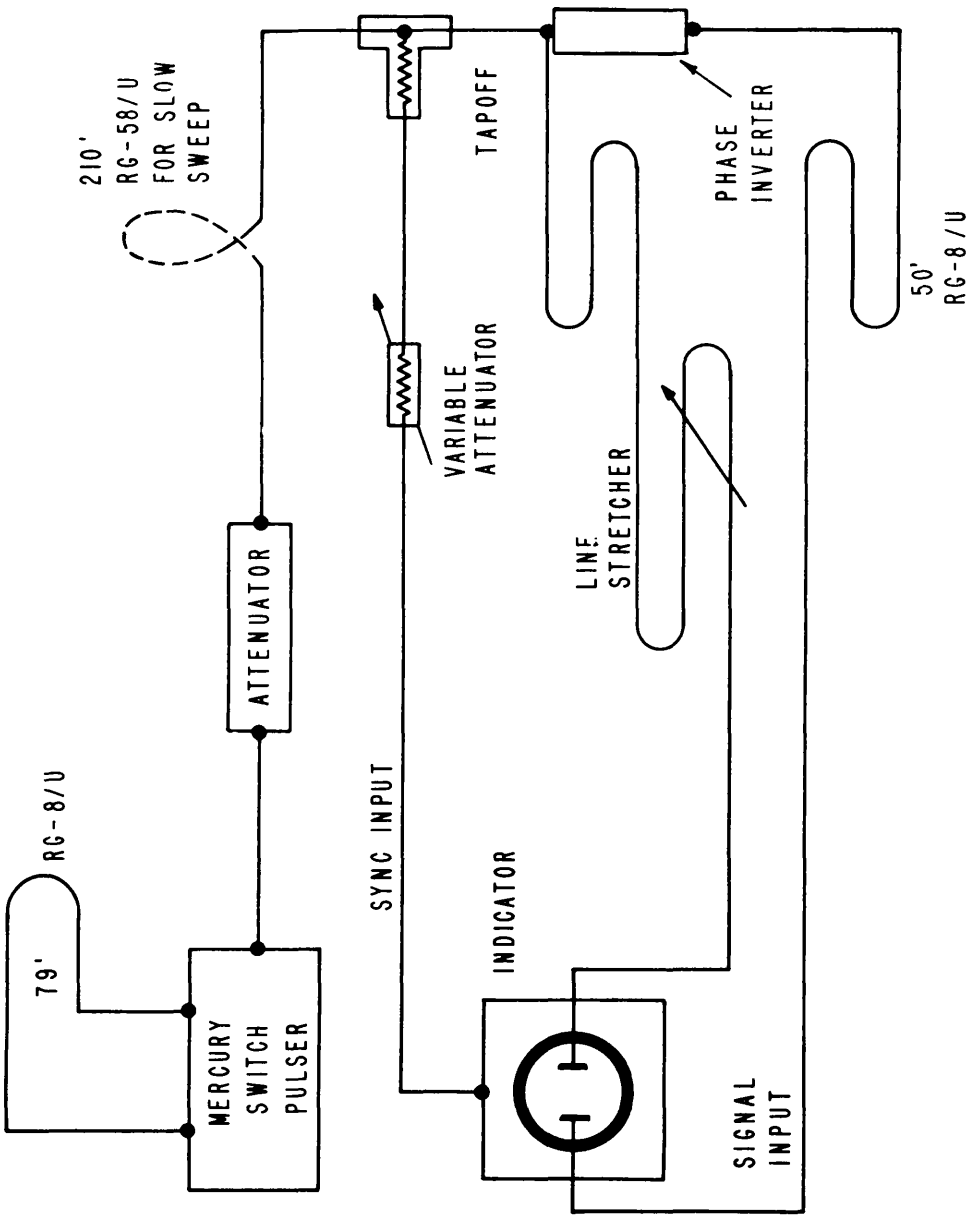

Figure 31 - Block diagram of system for measuring writing speed

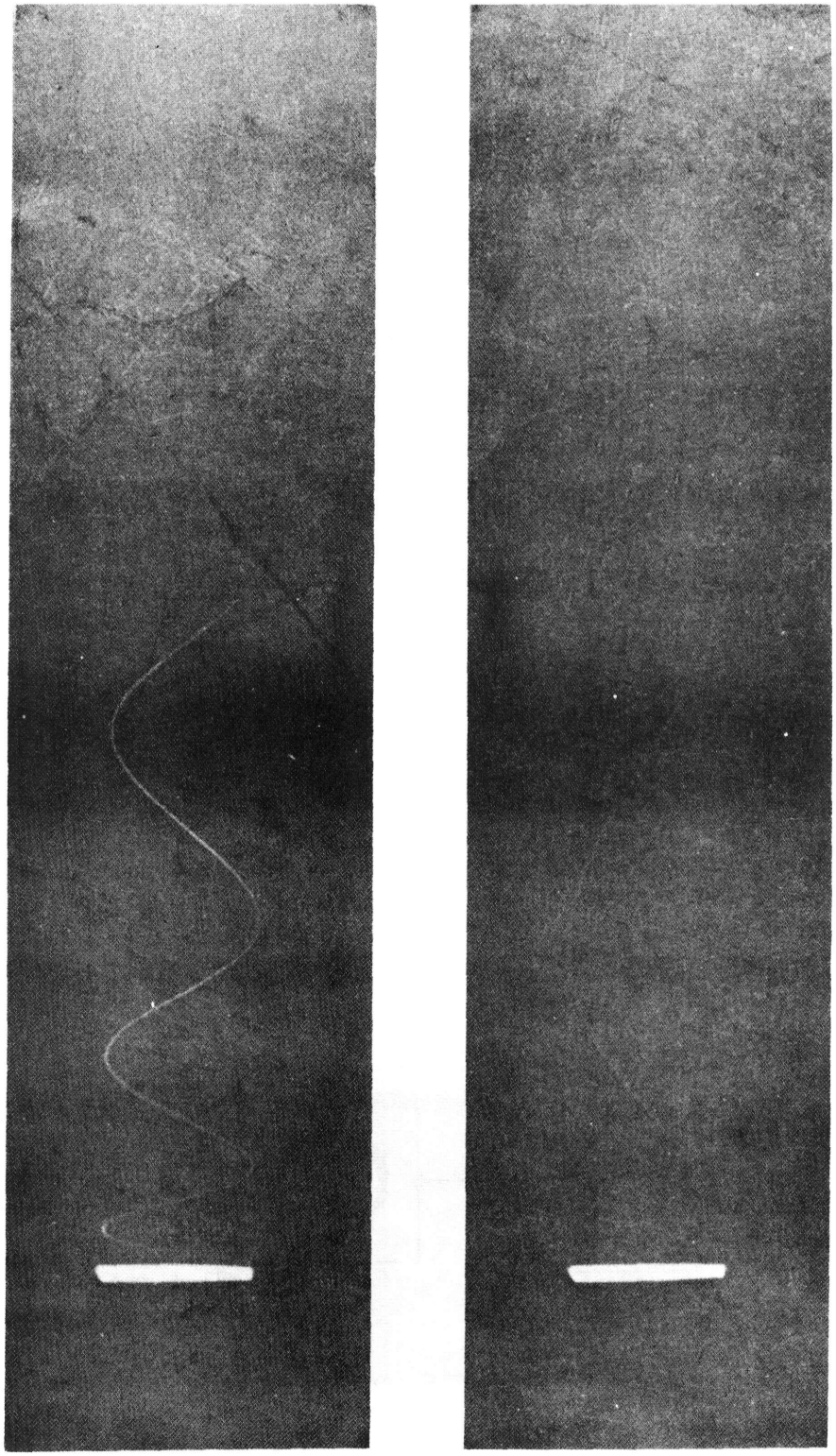

Figure 32 - Writing speed comparison

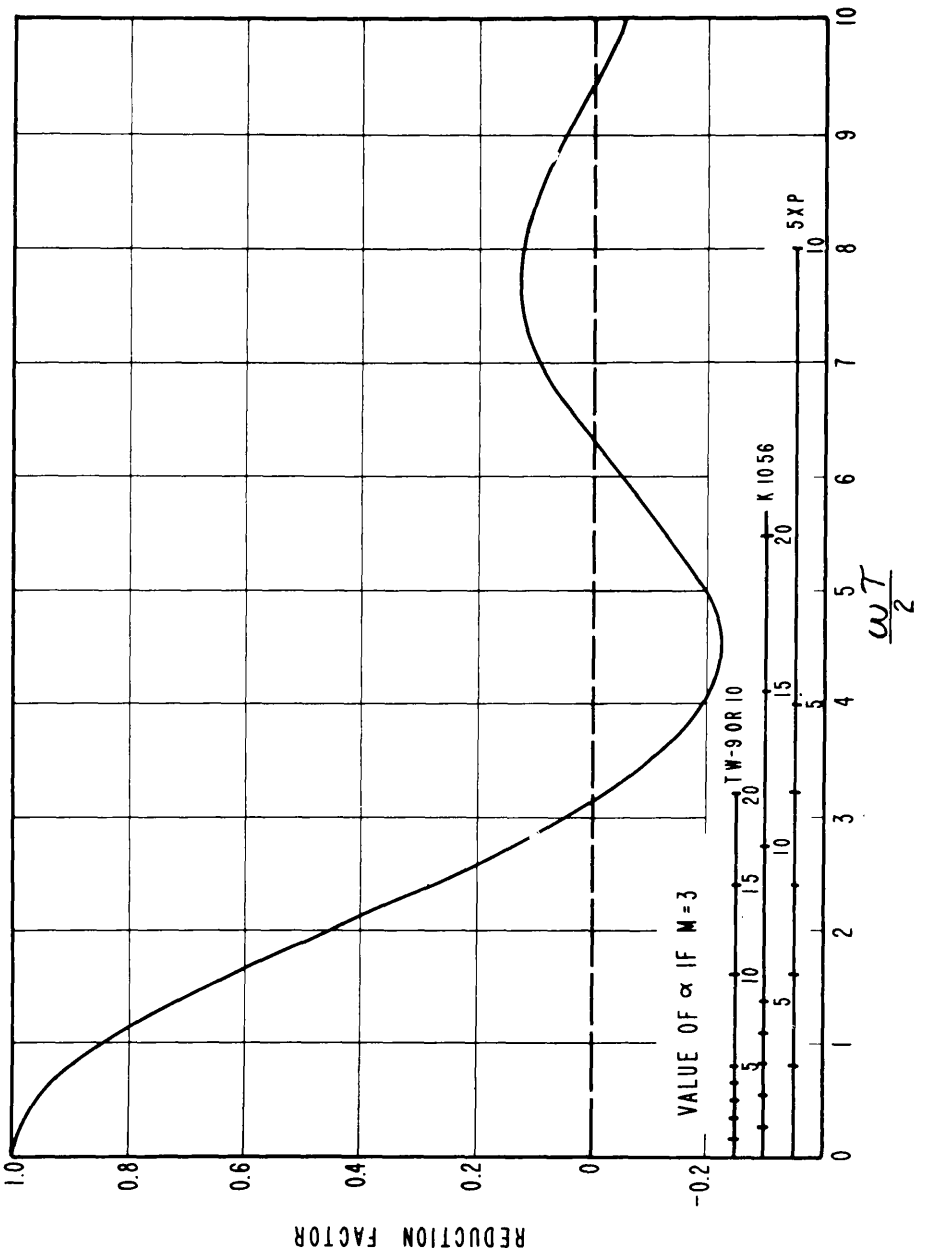

Figure 33 - Sensitivity reduction factor for deflection plates with sinusoidal input

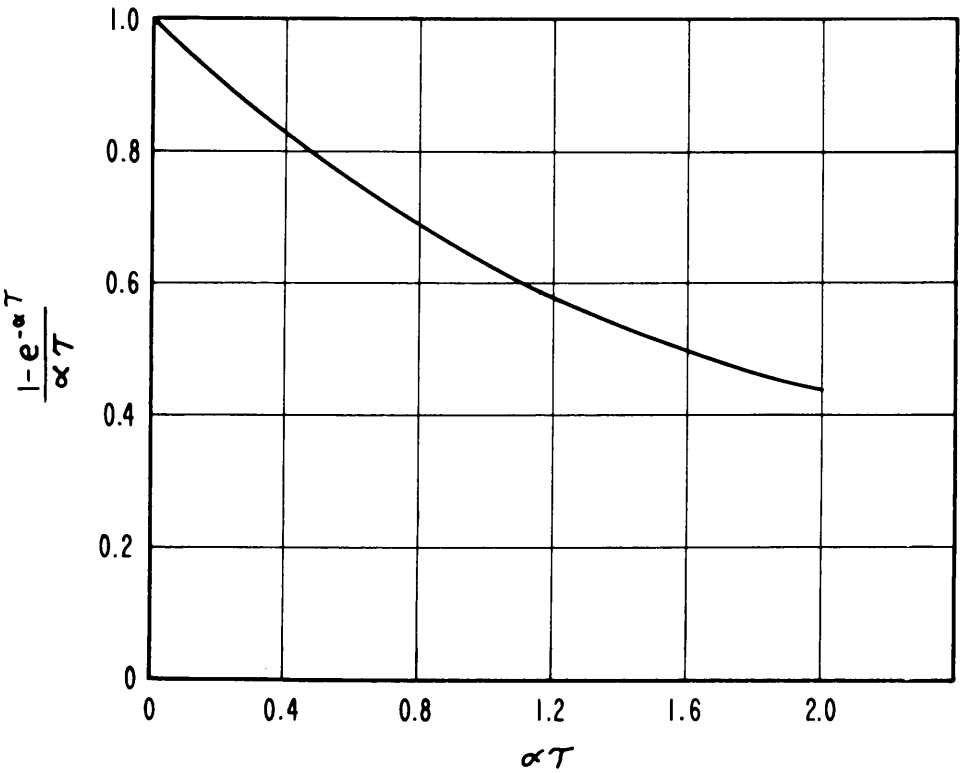

Figure 34 - Sensitivity reduction factor for deflection plates with exponential input

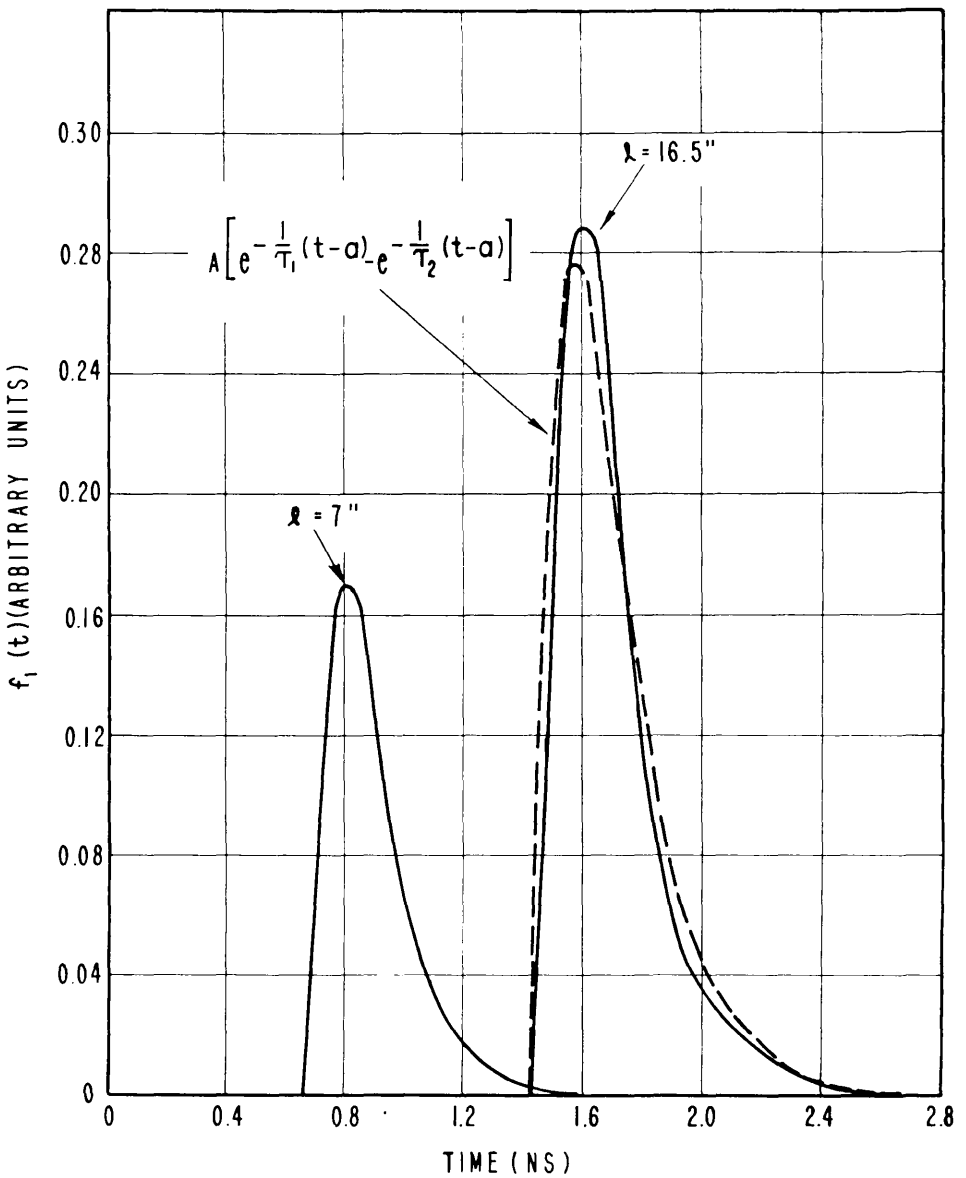

Figure 35 - Response of terminated detector to δ-function input

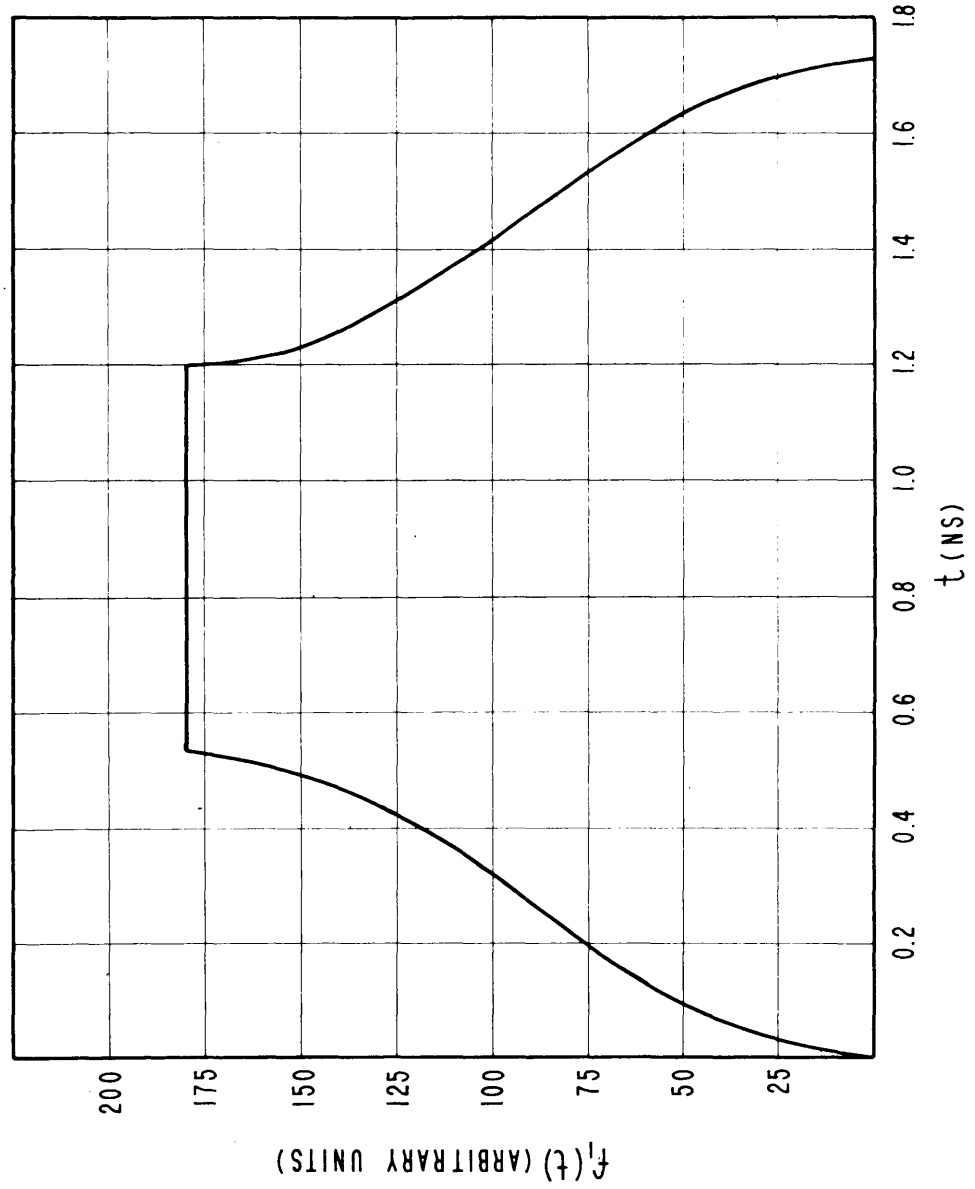

Figure 36 - Response of open-circuited detector to δ-function input

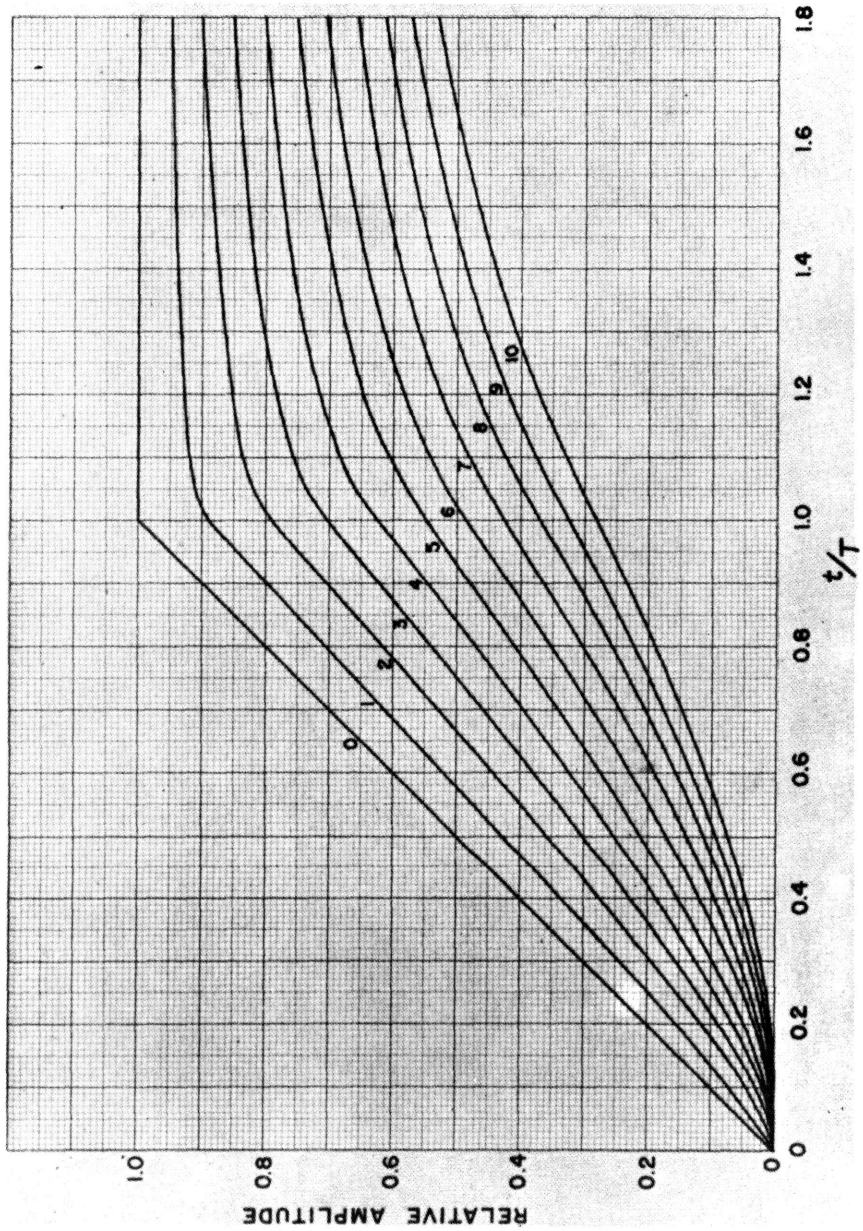

Figure 37 - Response of transmission line to ramp function input

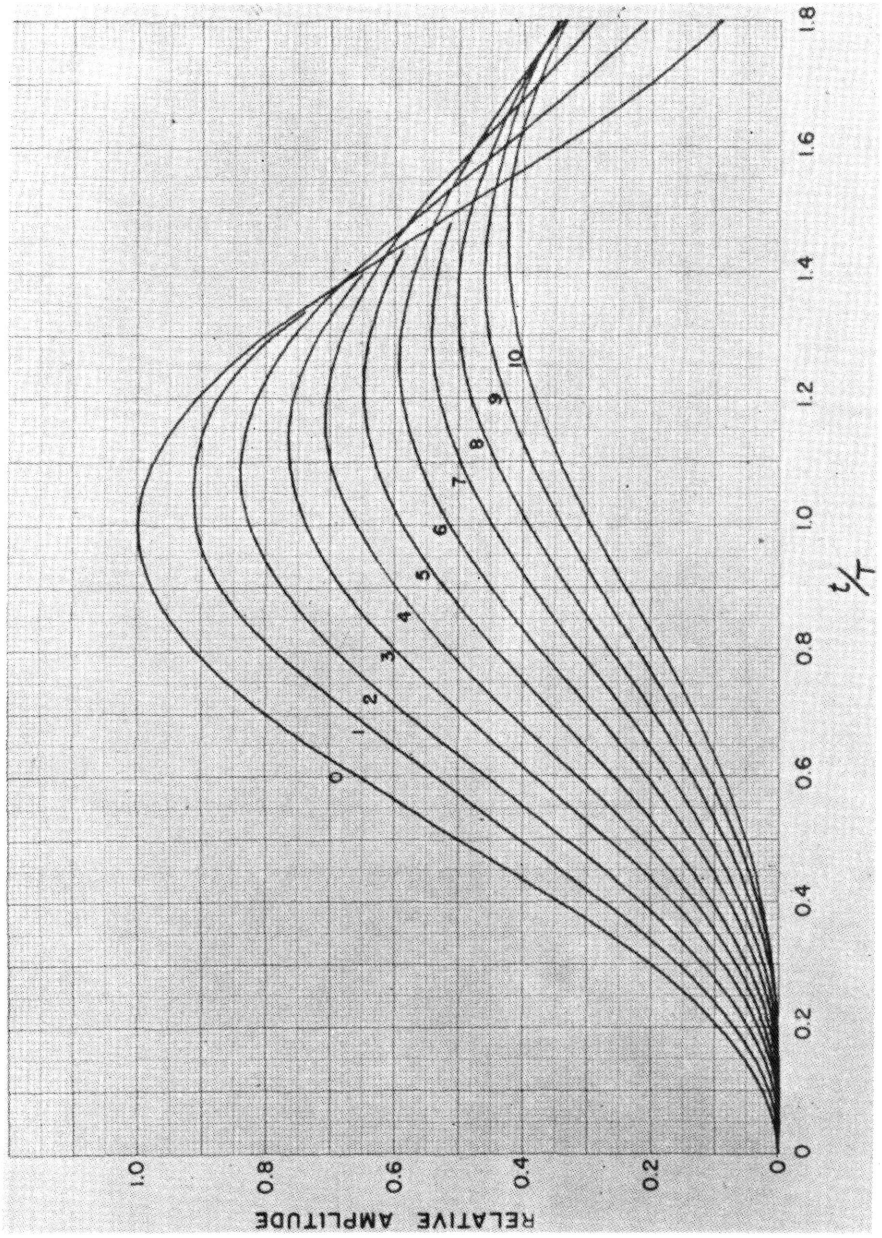

Figure 38 - Response of transmission line to cosine squared input

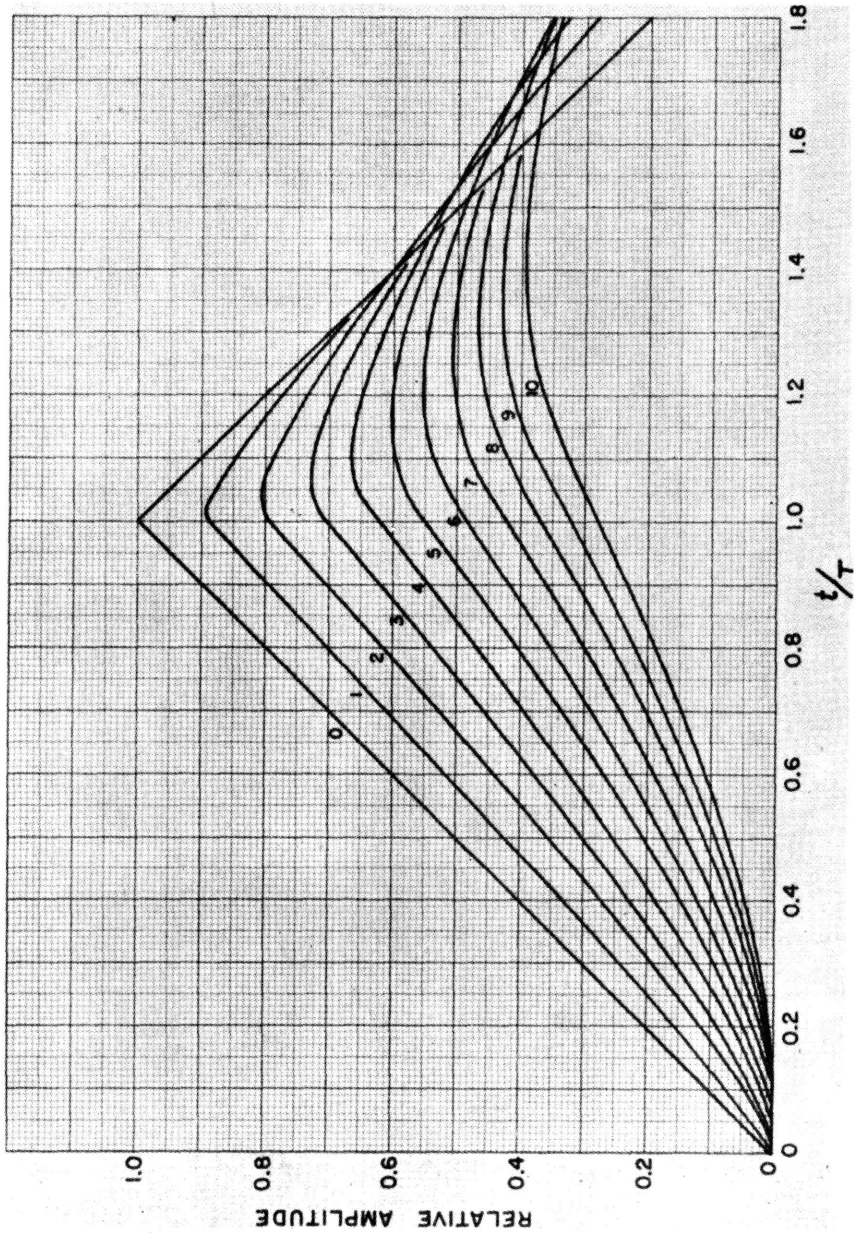

Figure 39 - Response of transmission line to triangular input

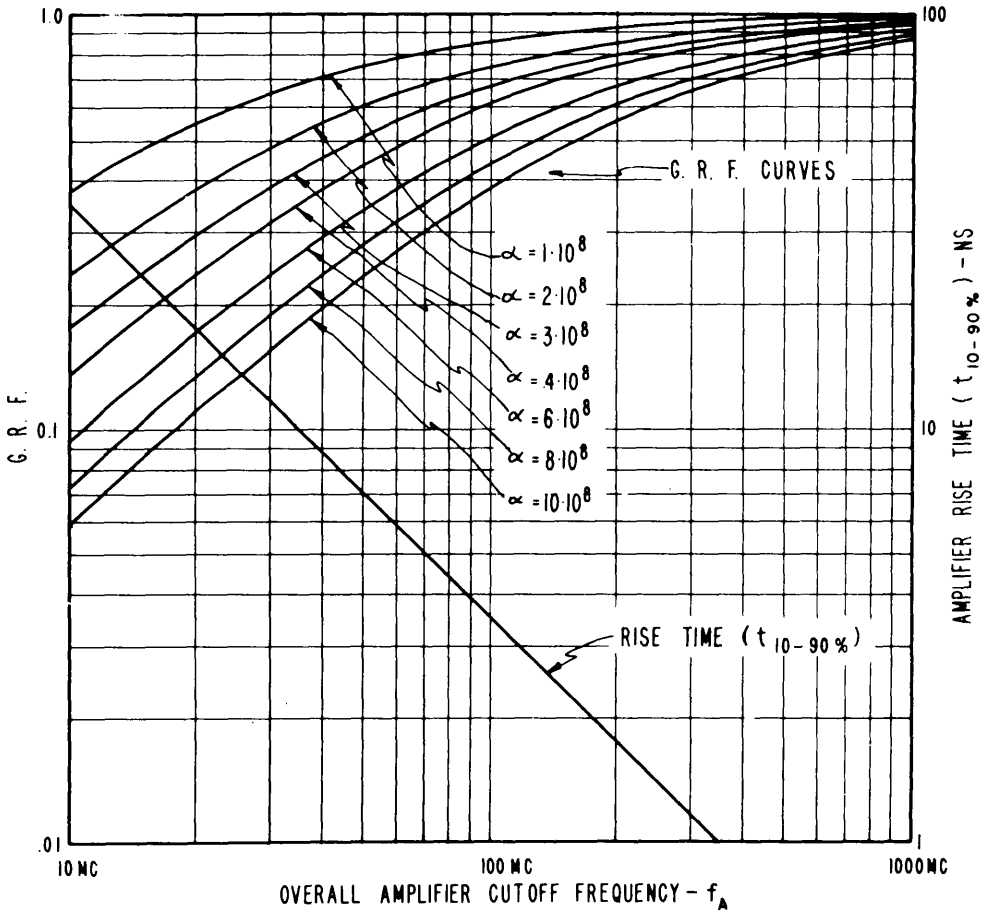

Figure 40 - Rise time and GRF vs. f_A

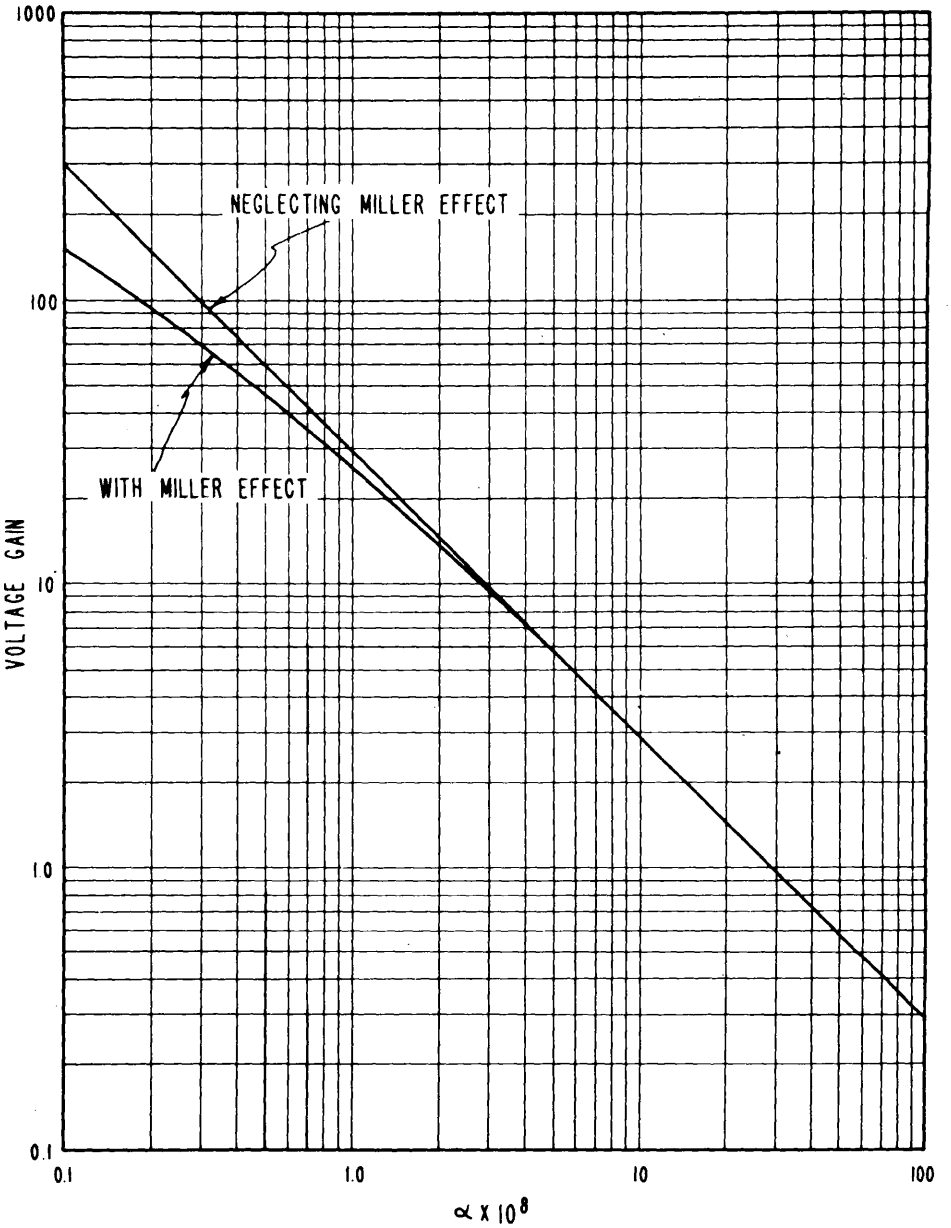

Figure 41 - Gain of single 418-A amplifier vs. alpha

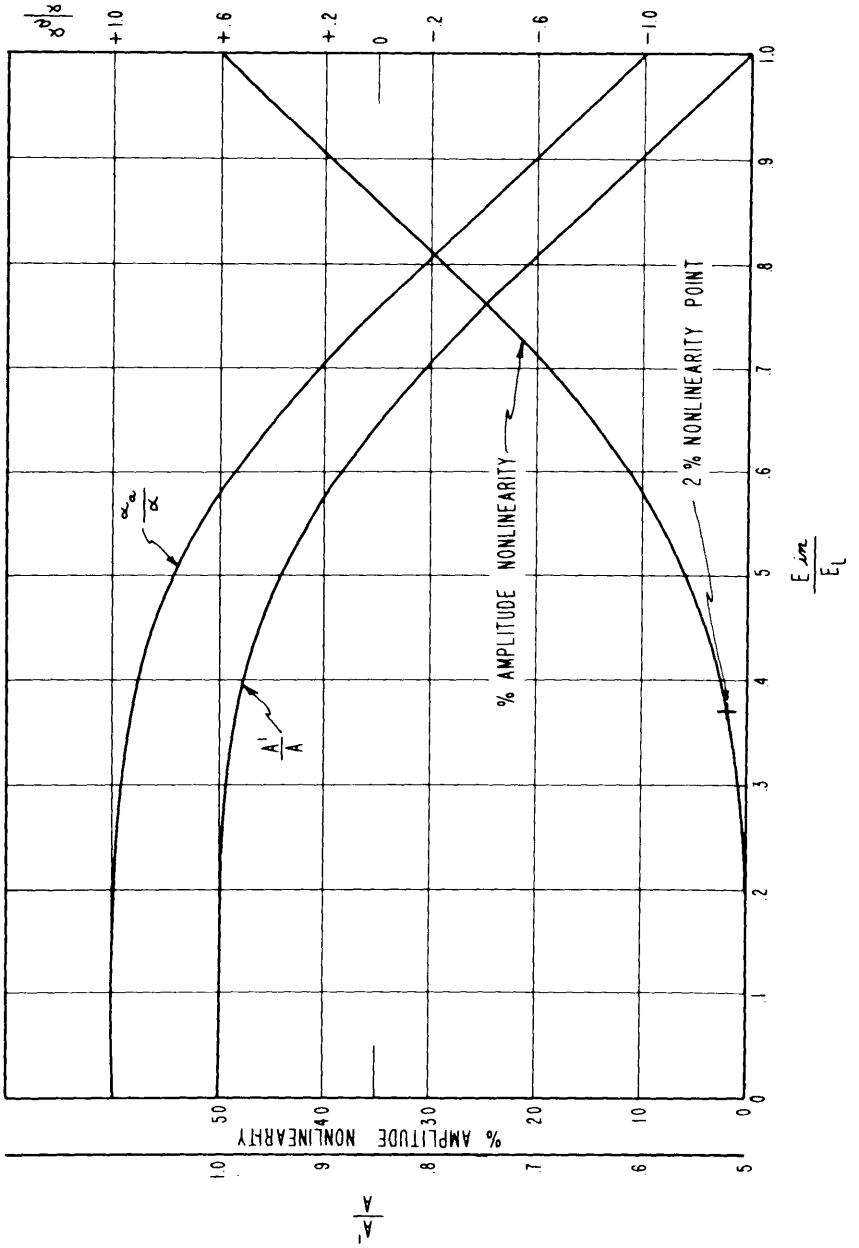

Figure 42 - Amplitude and alpha nonlinearity (Ivy amplifier)

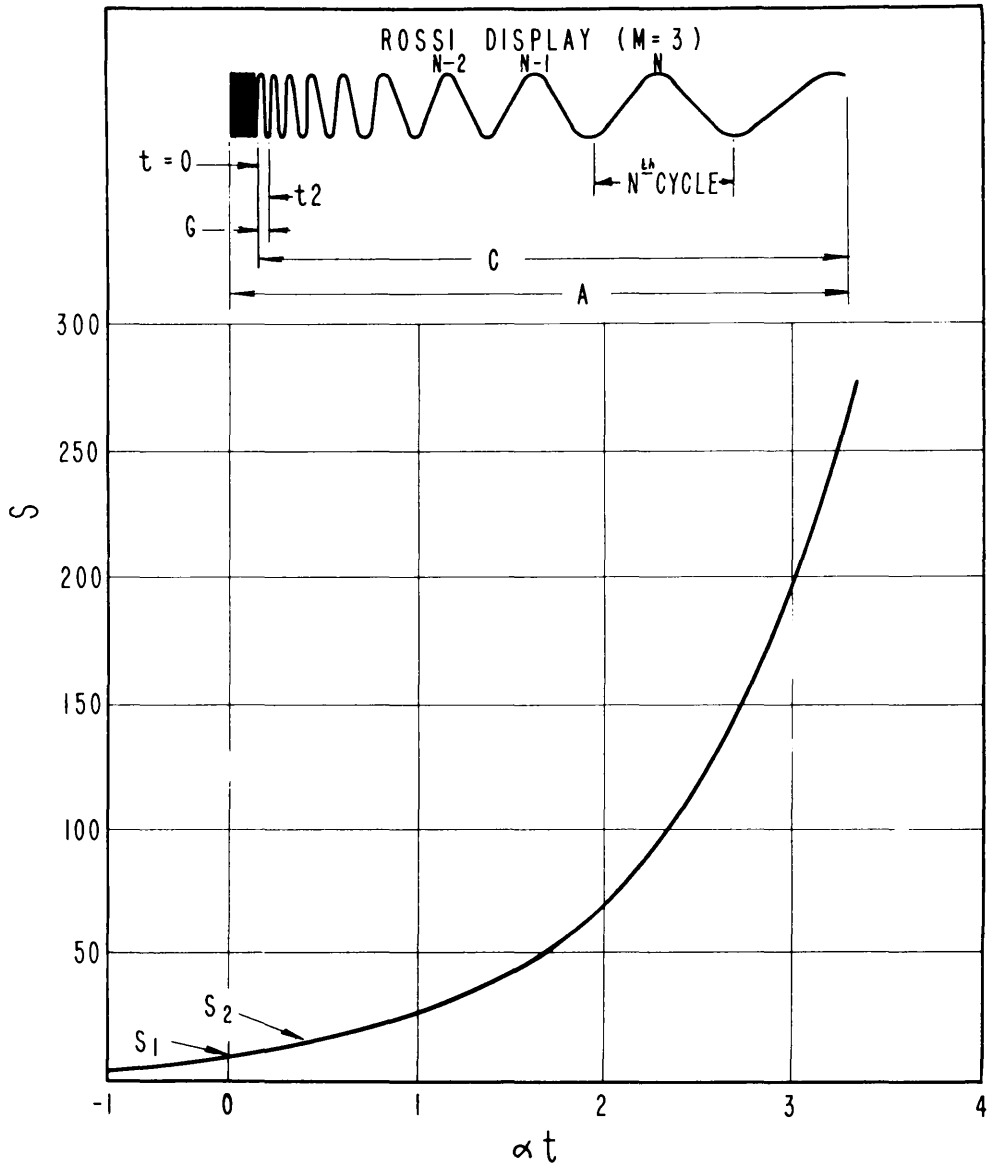

Figure 43 - The exponential signal and the Rossi display

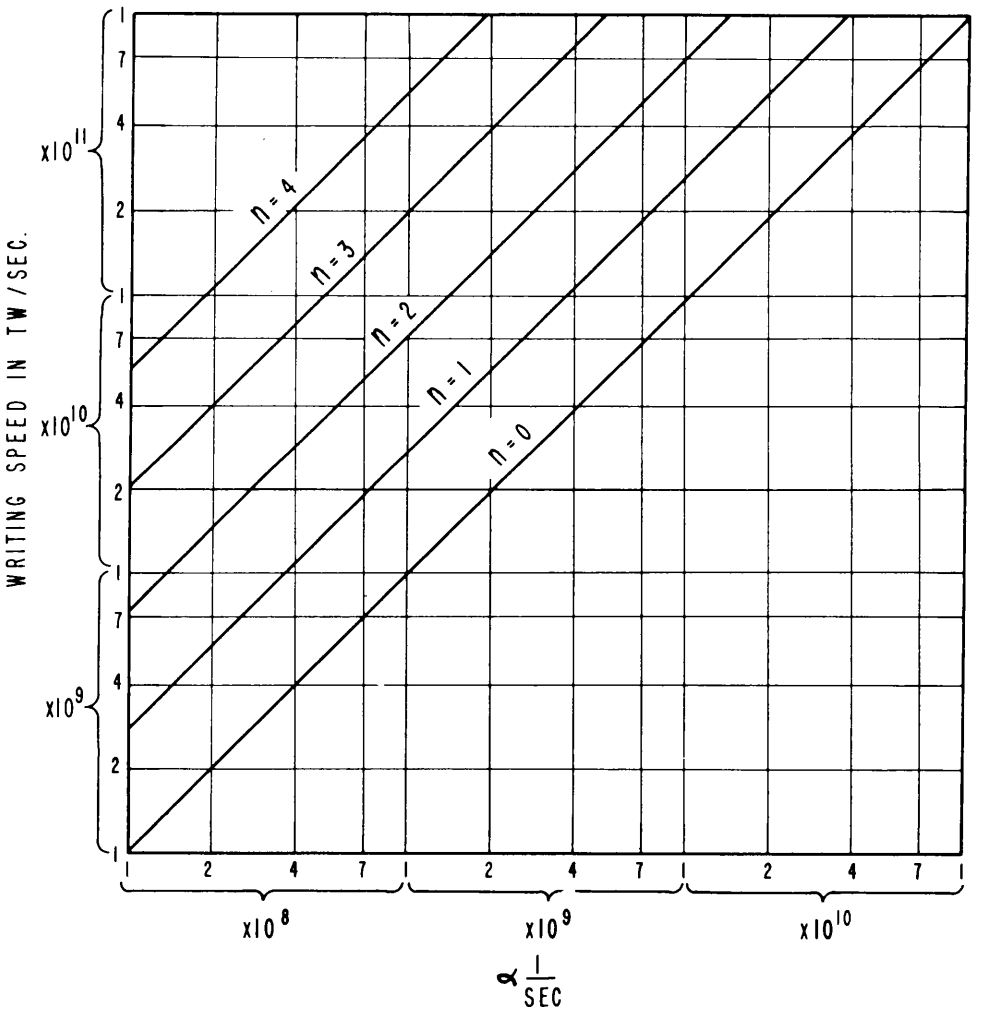

Figure 44 - Writing speed vs. alpha for Rossi display

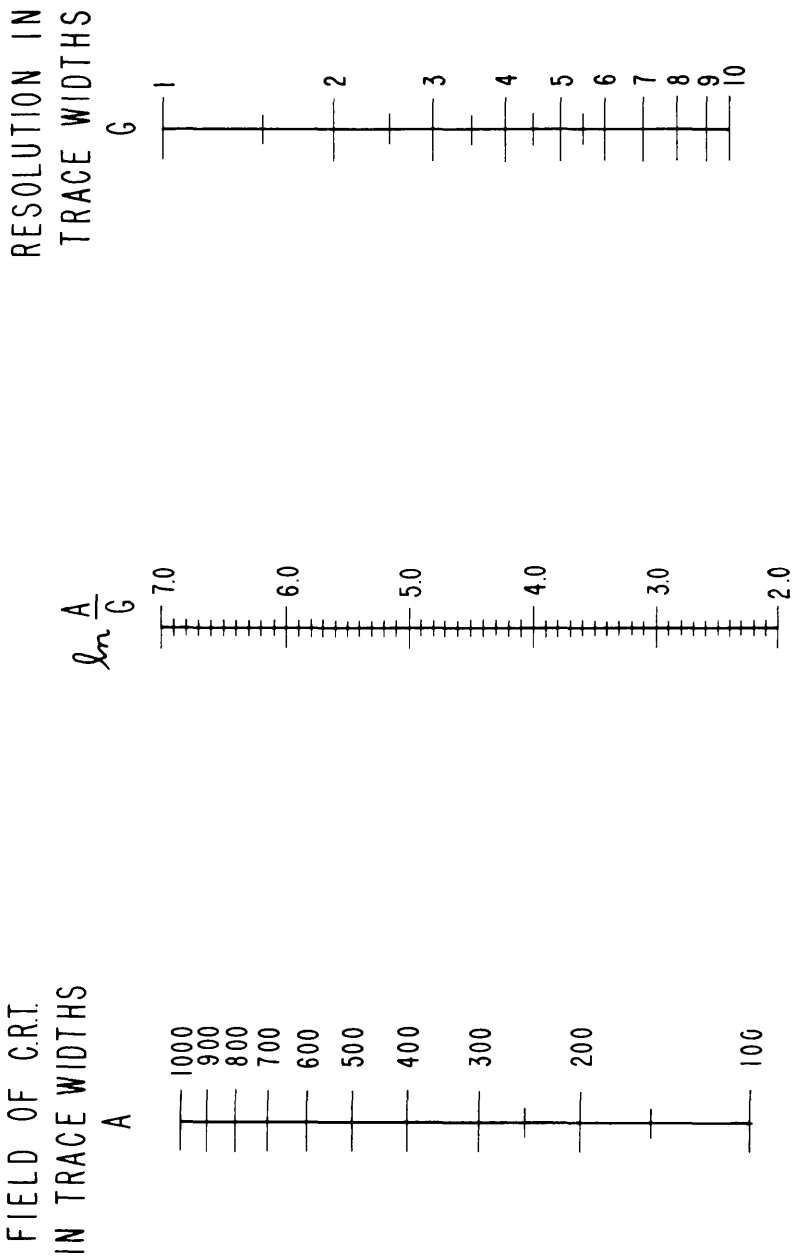

Figure 45 - Nomograph relating field, resolution and *ln* A/G

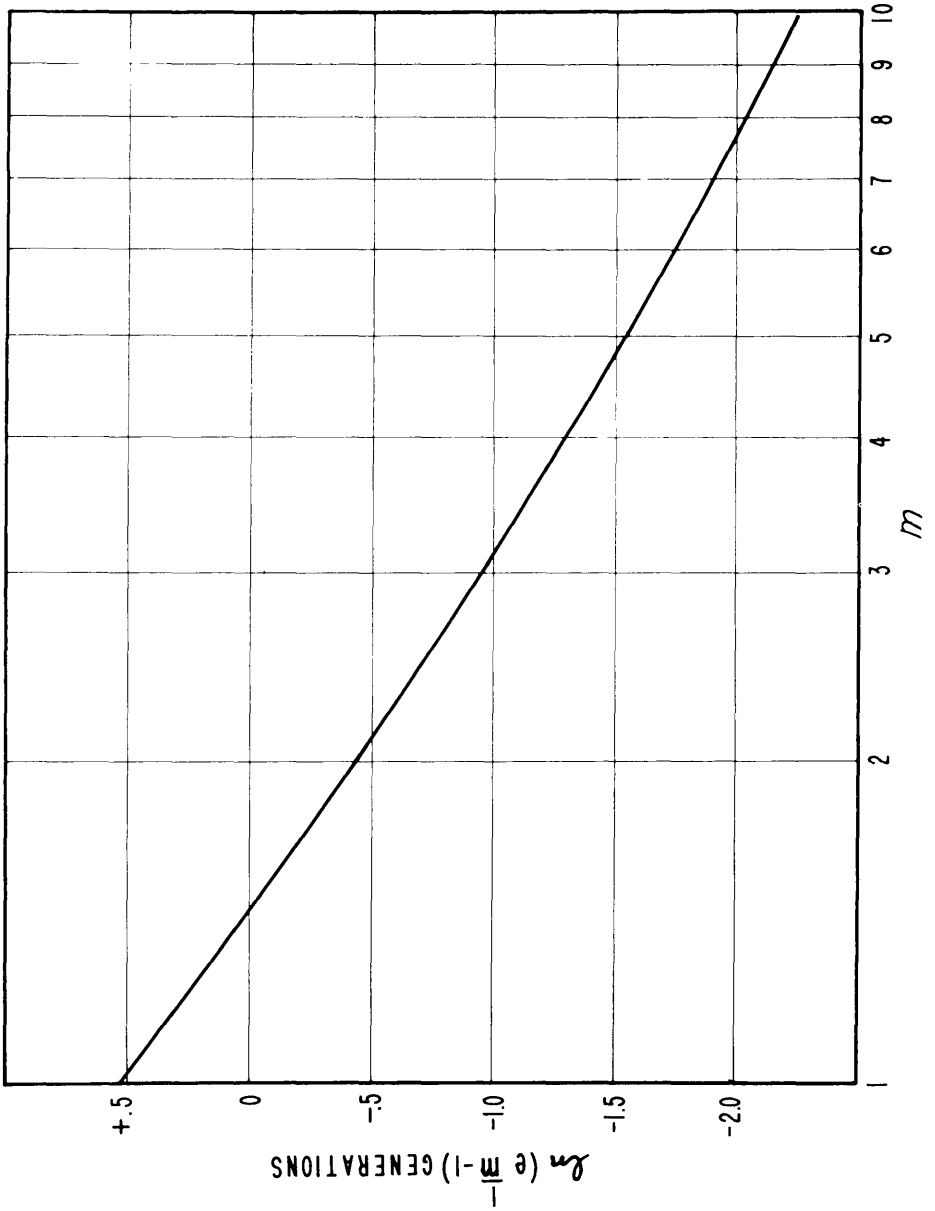

Figure 46 - $\ln(e^{\frac{1}{m}}-1)$ vs. m

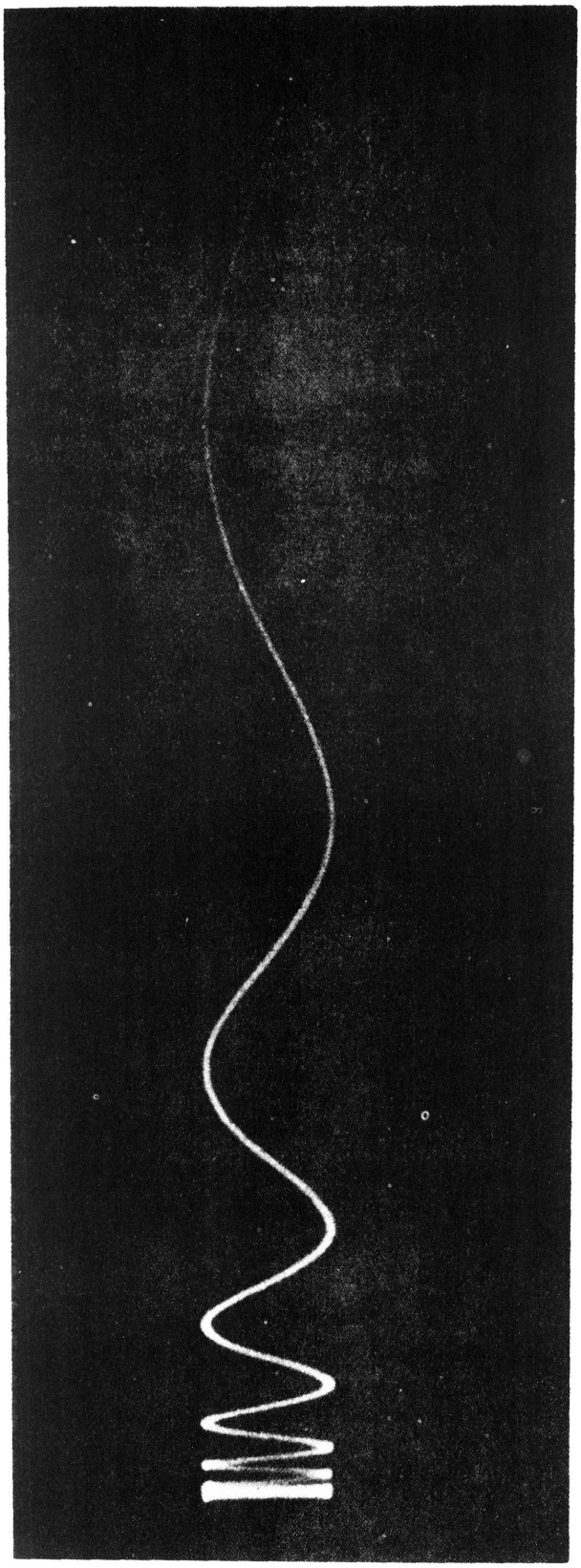

Figure 47 - Rossi display (f = 400 mc)

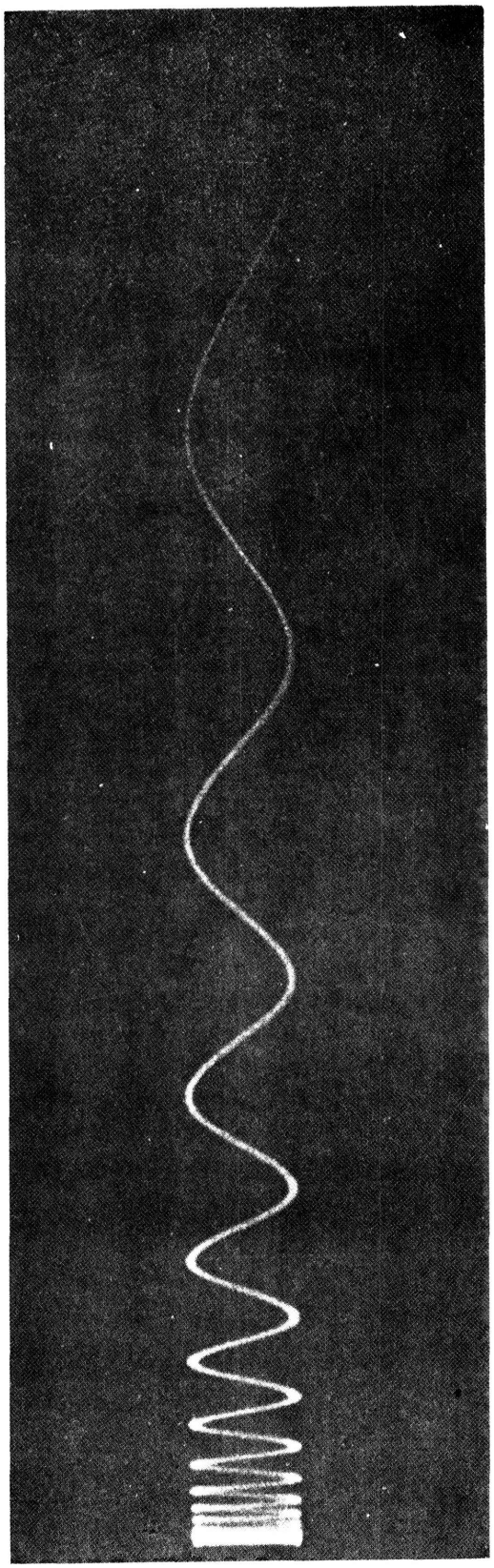

Figure 48 - Rossi display (f = 800 mc)

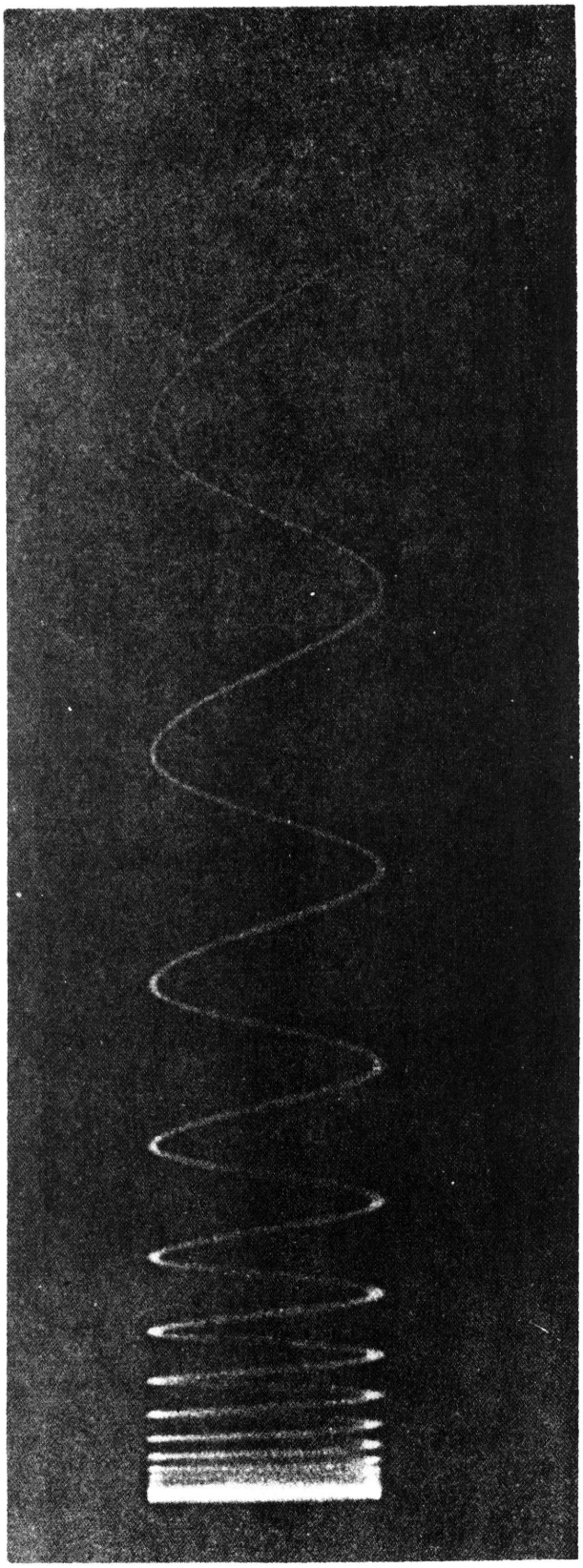

Figure 49 - Rossi display (f = 1000 mc)

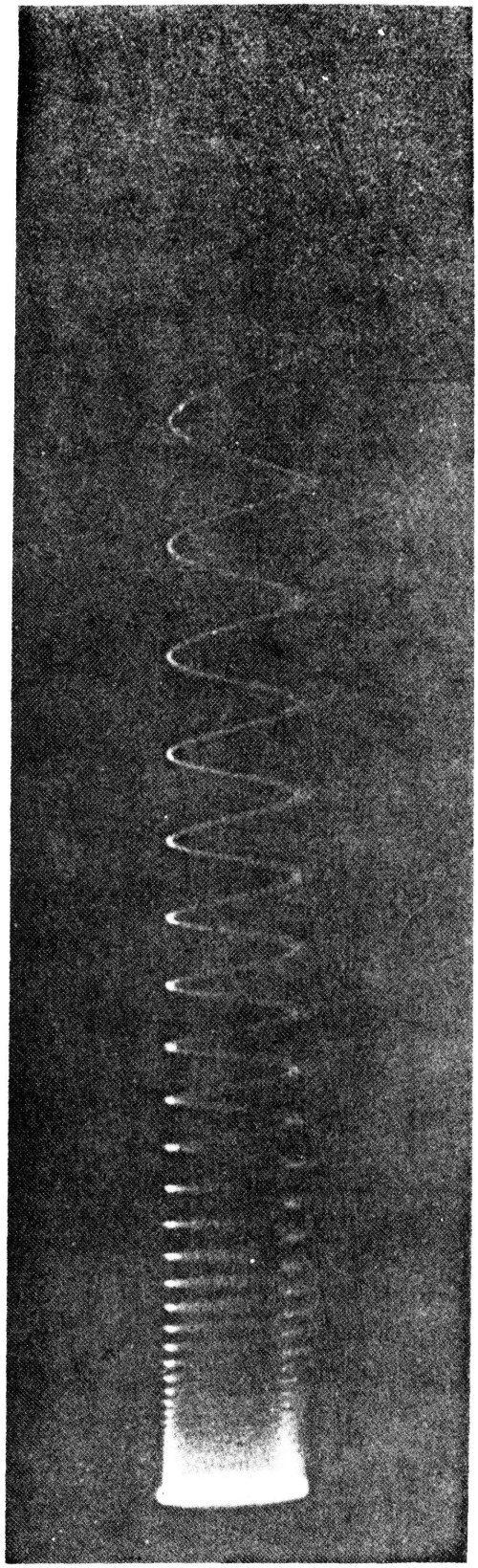

Figure 50 - Rossi display (f = 3000 mc)

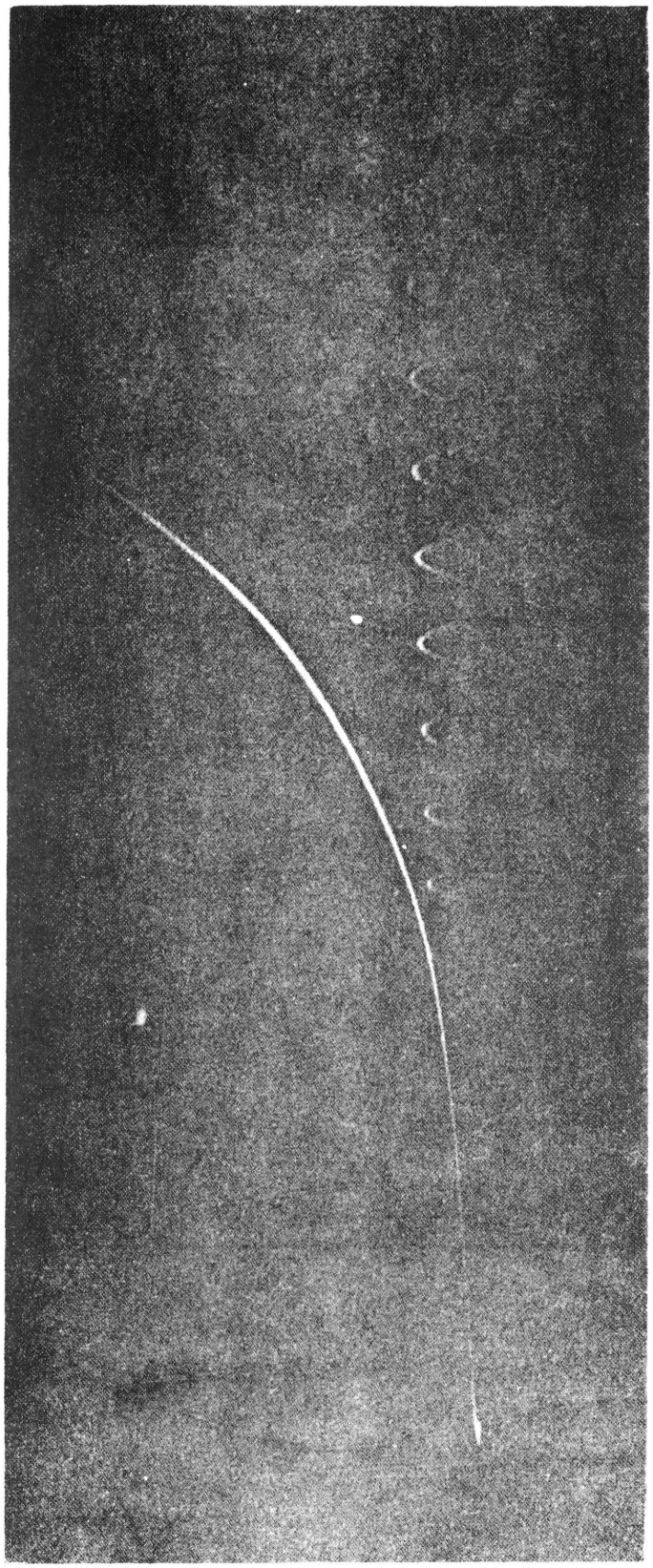

Figure 51 - Exponential signal displayed on linear time base

(α = 3.75 × 10^8)
(f = 1000 mc)

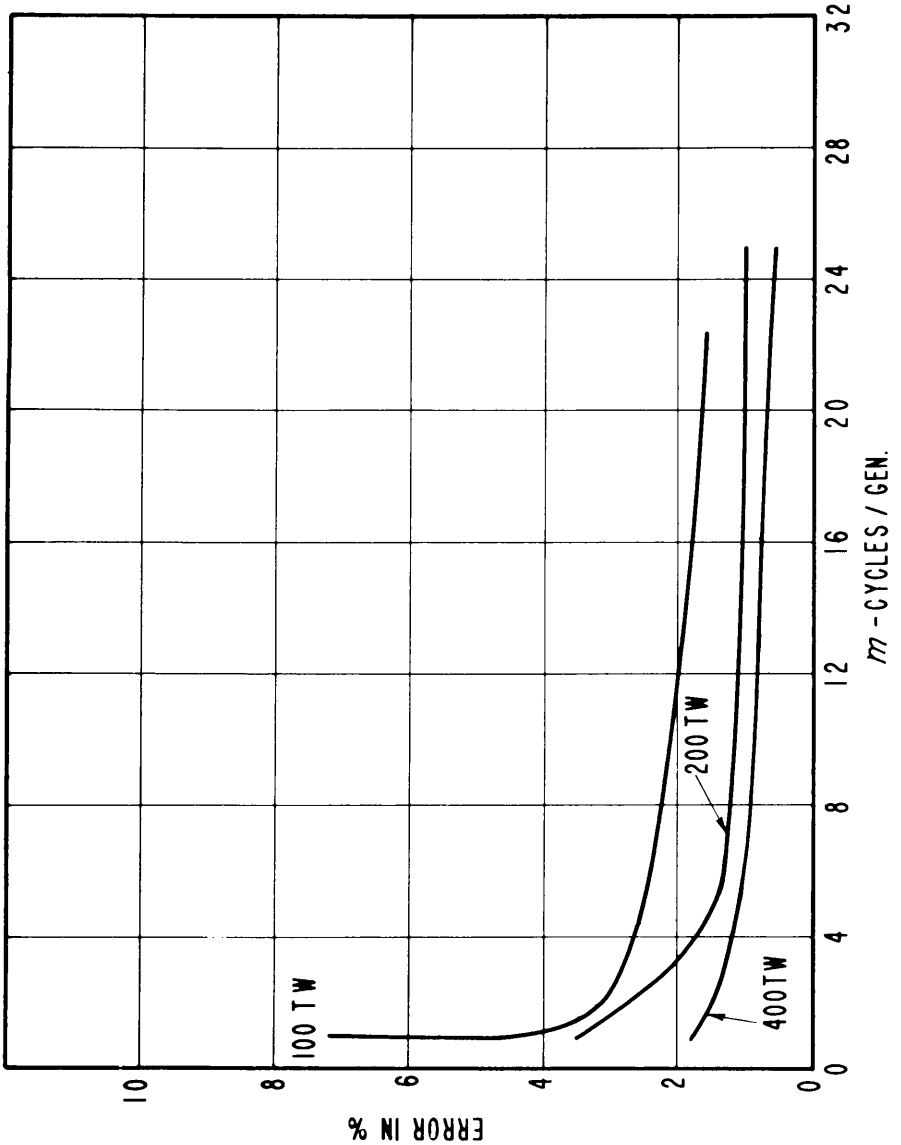

Figure 52 - Probable error in measurement of alpha vs. m